See

# COLLOID JOURNAL (USSR)

Volume XVI, Number 1

January-February, 1954

## IN ENGLISH TRANSLATION

CONSULTANTS BUREAU
152 West 42nd St., New York 18, N.Y.

*—An agency for the interpretation of international knowledge—*

Colloid Journal (U.S.S.R.) in English Translation, January-February, 1954

# TABLE OF CONTENTS

| | Page | Russ. page |
|---|---|---|
| 1. Autohesion of High Polymers. III. Effect of Molecular Weight, Shape of the Molecule, and Presence of Polar Groups on the Autohesion of High Polymers. S.S.Voyutsky and B.V.Shtarkh.. | 1 | 3 |
| 2. One Case of the Motion of a Cylindrical Body in a Visco-Plastic Disperse System. N.A.Gukasov .......................... | 9 | 10 |
| 3. Multicationic Exchange on Sulfocarbon and Wofatit. A.T.Davydov and I.Ya.Levitsky .......................... | 13 | 13 |
| 4. The Mechanism of Emulsification. L.Ya.Kremnev and A.A.Ravdel... | 19 | 17 |
| 5. Structural-Mechanical Properties of Enamel. G.V.Kukolev and L.D.Svirsky.......................... | 33 | 29 |
| 6. Structure and Properties of Loaded Rubber Mixtures. XII. Dielectric Properties of Carbon Black Mixtures with Natural Rubber. A.I.Lukomskaya and B.A.Dogadkin.................. | 41 | 36 |
| 7. Sulfides of Copper, Lead, and Zinc as Solid Emulsifiers. S.G.Mokrushin and T.P.Avilova.......................... | 49 | 44 |
| 8. Forces Retaining Dyestuff on the Fiber. F.I.Sadov............. | 57 | 51 |
| 9. Investigation of the Structure of Synthetic Polyamide Fibers. II. Integral Heats of Wetting of Capron Fiber by Water. S.M.Skuratov, N.V.Mikhailov, and E.Z.Fainberg.............. | 65 | 58 |
| 10. Flow of Clay Suspensions in Pipes. B.S.Filatov................ | 73 | 65 |
| 11. Effect of Electrolytes of the Aqueous Phase of Styrene Emulsions on the Dispersivity of the Latexes Formed. A.I.Yurzhenko and V.P.Gusyakov.......................... | 83 | 72 |
| 12. Vladimir Adolfovich Naumov (obituary).......................... | 91 | 79 |

# COLLOID JOURNAL

Journal of Theoretical and Applied Physics and
Chemistry of Colloids

Volume XVI (1954)
Number 1 (January-February)

Editor
A. V. Dumansky

Editorial Board
P.N.Antipov-Karataev, B.V.Deryagin, B.A.Dogadkin (Deputy Editor),
A.V.Dumansky, V.A.Kargin, S.M.Lipatov, P.A.Rebinder,
I.P.Serdobolsky (Secretary), M.P.Volarovich

A publication of the Academy of Sciences of the U.S.S.R

---

IN ENGLISH TRANSLATION

Copyright, 1954

CONSULTANTS BUREAU
152 West 42nd Street
New York 18, N.Y.

Printed in the United States

Annual subscription $80.00
Single issue 20.00

Note: The sale of photostatic copies of any portion of this copyright translation is expressly prohibited by the copyright owners. A complete copy of any paper in this issue may be purchased from the publisher for $7.50.

# AUTOHESION OF HIGH POLYMERS

## III. EFFECT OF MOLECULAR WEIGHT, SHAPE OF THE MOLECULE, AND PRESENCE OF POLAR GROUPS ON THE AUTOHESION OF HIGH POLYMERS

S. S. Voyutsky and B. V. Shtarkh

In our previous papers we formulated a concept of autohesion of high polymers as a diffusion process [1], and presented a detailed study of the effects, on the autohesion of polyisobutylene, of the rate of separation of the contacting polymer surfaces, contact pressure, time, and temperature of contact [2]. The object of the present study was to determine the effect of molecular size and shape, and also of the nature of the polymer, on the autohesion of high polymers.

The quantitative evaluation of autohesion of high polymers was carried out by the technique used successfully in our earlier studies.

In this technique the autohesion was determined by the force needed to separate two doubled strips of fabric, which were coated with the polymer in a volatile solvent before doubling. Complete evaporation of the solvent from the polymer was always carefully ensured before doubling. The doubling was always effected in the same conditions, established in our previous study [2]. The quantity of polymer on the fabric was never less than 0.03g/cm$^2$, and the pressure in doubling was 40 g/cm$^2$. The only factors to be varied, according to the aim of the experiment, were the time during which the layers of rubber were in contact, and the temperature during contact.

The separation of the joints was carried out on a TsNIKZ (Central Research Institute for Leather Substitutes) dynamometer with jaws which separate in a horizontal direction at a constant rate of 0.27 cm/sec. The dynamometer was fitted with an automatic recording device. From the diagrams obtained it was possible to determine the average resistance to separation and to calculate the work of autohesion from the formula:

$$Au = \frac{p2gl}{lb} = \frac{2pg}{b},$$

where p is the mean force of separation; l is the length of the working section of the joint; b - width of the joint; g - acceleration due to gravity.

The nature of separation of a joint was in each case carefully checked. Only those values of the work of autohesion were accepted which corresponded to a perfectly smooth surface of the layers of polymer on both strips of fabric after separation. If these surfaces were rough or if the polymer became detached from the fabric, the value measured was clearly not the autohesion but the cohesional strength or the adhesion of the polymer to the fabric.

*Effect of molecular weight on the autohesion of high polymers.* Samples of polyisobutylene with molecular weights of 20000, 100000, 150000, and 200000 were used for the experiments. In this series of experiments the polymer was applied to the fabric strips from benzene solution. Figure 1 shows the data on changes in the resistance to separation and the corresponding work of autohesion with changes in the duration of contact of the polyisobutylene layers.

It must be noted that in the case of polyisobutylene with molecular weight 20000, separation by the initial contact method was observed only for relatively small contact times. When the contact time exceeded 1 hour, the polymer surface on the fabric strips after separation was rough. This indicated that in this case the cohesional strength of the polymer was determined.

As is seen from the shape of the kinetic curves, the resistance to separation and the work of autohesion in all cases increases with increasing time of contact, and tends to a definite limit. The rate of increase of autohesion is greater for lower molecular weights of polymer, that is, for shorter molecules. Since the mobility of segments of isolated long chain molecules does not depend on the molecular weight for degrees of polymerization in excess of 15-20, the results indicate that the autohesion of high polymers of sufficiently high molecular weight is largely due to the diffusion of the ends of the chains.

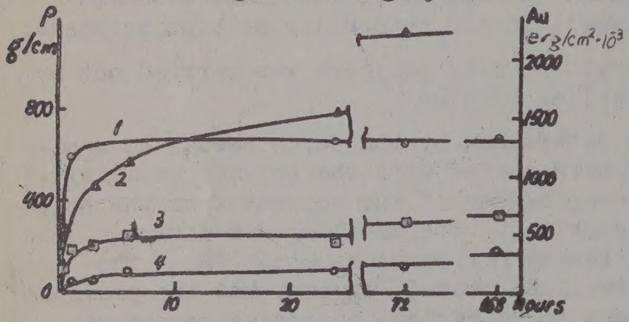

Fig. 1. Effect of contact time on the resistance to separation p and work of autohesion Au for polyisobutylenes of different molecular weight: 1-20000; 2-100000; 3-150000; 4-200000.

The results obtained do not permit any definite conclusions to be drawn concerning the limit of autohesion of the different polymers, corresponding to the cohesional strength of the material. However, the shape of the curves does not contradict the generalization that the cohesional strength of a polymer increases with molecular weight. In particular, from the curve for the polymer with molecular weight 200000 it seems likely that the maximum value of the autohesion, which is reached far beyond the limits of the diagram, will be greater than the maximum autohesion for all the other polymers. The curve for the polymer of molecular weight of 20000 is of interest. It is seen that this curve reaches its limit, which corresponds to 670 g/cm, in a contact time of the order of 1 hour. This is in full agreement with the fact that when doubled strips which have been in contact for more than 1 hour are separated, the surface of the polymer layer is rough. Evidently, in that case the cohesional strength of the polymer was determined.

Figure 2 shows changes of the resistance to separation and of the work of autohesion of polyisobutylenes of different molecular weights with variations of temperatures of contact. The contact time in this series of experiments was 5 min. It is seen that the curves are exponential in nature. This confirms that autohesion is diffusional in character. As we know, an exponential dependence of diffusion rate on temperature is found also in low-molecular substances[3].

With a knowledge of the dependence of autohesion on the contact temperature, and on the assumption that the resistance to separation is a measure of the depth to which the segments of the chain molecules diffused during contact, it is easy to calculate the activation energy of autohesion. This is the energy required for a segment of the diffusing molecule which constitutes a kinetic entity to enter a gap between the molecules of the layer into which it diffuses, and to move in this gap. The activation energy is usually calculated by means of an equation analogous to the Arrhenius equation

$$p = p_0 e^{-(E/RT)} \qquad (1)$$

where p is the resistance to separation of the joint; $p_0$ is a constant; E is the activation energy of the process; R is the gas constant; T is the absolute temperature. According to this equation, a straight line should be obtained by plotting the logarithm of the resistance to separation along the ordinate axis, and the reciprocal of the absolute temperature along the abscissa axis. Figure 3 shows such graphs for all the polyisobutylenes studied. It is seen that all the experimental points lie fairly well on straight lines. It is interesting that all the lines are practically parallel and that the corresponding value of the activation energy, independently of the molecular weight of the polymer, is 2390 cal. Evidently the activation energy is the same in all cases, because the kinetic entities which participate in the diffusion process are of the same nature. The question arises, how can the same value of activation energy for the autohesion of polyisobutylenes of different molecular weight be reconciled with the increase in the diffusion rate which is observed with decreasing degree of polymerization It appears that the explanation lies in the fact that the ends of the molecules, which are more numerous in low molecular polyisobutylenes, diffuse more rapidly into the polymer layer than do the middle portions of the molecules. This is quite understandable, as the probability of entry of the ends of a molecule into the gap between the molecules of the layer into which the diffusion takes place must definitely be greater, for steric reasons, than the probability of entry of a middle portion of a molecule into the same gap. It must then be assumed that the different autohesion of polyisobutylenes of different degrees of polymerization is due to differences in the value of the pre-exponential term in Equation (1), which, when the Arrhenius equation is applied to diffusion, represents the probability of entry of a molecule into a pore.

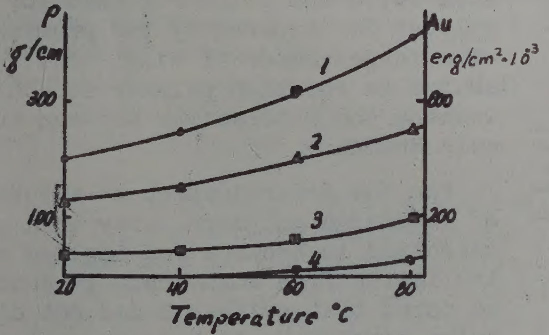

Fig. 2. Dependence of the contact temperature on the resistance to separation p and the work of autohesion Au for polyisobutylenes of different molecular weight; 1-20000; 2-100000; 3-150000; 4-200000.

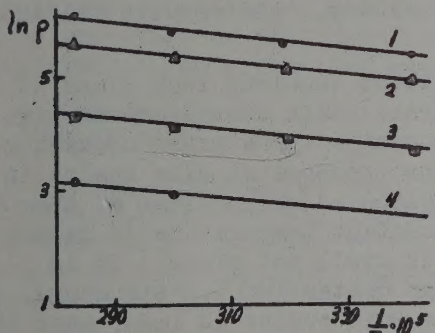

Fig. 3. Dependence of ln p on 1/T for polisobutylenes of different molecular weight: 1-20000; 2-100000; 3-150000; 4-200000.

Effect of shape of the polymer molecule on autohesion. Two butadiene polymers, A and B, were taken, with different contents of the 1,4-and 1,2-structures, which were studied in detail by Tolstukhina [4]. Table 1 shows the contents of the 1,4-

and 1,2-structural units in the polymers, determined by Prilezhaev's method and the zoning method, and the molecular weights of the polymers, determined osmometrically.

TABLE 1
Characteristics of the Polybutadienes.

| Polymer | Content (in %) of the structural units in the main chain | | Molecular weight |
|---|---|---|---|
| | 1,4- | 1,2- | |
| A | 30 | 57 | 101000 |
| B | 65 | 31.5 | 72000 |

TABLE 2
Resistance to Separation and Work of Autohesion of Polybutadienes with Different Contents of 1,4- and 1,2-Structural Units in the Main Chain

| Polymer | Resistance and Work | Contact temperature in° | |
|---|---|---|---|
| | | 20 | 60 |
| A | p(g/cm) | 34 | 284 |
| | Au(erg/cm$^2\cdot10^{-3}$) | 66 | 560 |
| B | p(g/cm) | 54 | 123 |
| | Au(erg/cm$^2\cdot10^{-3}$) | 106 | 241 |

It is very significant that it was established by a study of the plastic flow of polymers A and B in the solid state that the coefficient of true viscosity of butadiene polymers decreases with increase of the content of 1,4-structural units in the molecule. However, Tolstukhina's study of the rate of stress relaxation in butadiene polymers showed that the relaxation processes were more rapid for polymer A than for polymer B. Apparently the presence of a large number of vinyl side chains in the high polymer molecule weakens the interaction between the main chains.

For the determination of autohesion of butadiene polymers, they were dissolved in benzene and applied to the fabric from solution. It should be noted that polymer B did not dissolve completely in benzene, and to obtain a smooth polymer surface on the fabric strips it was necessary to separate off by filtration a small amount of a gel fraction. The same method was used by Tolstukhina in the preparation of solutions of this polymer. The fabric strips were doubled in the usual manner, with a contact time of 5 minutes and at temperatures of 20 and 60°. The separation of the joints was carried out in the usual way. The results are shown in Table 2.

It is seen from the results of experiments in which doubling took place at 20° that large numbers of double bonds in the main valency chain correspond to high values of resistance to separation and work of autohesion for a given contact time. These results confirm our previous view [1] that the presence of side chains in polymer molecules should hinder the diffusion of molecules or portions of them from one volume of the polymer into another. When the contact temperature is raised to 60°, the position is reversed. The cause of this is still not clear. It is possible that in the case of the polymer with a high content of 1,2-structure, in which, as we have seen, the interaction between the main chains is less, when the temperature increases the whole molecules begin to diffuse, and not segments of them.

Effect of the number of polar groups in the high polymer molecule on autohesion. These experiments were carried out with butadiene copolymers which contained different amounts of acrylonitrile. Polymers with contents of 11.7; 19.6; 28.0; and 36.9% of acrylonitrile were used. The butadiene-nitrile copolymers were applied to the fabric strips from dichlorethane solution. The contact time of the coated strips during doubling was 5 minutes.

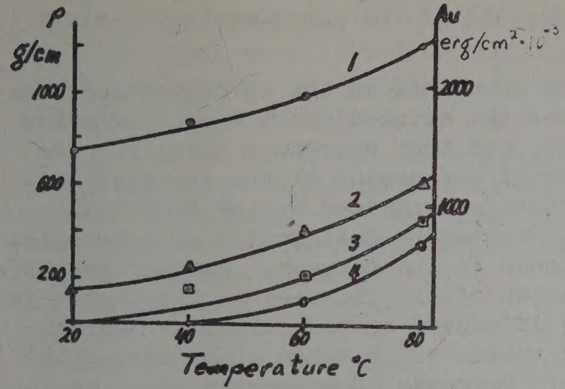

Fig. 4. Effect of contact temperature on resistance to separation p and work of autohesion Au for butadiene-nitrile copolymers containing: 1-11.7%; 2-19.6%; 3-28%; 4-36.9% acrylonitrile in the molecule.

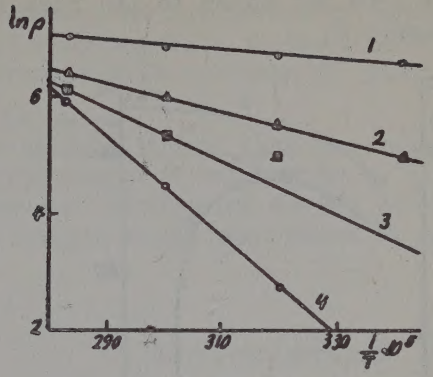

Fig. 5. Dependence of ln p on 1/T for butadiene-nitrile copolymers containing: 1-11.7%; 2-19.6%; 3-28%; 4-36.9% acrylonitrile in the molecule.

Figure 4 presents data on the resistance to separation and work of autohesion for various butadiene-nitrile copolymers at different doubling temperatures. As in the case of the polyisobutylenes, the curves are exponential in character. It is interesting to note that with higher contents of polar groups in the copolymer the resistance to separation at normal temperatures is less, but the slope of the curve with increase of temperature is steeper. This is evidently to be explained by the fact that the poalr groups, as the result of formation of bonds between them, strongly hinder thermal movement at low temperatures. As the temperature rises and thermal movement increases, the polar bonds are destroyed and the diffusion capacity increases sharply.

Figure 5 shows graphs for ln p against 1/T for the polymers studied. On the whole the experimental points lie fairly well on straight lines. It is interesting that the slope of the curve is greater with higher contents of polar groups in the copolymer. The activation energy calculated from these graphs was as follows:

| | |
|---|---|
| Content of acrylonitrile in the copolymer, % | 11.7, 19.6, 28.0, 36.9 |
| Value of E in kcal | 1.53, 4.76, 8.67, 16.59. |

Our explanation for the increase of activation energy with increased content of acrylonitrile in the copolymer is that as the polarity of the polymer increases, so there is an increase in the energy needed for a segment of the molecule to penetrate into the space between the molecules of the polymer into which the former molecule is diffusing.

Effect of formation of spatial structures in the polymer on its autohesion. In this series of experiments we studied the effect of cross-bonding of natural rubber molecules by sulfur bridges in vulcanization, on autohesion. In these experiments the fabric strips were coated with benzene solutions of smoked sheet, to which 5% sulfur, 1% thiuram, and 2% zinc oxide on the weight of the rubber had been previously added on rolls. Before doubling, the strips were heated at 100° for various periods, which resulted in different degrees of vulcanization of the rubber strips. Otherwise the preparation and separation of the joints was as usual. In addition to these experiments, a special control series of experiments was performed, which differed only in the fact that sulfur, thiuram, and zinc oxide were not added to the rubber. The results of the experiments are shown in Figure 6.

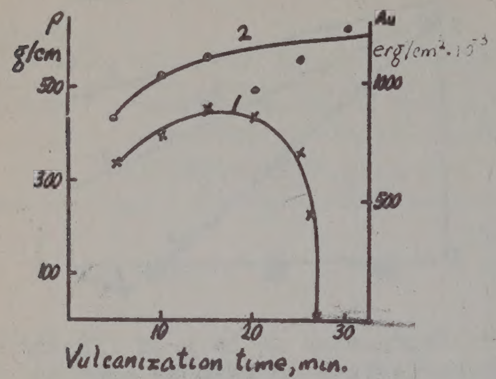

Fig. 6. Effect of vulcanization on resistance to separation p and work of autohesion Au of natural rubber: 1-with sulfur, thiuram, and zinc oxide; 2- without additions.

It is seen that as the vulcanization time increases the autohesion at first increases somewhat, and then decreases sharply. The increase of autohesion at the start of vulcanization is explained by the fact that heating favors the destruction of intermolecular bonds in the polymer. Another possible explanation of the increase of autohesion is that it is caused by the oxidative degradation of rubber which takes place during the process. Decrease of molecular size, as was seen in the case of polyisobutylene, may favor autohesion of the high polymer. During this time the partial formation of bridges between the individual molecules does not yet appreciably affect autohesion.

The sharp decrease of autohesion when the time of heating is increased to 25 min. is apparently due to the fact that then sulfur bonds already begin to be formed between the separate aggregates formed during the first stage of vulcanization. A sort of jump occurs, in which the polymer containing large numbers of sulfur bonds between individual linear molecules undergoes a transition into a qualitatively new state – a three-dimensional structure. It is clear that the formation of a spatial structure, as was shown earlier [1], should lead to complete disappearance of autohesion in the polymer.

In the control experiments the autohesion increases continuously with increasing time of thermal treatment, tending to a definite limit. The fact that the value of the autohesion in the control series is always higher is explained by the impossibility of formation of sulfur bridges.

Finally it should be noted that the curve for changes of autohesion with increase of heating time of the polymer to which sulfur and accelerators had been added may serve to characterize structural changes in the polymer during vulcanization. In this respect it presents considerable advantages, for example, over the curve which characterizes the addition of sulfur. This latter, as is known [5] changes steadily throughout the whole time of heating and the instant of formation of a spatial structure cannot be detected on it.

## SUMMARY

1. It is shown for polyisobutylenes of different molecular weight that increase in the size of the chain molecule retards autohesion, but increases the limiting value to which the work of autohesion tends with increasing contact time.

2. Investigation of the temperature dependence of autohesion of polyisobutylenes showed that the activation energy does not depend on the molecular weight of the polyisobutylene.

3. It is shown for polybutadienes with varying contents of 1,4-and 1,2-structures that autohesion decreases with increase in the number of short side

groups in the molecule, which apparently hinder diffusion by purely steric causes.

4. Investigation of the temperature dependence of autohesion of butadiene-nitrile copolymers with different contents of acrylonitrile in the molecule showed that the activation energy of autohesion increases with increase of polar nitrile groups in the polymer.

5. It is shown for the vulcanization of natural rubber that the formation of a spatial structure results in complete disappearance of autohesion in high polymers. It is shown that the kinetics of changes of autohesion during vulcanization can effectively characterize the structural changes which take place in the polymer during the process.

Central Research Institute
for Leather Substitutes, Moscow.

Received March 5, 1953

## LITERATURE CITED

[1] S. S. Voyutsky and Yu. L. Margolina, Prog. Chem. 18, 449 (1949).

[2] S. S. Voyutsky and V. M. Zamazy, Proc. Acad. Sci. USSR, 81, 63 (1951); Colloid J., 15, 407 (1953). 1)

[3] R. Barrer, Diffusion in Solids, p 148 (1948).

[4] F. S. Tolstukhina, Study of the Effect of Structure of Butadiene Polymers on their Physico-Chemical and Mechanical Properties. Author's summary of dissertation, Moscow Institute of Fine Chemical Technology (1952).

[5] B. A. Dogadkin, Chemistry and Physics of Rubber, State Chemical Press, pp.301-305 (1947).

---

1) See Consultants Bureau Translation, p.421.

# ONE CASE OF THE MOTION OF A CYLINDRICAL BODY IN A VISCO-PLASTIC DISPERSE SYSTEM

N. A. Gukasov

In the solution of various applications of the theory of flow of visco-plastic bodies (theory of the Lawaczeck apparatus, problem of hydromechanical friction in drilling operations, etc.) it is necessary to examine problems of motion of a long cylindrical body in a cylindrical pipe. The aim of the present study is to solve this problem on the following assumptions: 1) the cylindrical body is sufficiently long for the frontal resistance of this body to be neglected in comparison with friction on its sides; 2) the body has no weight; 3) the body moves coaxially in the pipe; 4) in view of the slowness of movement, inertia forces may be neglected; 5) the cylindrical pipe is closed at the lower end. The analogous problem for a Newtonian liquid was solved by Pirverdyan [1] in relation to the problem of flow of a two-phase liquid.

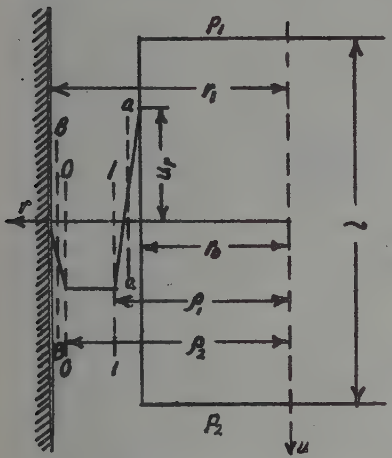

Fig. 1. Flow of a plastic liquid in an annular space.

Figure 1 schmatically represents the flow of a plastic liquid in an annular space. The stream is separated by the core of the liquid into two independent regions, unconnected with each other, and therefore it is necessary to derive equilibrium equations separately for each region.

According to the Shvedov-Bingham law [1]:

$$\tau = \mu \frac{du}{dr} + \theta$$

where $\tau$ is the tangential shear stress; $\mu$ is the absolute viscosity; $\theta$ is the time of commencement of flow; $\frac{du}{dr}$ is the velocity gradient.

To solve the problem, we denote by $\underline{u_1}$ and $\underline{u_2}$ the respective velocities of the clay suspensions for the region with positive and negative values of $\frac{du}{dr}$; $u_0$ is the velocity of the core of the clay suspension; $\underline{l}$ is the length of the moving cylinder; $\underline{p_1}$ and $\underline{p_2}$ are the pressures at the upper and lower ends of the moving cylinder, respectively; $\gamma$ is the specific gravity of the clay suspension; $\underline{r_0}$ and $\underline{r_1}$ are the radii of the moving and stationary cylinders respectively; $\rho_1$ and $\rho_2$ are the radii of the core of clay suspension, when;

$$\frac{\underline{p_2 - p_1}}{\underline{l}} = k; \quad r_a = \frac{\underline{r_0}}{r_1}; \quad \rho_a = \frac{\rho_1}{r_1}; \quad \rho_b = \frac{\rho_2}{r_1}; \quad r_b = \frac{r_1}{r_1} = 1.$$

The equilibrium equation for $\underline{a}$ - $\underline{a}$ (see Figure 1), which includes the ring of clay suspension around the weightless cylinder, is written:

$$2\pi r\left(\mu\frac{du_1}{dr}+\theta\right)\underline{l}+\pi(r^2-r_0^2)\gamma\underline{l}-p_2\pi r^2+p_1\pi r^2=0. \qquad (1)$$

Analogous equations are written for $\underline{b}$ - $\underline{b}$; I - I, and II - II respectively (see Figure 1):

$$-2\pi r\left(-\mu\frac{du_2}{dr}+\theta\right)\underline{l}+\pi(r^2-r_0^2)\gamma\underline{l}+p_1\pi r^2-p_2\pi r^2=0. \qquad (2)$$

$$2\pi\rho_1\theta\underline{l}+\pi(\rho_1^2-r_0^2)\gamma\underline{l}-p_2\pi\rho_1^2+p_1\pi\rho_1^2=0 \qquad (3)$$

$$-2\pi\rho_2\theta\underline{l}+\pi(\rho_2^2-r_0^2)\gamma\underline{l}-p_2\pi\rho_2^2+p_1\pi\rho_2^2=0. \qquad (4)$$

From Equations (1) and (2), knowing that when

$$r=r_0,\ u_1=-u_t;\quad r=\rho_1,\ u_1=u_0;\ r=r_1,\ u_2=0;\quad r=\rho_2,\ u_2=u_0,$$

we derive an expression for $u_1$, $u_2$, $u_0$ and $u_t$:

$$u_1=\frac{\gamma r_a^2 r_1^2}{2\mu}\ln\frac{r\rho_b}{r_1\rho_\alpha}+\frac{r_1^2(\gamma-k)}{4\mu}\left(1+\rho_a^2-\rho_b^2-\frac{r^2}{r_1^2}\right)-\frac{\theta}{\mu}r_1\left(1-\rho a-\rho b+\frac{r}{r_1}\right), \qquad (5)$$

$$u_2=\frac{\gamma-k}{4\mu}(r_1^2-r^2)+\frac{\gamma r_a^2 r_1^2}{2\mu}\ln\frac{r}{r_1}-\frac{\theta}{\mu}(r_1-r), \qquad (6)$$

$$u_0=\frac{\gamma-k}{4\mu}r_1^2(1-\rho_b^2)+\frac{\gamma r_a^2 r_1^2}{2\mu}\ln\rho_b-\frac{\theta}{\mu}r_1(1-\rho_b), \qquad (7)$$

$$u_t=\frac{k-\gamma}{4\mu}r_1^2(1+\rho_a^2-\rho_b^2-r_a^2)+\frac{\theta}{\mu}r_1(1-\rho_b-\rho_a+r_a)-\frac{\gamma r_a^2 r_1^2}{2\mu}\ln\frac{r_a\rho_b}{\rho_a} \qquad (8)$$

where $\underline{u_t}$ is the velocity of the moving cylindrical body.

From Equations (3) and (4) we have:

$$\frac{k}{\gamma}=1-\frac{r_a^2}{\rho_a\rho_b};\quad \frac{\theta}{\gamma r_1}=\frac{r_a^2(\rho_b-\rho_a)}{2\rho_a\rho_b}.$$

We determine the amount of flow in the space between the moving and stationary cylinders:

$$q=2\pi\int_{r_0}^{r_1} ru\,dr$$

or

$$q=2\pi\int_{r_0}^{\rho_1} ru_1\,dr+\pi(\rho_2^2-\rho_1^2)u_0+2\pi\int_{\rho_2}^{r_1} ru_2\,dr.$$

Substituting expressions for $\underline{u_1}$, $\underline{u_0}$, and $\underline{u_2}$, and putting $\Pi=\frac{2\mu q}{\pi\gamma r_1^4}$, we have:

$$\Pi = \frac{r_a^2}{4\rho_a\rho_b}\left[(\rho_a^2 - r_a^2)^2 + (1 - r_a^2)^2 - (r_a^2 - \rho_b^2)^2\right] -$$

$$- \frac{r_a^2}{\rho_a\rho_b}(\rho_b - \rho_a)\left[r_a^2\left(\rho_a + \rho_b - \frac{2}{3}r_a - 1\right) + \frac{1}{3}(1 - \rho_a^3 - \rho_b^3)\right] +$$

$$+ r_a^4 \ln\frac{\rho_a}{r_a\rho_b} - \frac{r_a^2}{2}(\rho_a^2 - r_a^2 - \rho_b^2 + 1). \qquad (9)$$

Since the end of the vessel is closed, the amount of liquid pressed out equals the amount of liquid which flows down, or:

$$\pi r_0^2 u_t = q,$$

then

$$\Pi = -\frac{r_a^4}{2\rho_a\rho_b}(\rho_a^2 - r_a^2 - \rho_b^2 + 1) + \frac{r_a^4(\rho_b - \rho_a)}{\rho_a\rho_b}(1 - \rho_a - \rho_b + r_a) + r_a^4 \ln\frac{\rho_a}{r_a\rho_b} \qquad (10)$$

Term-by-term subtraction of Equation (10) from Equation (9) gives:

$$\rho_a(4r_a^3 + 2\rho_b^3 + 6r_a^2\rho_b - 6\rho_b + 4) +$$

$$+ \rho_b(\rho_b^3 - 4r_a^3 - 4) + 3(1 - r_a^4) =$$

$$= \rho_a^4 + 2\rho_a^3\rho_b.$$

Denoting the left and right sides of this Equation by $\alpha$, we have:

$$\rho_a^4 + 2\rho_a^3\rho_b = \alpha;$$

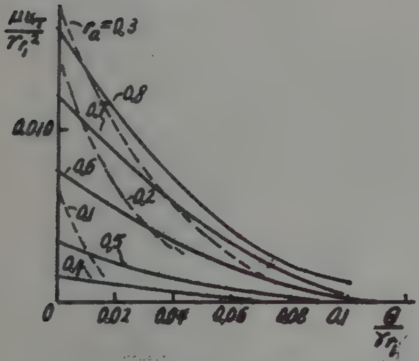

Fig 2. Graph for the dependence of $\frac{\mu u_t}{\gamma r_1^2}$ on $\frac{\theta}{\gamma r_1}$.

$$\rho_a(4r_a^3 + 2\rho_b^3 + 6r_a^2\rho_b - 6\rho_b + 4) + \rho_b(\rho_b^3 - 4r_a^3 - 4) + 3(1 - r_a^4) = \alpha.$$

Graphical solution of these two Equations makes is possible to find their roots, and hence the dependence $\rho_b = \underline{f}(\rho_a)$. With a knowledge of the dependence $\rho_b = \underline{f}(\rho_a)$, it is possible to plot the dependence $\mu u_t/\gamma r_1^2 = \psi(\theta/\gamma r_1)$ (see Figure 2).

When $\theta/\gamma r_1 = 0$, the curve for $\mu u_t/\gamma r_1^2 = \psi_1(r_a)$ coincides with the curve which may be plotted by means of Formula (17) given in Pirverdyan's paper.

In conclusion, I express my gratitude to A. M. Pirverdyan for his guidance in the present investigation.

State Research and Development Institute,
Baku.

Received April 25, 1953

LITERATURE CITED

[1] Cited from R.I. Shishchenko, Hydraulics of Clay Suspensions, Azerbaidzhan Oil Works Press (1951).

# MULTICATIONIC EXCHANGE ON SULFOCARBON AND WOFATIT

A.T. Davydov and I. Ya. Levitsky

Studies of exchange absorption of ions on different adsorbents usually deal with exchanges between two ions. Such cases of ion exchange are of interest in the theoretical treatment of the problem and are met with very rarely in practice.

In the practical utilization of ion exchangers we always deal with the adsorption of several ions, that is, with multi-ionic exchange.

In his study of the conditions of multicationic exchange on glauconite, Nikolsky [1] gives an equation which is applicable both to exchange adsorption and to chemical absorption. Antipova-Karateeva [2] studied the exchange of three cations on soil, and obtained satisfactory results. Gapon [3], in a study of the conditions of multicationic exchange reactions, found it possible to regard this process as independent for each individual ion in its adsorption or exchange from a mixture for other ions.

To verify this for synthetic ion exchangers, we studied exchange reactions with three cations [4]. In the present study we have attempted to extend Gapon's views to exchange with four cations, as represented by the following scheme:

$$\Pi\ [(M_1)_{\frac{1}{m}},(M_2)_{\frac{1}{n}},(M_3)_{\frac{1}{z}}] + \frac{1}{p}(M_4) \rightleftharpoons \Pi\ (M_4)_{\frac{1}{p}} + \left[\frac{1}{m}(M_1),\frac{1}{n}(M_2),\frac{1}{z}(M_3)\right] \qquad (1)$$

where $\Pi$ is the adsorbent, and $\underline{m}$, $\underline{n}$, $\underline{z}$ and $\underline{p}$ are the valencies of the exchanging cations $\underline{M_1}$, $\underline{M_2}$, $\underline{M_3}$, and $\underline{M_4}$.

On the basis of the laws found in the study of three-cation exchange [4], Scheme (1) may be represented as three independent biary reactions, and in conditions of adsorptional equilibrium between the liquid and the solid phases the corresponding constants for exchange adsorption may be derived. If we denote by $\Gamma_1$, $\Gamma_2$, $\Gamma_3$, and $\Gamma_4$ the amounts (in g-equiv, of the adsorbed cations $M_1$, $M_2$, $M_3$, and $M_4$, and if $c_1$, $c_2$, $c_3$, and $c_4$ denote the concentrations of the same cations in the equilibrium solution then the pairs of reactions may be denoted as follows:

$$K_1\Gamma_1 c_4^{1/p} = K_2\Gamma_4 c_1^{1/m} \qquad (2)$$

$$K_3\Gamma_2 c_4^{1/p} = K_4\Gamma_4 c_2^{1/n} \qquad (3)$$

$$K_5\Gamma_3 c_4^{1/p} = K_6\Gamma_4 c_3^{1/z} \qquad (4)$$

From the three above equations we have the three constants for the exchange reactions:

$$\frac{\Gamma_1}{\Gamma_4} = \frac{K_2}{K_1} \cdot \frac{c_1^{1/m}}{c_4^{1/p}} \tag{5}$$

$$\frac{\Gamma_2}{\Gamma_4} = \frac{K_4}{K_3} \cdot \frac{c_2^{1/n}}{c_4^{1/p}} \tag{6}$$

$$\frac{\Gamma_3}{\Gamma_4} = \frac{K_6}{K_5} \cdot \frac{c_3^{1/z}}{c_4^{1/p}} \tag{7}$$

Simplification of the equations obtained by division of Equation (5) by (6) and by (7), gives the following equations:

$$\frac{\Gamma_1}{\Gamma_2} = K'' \frac{c_1^{1/m}}{c_2^{1/n}} \tag{8}$$

$$\frac{\Gamma_1}{\Gamma_3} = K''' \frac{c_1^{1/m}}{c_3^{1/z}} \tag{9}$$

By multiplying together the left-hand sides and the right-hand sides of Equations (8) and (9), we obtain the equation for the isotherm of the exchange reaction for four cations.

$$\frac{(\Gamma_1)^2}{\Gamma_2 \cdot \Gamma_3} = K \frac{\left(c_1^{1/m}\right)^2}{c_2^{1/n} \cdot c_3^{1/z}} \tag{10}$$

If the capacity of the adsorbent for the cations, determined experimentally in the present study, is denoted by $\Gamma_{1\infty}$, $\Gamma_{2\infty}$, and $\Gamma_{3\infty}$, then the exchange value of these cations will be given by the following equations:

$$\Gamma_1 = \Gamma_{1\infty} - mc_1 \; ; \tag{11}$$

$$\Gamma_2 = \Gamma_{2\infty} - nc_2 \; ; \tag{12}$$

$$\Gamma_3 = \Gamma_{3\infty} - zc_3 \; . \tag{13}$$

Substitution of the values of $\Gamma_1$, $\Gamma_2$, and $\Gamma_3$ in Equation (10) gives it in a form suitable for calculation:

$$\frac{(\Gamma_{1\infty} - mc_1)^2}{(\Gamma_{2\infty} - nc_2)\,(\Gamma_{3\infty} - zc_3)} = K'''' \frac{\left(c_1^{1/m}\right)^2}{c_2^{1/n} \cdot c_3^{1/z}} \; . \tag{14}$$

To verify Equation (14) we studied the exchange adsorption of the cations

To verify Equation (14) we studied the exchange adsorption of the cations $NH_4^+$, $Ca^{2+}$ and $Fe^{3+}$ on $K^+$, $Mg^{2+}$, and $Al^{3+}$ from solutions of different concentrations on Sulfocarbon and Wofatit-P. The experimental technique of this work was described in detail in an earlier publication [4]. The experimental and calculated data are shown in the Tables; exchange adsorption on Sulfocarbon in Table 1, and exchange adsorption on Wofatit in Table 2.

TABLE 1

Exchange Adsorption on Sulfocarbon,

| Concentration of cation | pH |  | Amount of cation displaced in g-equiv $\cdot 10^2$ per 100 g sulfocarbon |  |  | $\frac{(c_1^{1/m})^2}{c_2^{1/n} \cdot c_3^{1/z}} \cdot 10^2$ | $\frac{(\Gamma_{2\infty} - n^{c}{}_{2})(\Gamma_{3\infty} - z^{c}{}_{3})}{(\Gamma_{1\infty} - m^{c}{}_{1})^2}$ | $K''' \cdot 10^3$ |
|---|---|---|---|---|---|---|---|---|
|  | Initial solution | Equilibrium solution | $c_1(NH_4)$ | $c_2(Ca)$ | $c_3(Fe)$ |  |  |  |
| KCl | $(\Pi_{NH_4} + \Pi_{Ca} + \Pi_{Fe}) + K^+$ |  |  |  |  |  |  |  |
| 0.04 | 6.04 | 2.5 | 0.815 | 0.99 | 1.03 | 0.307 | 0.658 | 2.02 |
| 0.07 | 6.0 | 2.48 | 1.06 | 1.24 | 1.39 | 0.420 | 0.584 | 2.45 |
| 0.10 | 5.98 | 2.43 | 1.14 | 1.40 | 1.58 | 0.438 | 0.539 | 2.36 |
| 0.13 | 5.9 | 2.38 | 1.22 | 1.51 | 1.68 | 0.487 | 0.517 | 2.52 |
| 0.16 | 5.82 | 2.32 | 1.30 | 1.55 | 1.74 | 0.526 | 0.506 | 2.66 |
| 0.25 | 5.92 | 2.3 | 1.47 | 1.89 | 1.94 | 0.583 | 0.456 | 2.66 |
| 0.5 | 5.93 | 2.28 | 1.63 | 2.09 | 2.23 | 0.653 | 0.395 | 2.58 |
| 0.75 | 6.0 | 2.2 | 1.71 | 2.26 | 2.36 | 0.680 | 0 356 | 2.42 |
| 1.0 | 6.02 | 2.2 | 1.75 | 2.31 | 2.46 | 0.696 | 0.345 | 2.40 |
|  |  |  |  |  |  |  | $K_{av.}$ = 0.00245 |  |
| $MgCl_2$ | $(\Pi_{NH_4} + \Pi_{Ca} + \Pi_{Fe}) + Mg^{2+}$ |  |  |  |  |  |  |  |
| 0.04 | 5.78 | 2.32 | 0.86 | 1.10 | 1.17 | 0.326 | 0.634 | 2.07 |
| 0.07 | 5.74 | 2.24 | 1.10 | 1.25 | 1.52 | 0.437 | 0.560 | 2.44 |
| 0.1 | 5.82 | 2.14 | 1.18 | 1.47 | 1.62 | 0.456 | 0.530 | 2.36 |
| 0.13 | 5.72 | 2.1 | 1.26 | 1.59 | 1.71 | 0.491 | 0.508 | 2.49 |
| 0.16 | 5.8 | 2.1 | 1.34 | 1.69 | 1.78 | 0.531 | 0.494 | 2.62 |
| 0.25 | 5.88 | 2.14 | 1.51 | 1.94 | 2.23 | 0.580 | 0.397 | 2.30 |
| 0.5 | 5.85 | 2.04 | 1.71 | 2.21 | 2.59 | 0.667 | 0.322 | 2.15 |
| 0.75 | 5.9 | 2.04 | 1.87 | 2.37 | 2.65 | 0.766 | 0.310 | 2.37 |
| 1.0 | 5.89 | 2.0 | 2.00 | 2.42 | 2.78 | 0.846 | 0.286 | 2.42 |
|  |  |  |  |  |  |  | $K_{av.}$ = 0.00236 |  |
| $AlCl_3$ | $(\Pi_{NH_4} + \Pi_{Ca} + \Pi_{Fe}) + Al^{3+}$ |  |  |  |  |  |  |  |
| 0.04 | 2.74 | 2.32 | 1.02 | 1.52 | 1.94 | 0.313 | 0.451 | 1.46 |
| 0.07 | 2.8 | 2.28 | 1.14 | 1.77 | 2.20 | 0.349 | 0.393 | 1.37 |
| 0.1 | 2.88 | 2.38 | 1.18 | 1.87 | 2.33 | 0.358 | 0.381 | 1.37 |
| 0.13 | 2.91 | 2.32 | 1.26 | 1.95 | 2.49 | 0.391 | 0.332 | 1.30 |
| 0.16 | 2.9 | 2.38 | 1.30 | 1.99 | 2.56 | 0.410 | 0.320 | 1.31 |
| 0.25 | 2.96 | 2.3 | 1.34 | 2.16 | 2.69 | 0.410 | 0.290 | 1.19 |
| 0.5 | 3.2 | 2.26 | 1.43 | 2.34 | 2.78 | 0.439 | 0.267 | 1.17 |
| 0.75 | 3.0 | 2.21 | 1.51 | 2.42 | 2.91 | 0.475 | 0.242 | 1.15 |
| 1.0 | 3.04 | 2.29 | 1.59 | 2 47 | 2.95 | 0.519 | 0.232 | 1.20 |
|  |  |  |  |  |  |  | $K_{av.}$ = 0.00128 |  |

$\Gamma_{1\infty} = 0.162$, $\Gamma_{2\infty} = 0.183$, $\Gamma_{3\infty} = 0.126$

TABLE 2

Exchange Adsorption on Wofatit

| Concentration of cation | pH |  | Amount of cation displaced in g-equiv $\cdot 10^2$ per 100 g Wofatit |  |  | $\frac{(c_1^{1/m})^2}{c_2^{1/n} \cdot c_3^{1/n}} \cdot 10^2$ | $\frac{(\Gamma_{2\infty} - n^c{}_2)(\Gamma_{3\infty} - z^c{}_3)}{(\Gamma_{1\infty} - m^c{}_1)^2}$ | $K'''' \cdot 10^3$ |
|---|---|---|---|---|---|---|---|---|
|  | Initial solution | Equilibrium solution | $c_1(NH_4)$ | $c_2(Ca)$ | $C_3(Fe)$ |  |  |  |
| $KCl$ |  |  |  |  | $(\Pi_{NH_4} + \Pi_{Ca} + \Pi_{Fe}) + K^+$ |  |  |  |
| 0.05 | 6.0 | 2.32 | 1.02 | 1.12 | 1.25 | 0.256 | 0.407 | 1.73 |
| 0.1 | 5.96 | 2.43 | 1.18 | 1.54 | 1.65 | 0.443 | 0.323 | 1.43 |
| 0.25 | 5.9 | 2.25 | 1.51 | 1.90 | 2.15 | 0.593 | 0.231 | 1.37 |
| 0.5 | 5.8 | 2.21 | 1.67 | 2.14 | 2.25 | 0.677 | 0.211 | 1.46 |
| 0.75 | 5.93 | 2.27 | 1.71 | 2.29 | 2.41 | 0.622 | 0.182 | 1.13 |
| 1.0 | 5 98 | 2.6 | 1.83 | 2.35 | 2.51 | 0.750 | 0.165 | 1.24 |
|  |  |  |  |  |  |  | $K_{av.}$ = 0.00139 |  |
| $MgCl_2$ |  |  |  |  | $(\Pi_{NH_4} + \Pi_{Ca} + \Pi_{Fe}) + Mg^{2+}$ |  |  |  |
| 0.05 | 5.76 | 2.43 | 0.98 | 1.29 | 1.30 | 0.358 | 0.394 | 1.41 |
| 0.1 | 5.82 | 2.2 | 1.10 | 1.55 | 1.70 | 0.378 | 0.310 | 1.17 |
| 0.25 | 5.7 | 2.25 | 1.30 | 1.97 | 2.00 | 0.446 | 0.249 | 1.11 |
| 0.5 | 5.8 | 2.24 | 1.47 | 2.19 | 2.25 | 0.516 | 0.204 | 1.05 |
| 0.75 | 5.9 | 2.14 | 1.59 | 2.27 | 2.30 | 0.589 | 0.197 | 1.16 |
| 1.0 | 5.8 | 2.27 | 1.67 | 2.37 | 2.40 | 0 629 | 0.180 | 1.13 |
|  |  |  |  |  |  |  | $K_{av.}$ = 0.00119 |  |
| $AlCl_3$ |  |  |  |  | $(\Pi_{NH_4} + \Pi_{Ca} + \Pi_{Fe}) + Al^{3+}$ |  |  |  |
| 0.05 | 2.78 | 2.37 | 0.94 | 1.49 | 1.55 | 0.289 | 0.333 | 0.962 |
| 0.1 | 2.9 | 2.4 | 1.06 | 1.67 | 1.80 | 0.331 | 0.283 | 0.936 |
| 0.25 | 3.02 | 2.37 | 1.22 | 2.00 | 2.05 | 0.386 | 0.237 | 0.913 |
| 0.5 | 3.06 | 2.31 | 1.39 | 2.24 | 2.41 | 0.445 | 0.176 | 0.782 |
| 0.75 | 2.9 | 2.26 | 1.43 | 2.39 | 2.56 | 0.447 | 0.148 | 0.662 |
| 1.0 | 3.0 | 2.34 | 1.51 | 2.54 | 2.61 | 0.482 | 0.138 | 0.666 |
|  |  |  |  |  |  |  | $K_{av.}$ = 0.000815 |  |

$\Gamma_{1\infty} = 0.174$, $\Gamma_{2\infty} = 0.189$, $\Gamma_{3\infty} = 0.104$.

## SUMMARY

1. A study of four-cation exchange on Sulfocarbon and Wofatit is described, and Gapon's views on the independent exchange of individual ions in a mixture are generally confirmed.

2. The equation for the exchange of four cations is verified, and satisfactorily constant values are obtained.

3. In all the systems studied an appreciable decrease of pH of the equilibrium solutions was observed both for Sulfocarbon and for Wofatit-P.

4. In contrast to the method of calculation used by Gapon [3], where the value of $\Gamma_\infty$ (adsorption capacity) was found by extrapolation, in our experiments the value of $\Gamma_\infty$ was found experimentally, and was greater than the value for the maximum adsorption of each ion in all cases.

Chemical Research Institute,
Kharkov State University

Received April 8, 1953

# LITERATURE CITED

[1] B.P.Nikolsky and V.I.Paramonova, Prog. Chem., 8, 1535, (1939).

[2] T.F.Antipova-Karataeva, and I.N.Antipov-Karataev, Pedology, No. 1 (1940).

[3] E.N.Gapon, J.Gen.Chem. 3, 6 (1933).

[4] A.T.Davydov and I.Ya.Levitsky, Trans. Chem. Inst., Kharkov State University, 10 (1953).

# THE MECHANISM OF EMULSIFICATION

L.Ya. Kremnev and A.A. Ravdel'

Recently Rebinder [1] developed a concept of the mechanism of emulsification as a process of deformation of large drops of the disperse liquid in the emulsion into cylinders of unstable dimensions. It is assumed that a drop stretched into a cylinder disintegrates spontaneously when the length $l$ of the cylinder exceeds the perimeter of its base, $\pi D$

$$l > \pi D. \tag{1}$$

When condition (1) is satisfied, the surface of the products of disintegration is less than the surface of the original cylinder, which is the cause of the spontaneous disintegration, accompanied by a decrease of surface energy.

This simple and elegant mechanism of dispersion is seen in its purest form in our experiments on the flow of highly concentrated emulsions through capillaries under the influence of a pressure difference [2], that is, in the motion of a structurized system limited by the walls of a capillary. The forcing of such an emulsion through a capillary, even at a low velocity, invariably results in subdivision of the droplets and an increase in the degree of dispersion of the system.

It must be admitted that, on energy considerations, favorable conditions for disintegration may also arise in compression of droplets, which doubtless occurs, for example, during emulsification by rubbing or shaking of liquids or by movement of a spiral (plunger) in an emulsion [3]. Nevertheless, in the elucidation of the mechanism of emulsification, the possiblity of dispersion by compression of the droplets has not been considered thus far.

It must be borne in mind in the examination of irreversible deformation of droplets that the surface of droplets of different radii is always less that the surface of droplets of equal radius if formed in each case form the same large drop. Therefore, deformation by extension or compression must always end in the disintegration of the large drop into droplets of unequal dimensions, since on energy grounds the formation of equal drops is less favorable. Then condition (1) cannot be exclusive, determining uniquely the spontaneous disintegration of the deformed drop. In compression this condition is not applicable, while in extension the critical ratio between $l$ and $D$ will be determined by the dimensions of the droplets formed during disintegration. Evidently, the optimum disintegration conditions may be established by an analysis of the dispersion process.

## Analysis of the Process of Deformation and Spontaneous Disintegration of Drops

1. Let a drop of a pure liquid of volume $V_0$ be deformed into a cylinder of

the same volume, of height $h$ and base radius $a$, and let it break up into 2 droplets of volumes $V$ and $V_1$, with radii $r$ and $r_1$ and surface areas $S$ and $S_1$. The condition of spontaneous disintegration is the decrease of the surface area of the droplets ($S + S_1$) in comparison with the surface area of the cylinder $S_o$, and the corresponding decrease in the store of free energy at constant surface tension, $\sigma$.

Let us determine the ratios between $h$ and $a$ and also between $r$ and $r_1$ for which the most favorable conditions for the spontaneous disintegration of the cylinder are set up.

Assume that

$$h = Ka \text{ and } r_1 = nr, \tag{2 and 3}$$

when $n$ can have any positive value from 0.

The ratio between $S + S_1$ and $S_o$, equal to $\beta = \frac{S + S_1}{S_o}$ (value of $\beta < 1$), determines the possibility of spontaneous disintegration; it is of the form:

$$\beta = \frac{4\pi(r^2 + r_1^2)}{2\pi a(a + h)} \quad \text{or} \quad \beta = \frac{2r^2(n^2 + 1)}{a^2(1 + K)}. \tag{4}$$

Eliminate $r^2/a^2$ from Equation (4); for this put:

$$V_o = V + V_1 \quad \text{or} \quad \pi a^2 h = \frac{4}{3}\pi(r_1^3 + r^3).$$

According to (2) and (3):

$$\pi a^3 K = \frac{4}{3}\pi r^3(n^3 + 1),$$

and therefore

$$\frac{a^2}{r^2} = \left[\frac{4(n^3 + 1)}{3K}\right]^{2/3}. \tag{5}$$

Taking (5) into account, we have from Equation (4):

$$\beta = \frac{2(n^2 + 1)\left[\frac{3K}{4(n^3 + 1)}\right]^{2/3}}{1 + K}, \tag{6}$$

where $\beta$ is expressed as a function of $n$ and $K$.

The limiting value of $\beta$ will be obtained when $\beta' = 0$ and $n = \text{const}$:

$$\frac{2}{3}K^{-1/3}(1 + K) - K^{2/3} = 0, \tag{7}$$

whence $K = 2$.

Since $\beta''$ is less than zero, when $K = 2$ the function is a maximum; that is, for a cylinder height equal to the diameter of the base, $\beta$ has a maximum value for all values of $n$, and under these conditions we have the most unfavorable case of disintegration from the energy viewpoint.

Variations of $\beta$ as a function of $K$, according to Equation (6), are shown in Figure 1 for values of $n$ from 0 to 10, or for droplet volume ratios from 0 to $10^3$.

As is seen from the curves of Figure 1, the value of β is determined by the value of $n$, and increases with decrease of the latter. When $n = 1$, or when the cylinder falls into two droplets of equal radius, β assumes its highest values for all values of $K$, and therefore curve 4 represents the upper limit of changes of β. It is seen from the course of this curve that the cylinder can only disintegrate spontaneously wehn $K < 0.9$ and $K > 5.4$ ($\beta < 1$). When $K = 0.9$ and $5.4$ (Curve 4), and also when $n = 2.08$ and $K = 2$ (Curve 3), the existence of the cylinder and of two droplets resulting from its disintegration are equivalent from the energy viewpoint ($\beta = 1$). Similar points may be obtained also on the intermediate curves between Curves 4 and 3 when $1 < n < 2.08$, but as $n = 2.08$ is approached these points will lie nearer to the maximum value of β.

The optimum conditions for spontaneous disintegration occur when

$$n = 10 \left(\frac{V_1}{V} = 1000\right)$$

and the Curve 1 which corresponds to this case lies below all the other curves. This curve represents the lower limit of changes of β, as when $n = 0$, in conditions of deformation of the drop into a cylinder without disintegration, and when $n \geqslant 1$, when one of the droplets formed has a very small volume $\left(\frac{V_1}{V} \geqslant 1000\right)$, changes of β lie on Curve 1.

Thus, deviations from $K = 2$ in either direction favor disintegration, and, which is very important, the disintegration should be accompanied by the appearance of very small droplets which separate off from the large deformed drops, which is in full agreement with our views (see above). This may be the cause of the formation of Plateau's spherule during detachment of drops.

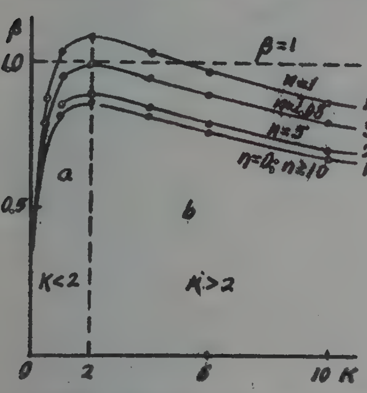

Fig. I. Variations of β as a function of $K$, according to Equation (6) for different values of $n$; a - compression region; b - extension region.

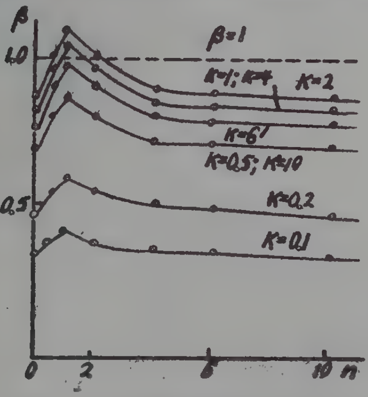

Fig. 2. Variations of β as a function of $n$ according to Equation (6) for different values of $K$.

The maximum value of β marks the boundary of two deformation regions: extension and compression. The right-hand, flatly descending branches of the curves represent extension of the drops. Evidently any value of $K > 2$ permits the spontaneous disintegration of an extended drop, and not only the condition $K > 2\pi$.

The branches of the curves to the left of the maximum, which enclose the compression region, are of special interest. The course of these branches indicates the possibility of transition of the cylinder into an unstable state by compression, that is, when $K < 2$, and this new fact should be taken into account in the study of the mechanism of emulsification. The sharp descent of these branches indicates the possibility of disintegration of the cylinder even at low degrees of compression and at considerably smaller deviations from $K = 2$ than in extension of the droplets. In agreement with the views presented above, the spontaneous disintegration of a drop in conditions of compression will also be accompanied by the appearance of a very small droplet.

The possibility of dispersion by the compression method can be clearly demonstrated by experiments in which a drop of mercury is compressed down to the critical dimensions between two glass plates. In such experiments the splitting off of small droplets may easily be seen. Continuous compression separates off a large number of small droplets of mercury from the flattened drop, so that intensive dispersion is very easily achieved. The result of compression differs significantly in this respect from the result of a single extension of a large droplet, which is accompanied by the separation of one small droplet, after which the extension must be repeated.

Figure 2 shows variations of $\beta$ with $n$ for different values of $K$. It is quite evident from the course of the curves that $\beta$ decreases significantly with increase of $n$ up to $n = 4 - 5$, and attains practically its lowest values when $n = 10$ in conditions both of extension and of compression. It is therefore unlikely that the volumes $V_1$ and $V$ of the droplets formed differ by more than a factor of 1000. Any deviation from $n = 1$ ($\beta$max) already allows the disintegration of a deformed droplet on energy grounds, if $\beta < 1$.

Evidently, the degree of deformation which determines the spontaneous disintegration and which is characterized by the value of $K$, is related to the properties of the liquid drop, but the nature of the relationship needs elucidation.

Therefore, $K > 2\pi$ is not an exclusive condition which determines uniquely the possibility of spontaneous disintegration of an extended drop. Disintegration may also set in at much lower values of $K$, which is confirmed by early work [4], and also when $K < 2$ in conditions of compression of the drop, if this can be achieved.

2. As a result of the action of surface tension forces, the cylindrical droplet will most probably assume the form of an ellipsoid, extended or compressed along its major axis.

Assume for the case of extension

$$\frac{a}{b} = K (K > 1), \qquad (8)$$

where $a$ and $b$ are the major and the minor half-axes of the ellipsoid, respectively.

Let the ellipsoid with volume $V_0$

$$V_0 = \frac{4}{3}\pi ab^2 = \frac{4}{3}\pi K b^3$$

and surface area $S_0$

$$S_0 = 4\pi ab = 4\pi K b^2$$

disintegrate, as before, into 2 drops with volumes $V_1$ and $V$, radii $r_1$ and $r$, and surface areas $S_1$ and $S$.

Retaining the condition (3) $r_1 = nr$, and also taking into account Equation (8), we have for β:

$$\beta = \frac{S_1 + S}{S_0} = \frac{r^2(n^2 + 1)}{Kb^2} . \tag{9}$$

We express β as a function of $n$ and $K$; for this, we eliminate $r^2/b^2$ from Equation (9); and we write

$$V_0 = V_1 + V \text{ or } \frac{4}{3}\pi Kb^3 = \frac{4}{3}\pi r_1^3 + \frac{4}{3}\pi r^3 = \frac{4}{3}\pi r^3(n^3 + 1),$$

and therefore

$$Kb^3 = r^3(n^3 + 1) \quad \text{and} \quad \frac{r^3}{b^3} = \frac{K}{n^3 + 1}. \tag{10}$$

In accordance with Formula (10), the Expression (9) becomes:

$$\beta = \frac{K^{2/3}(n^2 + 1)}{K(n^3 + 1)^{2/3}} = \frac{n^2 + 1}{(n^3 + 1)^{2/3}K^{1/3}} = \gamma K^{-1/3} \tag{11}$$

When $K$ = 1, the drop has its original sperical form and

$$\beta = \gamma = \frac{n^2 + 1}{(n^3 + 1)^{2/3}} \tag{11a}$$

For compression of the drop, $a$ and $b$ are transposed, so that $K = b/a$, and

$$\beta = \gamma K^{1/3}. \tag{11b}$$

In Equations (11) and (11b) the magnitude of γ is determined by the ratio of the droplets formed from the ellipsoid, while the value of $K$ is determined by the conditions necessary for division of the original drop. It seems feasible that a relationship exists between $K$ and $n$; in other words, a droplet separates off from the original drop, the dimensions of the former depending on the degree of deformation of the original drop. However, the nature of the relationship is unknown.

Let us assume that for a given degree of extension or compression of the drop which causes its division, the ratio of the dimensions of the droplets formed may be different. It is easily seen that γ tends to unity when $n \to 0$ and $n \to \infty$. Therefore the function γ should have a maximum value. Investigation by the usual methods shows that when $n = 1$, $\gamma_{max} = 1.26$. This shows that division into 2 drops of equal size (when $K = 1$) is impossible. It is further seen that even when $n = 5$, $\gamma \approx 1.03$, which differs by only 3% from the value of γ when $n \to \infty$. Therefore on energy considerations it is almost immaterial how the division of the original drop took place into two droplets, the radii of which are in the ratios of 5:1, or 10:1, etc. It also follows that as a first approximation our assumption that $n$ does not depend on $K$ is justified.

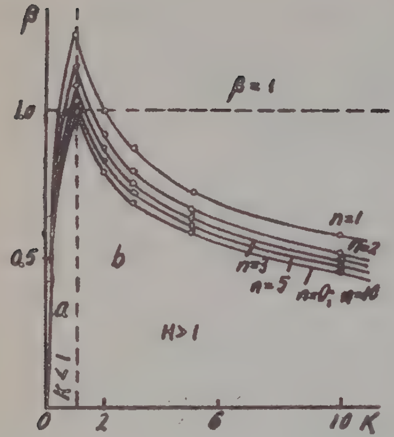

Fig. 3. Variation of β as a function of K, according to Equation (11) for different values of n; a - compression region, b - extension region.

The above is clearly demonstrated by the changes in β according to Equations (11, 11a and 11b), shown in Figures 3 and 4. Comparison of the curves in these Figures with the curves of Figures 1 and 2 confirms that the theoretical conditions of spontaneous disintegration are independent of the shape which the drop assumes on deformation. Deviation from n = 1 in either direction justifies, on energy grounds, disintegration with obligatory appearance both of a large drop and of a droplet of considerably smaller dimensions.

3. We may suppose that the ellipsoidal drop breaks up not into two, but into P droplets (P>2); analysis then leads to the following Expressions:

a) for extension of the drop

$$\beta = \frac{\sum_{1}^{P} n_i^2 + 1}{\left(\sum_{1}^{P} n_i^3 + 1\right)^{2/3}} K^{-1/3}; K > 1 \left(K = \frac{a}{b}\right); \qquad (12)$$

b) for compression of the drop

$$\beta = \frac{\sum_{1}^{P} n_i^2 + 1}{\left(\sum_{1}^{P} n_1^3 + 1\right)^{2/3}} K^{-1/3}; K < 1 \left(K = \frac{b}{a}\right) . \qquad (12a)$$

It is easily seen that when K = 1, and if the resultant droplets are equal in volume

$$n_1 = n_2 = n_3 = \ldots = n_i = n,$$

then changes in β in accordance with Equations (12) and (12a) fall along the upper curve of Figure 4. There is no doubt that if the droplets which are formed from the ellipsoid are unequal, their surface may be less that the surface area of the ellipsoid, and $\beta < 1$, which is the necessary condition for spontaneous disintegration. In any event, in that case also the appearance of small droplets together with large ones is quite obligatory.

4. We will now examine the repeated subdivision of a large drop. The mechanism of such subdivision may be represented as follows: the original drop divides into two drops, a larger and a smaller; the larger drop then divides and a still smaller droplet separates from it, etc., until the larger droplet formed becomes equal in size to the first of the smaller droplets. The conditions then arise for the subdivision of two equal largest drops, as the result of which 4 equal droplets

are formed (together with a number of smaller ones), etc.

We will again assume that the original droplet (ellipsoidal) with volume $V_o$ divides into a larger drop with volume $V'_1$ and a smaller droplet with volume $V$. Since

$$V_o = \frac{4}{3}\pi K b^3 \quad \text{and} \quad V = \frac{4}{3}\pi r^3,$$

then

$$\frac{V}{V_o} = \frac{r^3}{Kb^3}$$

and from Equation (10)

$$\frac{V}{V_c} = \frac{1}{n^3 + 1} = \alpha,$$

and therefore

$$V = \alpha V_o.$$

The first subdivision gives:

$$V_1 = \alpha V_o; \; V_1' = V_o(1 - \alpha);$$

The second subdivision:

$$V_2 = \alpha V_1'; \; V_2' = V_o(1 - \alpha)^2;$$

The m-th subdivision gives:

$$V_m = \alpha V_1'^{(m - 1)}; \; V_m' = V_o(1 - \alpha)^m.$$

Suppose that after the m-th subdivision the larger drop is equal to the first of the smaller droplets formed, then

$$V_m' = V_1 \quad \text{or} \quad V_o(1 - \alpha)^m = \alpha V_o$$

and the number m of the subdivisions which lead to this result is:

$$m = \frac{\log \alpha}{\log(1 - \alpha)} = \frac{\log \frac{1}{n^3 + 1}}{\log\left(1 - \frac{1}{n^3 + 1}\right)} \tag{13}$$

or

$$m \approx \frac{\log \frac{1}{n^3}}{\log\left(1 - \frac{1}{n^3}\right)}, \tag{13a}$$

since the difference between the values of m calculated from Equations (13) and (13a) even when n = 5 is only ~1%.

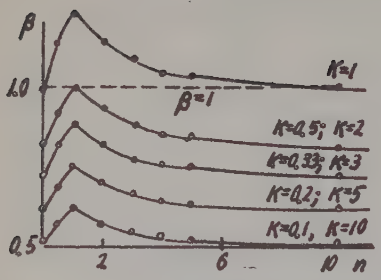

Fig. 4. Variation of β as a function of n, according to Equation (11) for values: K>1 - extension, and K<1 - compression.

The number m of the subdivisions is determined by the value of n, but from energy considerations $\frac{1}{n^3}$ should not exceed approximately 0.1. Some values of m from Equation (13) are shown in Table 1.

These are the more general results of an analysis of the subdivision process of the disperse phase of an emulsion into smaller droplets, without complication by other processes.

TABLE 1

Some Values of the Number of Subdivisions m.

| n | 2 | 3 | 5 | 10 |
|---|---|---|---|---|
| $\frac{1}{n^3}$ | 0.125 | 0.037 | 0.008 | 0.001 |
| m | 18 | 92 | 585 | 7700 |

## Critical Degree of Dispersion of Emulsions

In reality, it is necssary to take into account the opposite process which takes place during mechanical dispersion — coalescence of droplets. Let us examine the conditions for coalescence for different volume ratios between the disperse phase and the dispersion medium in the emulsion. Let $V_1$ = the volume of the disperse phase (benzene); $V_2$ = volume of the dispersion medium (water); $V$ = the volume of a droplet of benzene; $N = V_1/V$ = the total numberof droplets in the emulsion; $\varphi = \frac{V_1 + V_2}{N} = \frac{(V_1 + V_2)V}{V_1}$ = the average fractional volume of a droplet

The ratio of the fractional volume $\varphi$ to the droplet volume $V$ is

$$\frac{\varphi}{V} = \frac{(V_1 + V_2)V}{V_1 V} = \frac{V_1 + V_2}{V_1}$$

and the ratio of the diameter $d_\varphi$ to the diameter $d$ of the droplet is

$$\frac{d_\varphi}{d} = \left(\frac{\varphi}{V}\right)^{1/3} = \left(\frac{V_1 + V_2}{V_1}\right)^{1/3}.$$

It is seen that this ratic is independent of the droplet dimensions.

We now find the ratic $\frac{d_\varphi}{d}$ for different emulsions — from those of maximum concentration, with $V_1 = 99\%$ and $V_2 = 1\%$, to extremely dilute.

|  |  |  |  |  |
|---|---|---|---|---|
| $V_1$ | 99 | 50 | 10 | 1 |
| $V_2$ | 1 | 50 | 90 | 99 |
| $\frac{d_\varphi}{d}$ | 1.003 | 1.27 | 2.16 | 4.65 |

It is seen that in 99% emulsion the thickness of the layers of the dispersion medium between the droplets is only 0.003 of the droplet diameter. For droplet dimensions of approximately $10^{-5}$ cm the layer has a thickness of the order of the dimensions of a single molecule, so that even the formation of a protective layer of stabilizer is impossible. Displacements of such small droplets by Brownian movement should easily cause them to touch and coalesce. But for droplets of the order of approximately $10^{-4}$ cm in size, the thickness of the layers already reaches the dimensions of ten molecules, and the attachment of protective layers on the droplets and the formation of a stable emulsion becomes possible. It therefore follows that the smallest droplet dimensions in emulsions of maximum concentration should be about $10^{-4}$ cm.

In less concentrated emulsions, for example, 50%, the layer of the dispersion medium, with droplets of about $10^{-5}$ cm, has a thickness of the order of hundreds of molecules, and such an emulsion should be stable. In the same way, dilute emulsions of a greater degree of dispersion should be stable. To solve these problems, we will determine the coalescence rates of droplets in emulsions, on a basis of the theory of coagulation of colloidal solutions.

According to Smolukhovsky, the coagulation of monodisperse particles is described by the Equation

$$\varphi - \varphi_0 = K\tau_c, \qquad (14)$$

where $\varphi_0$ and $\varphi$ are, respectively, the initial and the final fractional volumes; $\tau_c$ is the time of coagulation, and K is the coagulation rate constant:

$$K = \frac{4kT}{3\eta},$$

where k is the Boltzmann constant; T is the temperature; $\eta$ is the viscosity of the dispersion medium (water).

At room temperature ($T = 298°$)

$$K = 5.5 \cdot 10^{-12}\ \text{cm}^3/\text{sec and } \tau_c \approx 1.8 \cdot 10^{11}(\varphi - \varphi_0)\text{sec}. \qquad (15)$$

According to Equation (14), the coagulation time depends not on the particle dimensions, but on the fractional volume. If the amount of the disperse phase is kept constant and the number of particles variable, the total number of particles (and the fractional volume) will be determined by the particle dimensions. In that case the coagulation time will depend on the particle dimensions. We shall calculate the coagulation time in the course of which the particle radius will increase 10 times, and, consequently, the fractional volume will increase 1000 times. Then in Equation (15) we may neglect $\varphi_0$ in comparison with $\varphi$, which corresponds to the larger particles fromed by coagulation, which gives

$$\tau_c = 1.8 \cdot 10^{11}\varphi. \qquad (15a)$$

In polydisperse systems coagulation proceeds at a somewhat greater rate, while on stirring it proceeds considerably more rapidly than in a medium at rest.

In that case the rate of coagulation depends on the rate of stirring, and in emulsification the coagulation time of the droplets will be less than that calculated from Equation (15a).

Let us examine the coalescence of droplets in the formation of emulsions of limiting concentration, as studied previously by us [5], when the concentration of the disperse phase was practically 99%, and also in the formation of less concentrated emulsions. If we assume the possibility of subdivision of the droplets of the disperse phase down to $r = 10^{-6}$ cm, it is possible with the aid of Equation (15a) to determine the coalescence rates of droplets of different dimensions from the data of Table 2.

TABLE 2

Coalescence Time of Droplets in Concentrated Emulsions

| r, cm | Concentration 99% | | Concentration 10% | | Concentration 1% | |
|---|---|---|---|---|---|---|
| | o<br>$cm^3$/particle | $\tau_c$<br>sec | o<br>$cm^3$/particle | $\tau_c$<br>sec | o<br>$cm^3$/particle | $\tau_c$<br>sec |
| $10^{-6}$ | $4.2 \cdot 10^{-18}$ | – | $4.2 \cdot 10^{-17}$ | – | $4.2 \cdot 10^{-16}$ | – |
| $10^{-5}$ | $4.2 \cdot 10^{-15}$ | $7.6 \cdot 10^{-4}$ | $4.2 \cdot 10^{-14}$ | $7.6 \cdot 10^{-3}$ | $4.2 \cdot 10^{-13}$ | $7.6 \cdot 10^{-2}$ |
| $10^{-4}$ | $4.2 \cdot 10^{-12}$ | $7.6 \cdot 10^{-1}$ | $4.2 \cdot 10^{-11}$ | 7.6 | $4.2 \cdot 10^{-10}$ | $7.6 \cdot 10$ |
| $10^{-3}$ | $4.2 \cdot 10^{-9}$ | $7.6 \cdot 10^{2}$ | $4.2 \cdot 10^{-8}$ | $7.6 \cdot 10^{3}$ | $4.2 \cdot 10^{-7}$ | $7.6 \cdot 10^{4}$ |

As is seen from Table 2, droplets $10^{-6}$cm in size coalesce practically instantaneously, regardless of the concentration of the emulsion; but to increase the size of a droplet by coalescence from 0.1 to 1 $\mu$ (even without stirring) requires very little time, and the time becomes appreciable only for 1% emulsions ($\tau_c = 76$ sec); on the other hand, $\tau_c$ rises considerably with further increase of droplet dimensions.

It was shown in Table 1 that 18 - 585 consecutive divisions are required to diminish a large droplet to the dimensions of the first small droplet split off. However short the time required for this might be, it definitely exceeds the coalescence time of droplets of size $< 1 \mu$ in emulsions of high and lower concentrations.

Consequently, all such droplets will coalesce. This has the important consequence that apparently it is impossible to achieve any lengthy lifetime for droplets appreciably less than 1 $\mu$ in the emulsification process.

Since the droplets $< 1 \mu$ will coalesce vigorously, the increase of the specific surface of the droplets will diminish sharply. This conclusion is in full agreement with our experimental results [6], according to which the specific surface of the droplets increased only 4.6 times during supplementary shaking of a polydisperse highly concentrated emulsion for 249 sec at a constant rate ($m = 600$). On the other hand, in the absence of coalescence the specific surface should increase several tens of times in such conditions. It is also interesting that in these experiments the degree of dispersion soon reached a very high value and the maximum on the curves showing the size distribution of the droplets was at $d = 1 \mu$, and about 94% of the droplets had these dimensions.

Up to now we confined ourselves to a study of the disintegration and coalescence of droplets of pure liquid in a pure dispersion medium. The presence of a surface-active stabilizer in the latter, however, cannot prevent the coalescence of droplets smaller than 1 μ. As is known from surface tension measurements, a considerable time is required for the adsorption of stabilizer molecules at the interphase boundary, which is caused by the low rate of diffusion of the molecules from the bulk of the dispersion medium toward the surface of the droplets. For soaps and also for high-molecular stabilizers the time of formation of the adsorptional layer is minutes of even tens of minutes [7]. Consequently, for droplet dimensions of the order of 1 μ, the time for adsorption of the stabilizer becomes commensurable with the rate of coalescence, and such droplets become stabilized.

Stirring increases the rate of coalescence and the rate of diffusion of the stabilizer to approximately the same extent. Therefore, the conditions of fixation of the adsorptional layer on the droplet surfaces remain the same, and droplets $<1$ μ cannot become stabilized.

The net result of the disintegration and coalescence processes, which act in the opposite directions, should be the formation of a relatively monodisperse emulsion with droplets of the order of 1 μ in size. It is just in droplets of this critical size that the possibility of stabilization and dying down of coalescence first appears. Our experimental data on the stabilization of w/o and o/w emulsions of limiting concentrations [5,8] fully confirm this conclusion. In such emulsions the content of droplets of $\sim 1$ μ in size is usually over 90%. A similar state of affairs is found for many other less concentrated emulsions [9].

## Aging of Emulsions

Experiment shows that completely stabilized emulsions are subject to aging, during which the droplets increase in size. In accordance with what was said above, coalescence in aging emulsions is practically impossible, owing to the fact that the droplets are coated by continuous protective layers. However, this does not exclude a process analogous to isothermal distillation of the droplets.

To study such a process let us assume that the droplets of the disperse phase and the dispersion medium are mutually saturated solutions. The concentration of the dispers phase at the droplet surface should be increasingly supersaturated with decreasing droplet diameter. As a result of this, diffusional flow takes place from the surfaces of the small droplets to the surfaces of the larger drops, and the disperse phase substance condenses on the latter.

In accordance with the Gibbs-Thompson Equation we may write

$$\ln \frac{c_r}{c_o} = \frac{2\sigma M}{RTr\delta}, \qquad (16)$$

where $c_r$ is the supersaturation concentration of the disperse phase at the surface of a drop of radius $r$; $c_o$ is the saturation concentration in the bulk of the dispersion medium; $\sigma$ is the surface tension at the interphase boundary; $M$ and $\delta$ are the molecular weight and the density of the disperse phase, respectively.

The rate of dissolution of a droplet may be likened to the rate of evaporation in a medium at rest:

$$\Delta m = 4\pi r D(c_r - c_o) \text{ g/sec}, \tag{17}$$

where $\Delta m$ is the rate of dissolution from the whole surface of the drop, and $D$ is the coefficient of diffusion of the droplet substance in the dispersion medium.

Substitution of $c_r$ from Equation (16) into (17) gives:

$$\Delta m = 4\pi r D c_o\left(e^{\frac{2\sigma M}{RTr\delta}} - 1\right). \tag{18}$$

By introducing the mass of the drop $m = \frac{4}{3}\pi r^3\sigma$, we obtain:

$\Delta m = -4\pi r^2\delta\frac{dr}{d\tau_n}$ ($\tau_n$ is the time of isothermal distillation) and

$$-4\pi r^2\delta\frac{dr}{d\tau_n} = 4\pi r D c_o\left(e^{\frac{2\sigma M}{RTr\delta}} - 1\right).$$

Since the values of $\sigma$, $M$, and $\delta$ for the usual liquids which form the disperse phase of emulsions are such that $\frac{2\sigma M}{RTr\delta} < 1$, up to $r = 10^{-6}$ cm, it is possible to resolve the exponent into a series, and take only the first two terms. Then

$$-4\pi r^2\delta\frac{dr}{d\tau_n} = 4\pi r D c_o\frac{2\sigma M}{RTr\delta}$$

or

$$-r^2 dr = \frac{2\sigma M D c_o}{RT\delta^2}d\tau_n. \tag{19}$$

Integration of Equation (19) in the limits $r_o(\tau_n = 0)$ to $r$ at $\tau_n$, gives

$$\tau_n = \frac{RT\delta^2}{6\sigma M D c_o}(r_o^3 - r^3). \tag{20}$$

Let us apply Equation (20) to emulsions of benzene in water. In this case $\sigma = 35$ dyne/cm; $c_o \simeq 7.10^{-4}$ g/cm$^3$ when $T = 298°$. The coefficient of diffusion of benzene in water is taken as $D = 1$ cm$^2$/day (by analogy with oxalic acid or phenol at concentrations $2.5 \times 10^{-3} - 8 \times 10^{-3}$ g/cm$^3$); then

$$\tau_n = 1.38 \cdot 10^9(r_o^3 - r^3) \text{ days}. \tag{20a}$$

If $r = 0.1r_o$ (the drop dimensions decrease 10 times during dissolution), then we have from Equation (20a): $\tau_n = 1.38 \cdot 10^9 r_0^3(1 - 0\ 001) \approx 1.38 \cdot 10^9 r_0^3$ days, and for droplets with different values of $r_0$, the intitial dimensions, $\tau_n$ will be

| $r_0$ cm | $1 \cdot 10^{-5}$ | $1 \cdot 10^{-4}$ | $5 \cdot 10^{-4}$ | $1 \cdot 10^{-3}$ |
|---|---|---|---|---|
| $\tau_n$ | 0.12 sec | 2 min | 4 hours 10 min | 1.38 days |

These results show that droplets of initial radius $r_0 = 10^{-5}$ cm distil into larger drops in a fraction of a second, while droplets with radius of the order of 1 $\mu$ require a time measured in minutes and hours. This value is less than the true time, as the presence of an adsorptional layer not only decreases $\sigma$, which is taken into account in Equation (20a), but it also decreases the whole exponent by a value which depends on the surface charge. However, this value cannot decrease the exponent significantly and affect the found values of $\tau_n$ appreciably.

Our results for emulsions are in agreement with the theoretical views, developed by Todes, on the increase of the size of sol particles, and the corresponding calculations for aerosols [10].

It follows from all the above that, for a radius of the order of 1 $\mu$, the rate of distillation of droplets is commensurable with the rate of their coalescence. Therefore, the increase in size of the droplets may proceed by these two routes in different ratios, until the droplets reach the critical size. Coalescence then ceases as the particles become coated with protective layers. At the same time, increase in the size of the droplets, even if retarded, should undoubtedly occur during aging of emulsions, which results in a decrease of the degree of dispersion of the latter.

## SUMMARY

1. Deformation of droplets of the disperse phase of an emulsion, favorable for spontaneous disintegration, may result both from extension and from compression at different ratios between the dimensions of the deformed droplets.

2. The droplets formed by the spontaneous disintegration of deformed drops are unequal in size.

3. Simultaneously with the disintegration of large drops, coalescence of small droplets of dimensions up to 1 $\mu$ takes place. In addition to coalescence, isothermal distillation of droplets may also lead to increase in the size of the small droplets.

4. Droplets which attain 1 $\mu$ in size become stabilized when the rate of adsorption oi the stabilizer becomes commensurable with the rate of coalescence of the droplets.

5. Both highly concentrated and also other emulsions have a characteristic critical degree of dispersion, which corresponds to a droplet size in the region of $\sim 1 \mu$.

6. When the critical degree of dispersion is reached, isothermal distillation of the droplets does not cease, which to some extent explains the fall in the degree of dispersion of emulsions during aging.

7. In the industrial production of emulsions it should be taken into account that the formation of highly disperse emulsions of the critical degree of

dispersion can be achieved in certain conditions of mechanical dispersion.

The Lensoviet Institute of Technology
Leningrad

Received February 21, 1953

## LITERATURE CITED

[1] P.A.Rebinder, Colloid J., 8, 157 (1946); article in "Colloids in the Food Industry", Moscow, Food Industry Press (1949).

[2] L.Ya.Kremnev and S.A.Soskin, Colloid J., 10, 209 (1948); L.Ya.Kremnev and V.S.Kuprik, Proc. Acad. Sci., USSR, 80, 623 (1951); Colloid J., 14, 98 (1952).[1]

[3] L.Ya.Kremnev, Proc. Acad. Sci., USSR, 79, 655 (1951); Colloid J., 13, 394 (1951); S.E.Bresler, M.D.Kats, and L.Ya.Kremnev, J.Phys. Chem., 5, 602 (1934).

[4] Lederer, Wien. Ber. 121, 17, (1912).

[5] L.Ya.Kremnev et al, J. Gen. Chem., 16, 2004, (1946); Trans. Leningrad Inst. Tech., 13, 110 (1947); Colloid J., 9, 269 (1947); 10, 18 (1948); 10, 436 (1948).

[6] L.Ya.Kremnev and S.A.Soskin, Colloid J., 9, 269 (1947).

[7] Harkins and Zollman J. Am. Chem. Soc. 48, 69 (1926); P.A.Rebinder, and N.N.Petrova, Bull. Acad. Sci. USSR, Chem. Ser., 4-5, 1085 (1937); K.F.Zhigach and P.A Rebinder, J. Phys Chem, 13, 94 (1939).

[8] L.Ya.Kremnev and N.I.Kuibina, Colloid J., 13, 38 (1951).

[9] Clayton, Emulsions. Moscow (1950).

[10] O.M.Todes, Problems of Kinetics and Catalysis, v.7, p.137, Academy of Sciences USSR Press, Moscow (1949).

---

[1] See Consultants Bureau Translation, p. 107.

# STRUCTURAL- MECHANICAL PROPERTIES OF ENAMEL

G.V. Kukolev and L.D. Svirsky

Enameling is effected by applying enamel slip to a metal base followed by firing till it melts. The slip essentially consists of a suspension, the disperse phase of which is made up of polydisperse particles of enamel frit and clay. The dispersion medium is water containing electrolytes.

We studied the relationship $v = f(P)$ for enamel slips, where $v$ is the rate of efflux, and $P$ is the force, by determining the rate of efflux of the slip from a tube or by lowering the perforated plate of a mobilometer, under the influence of weights of columns of the slip or of loads, respectively. It was proved [1] that enamel slips of normal concentrations are characterized by a dynamic limiting shear stress $\theta_d$ and by mobility; these properties may, to a certain extent, be used to describe the covering behavior of such slips.

However, the results of these studies did not give a sufficiently complete concept of the rheological characteristics of enamel slips. As is known, $\theta d$ is found not only in plastic bodies with anomalous viscosity, which have also a static limiting shear stress, $\theta_s$ (Shvedov bodies), but also in pseudoplastic bodies, which do not have $\theta_s$ and also in Bingham-Volarovich bodies, in which $\theta_d$ and $\theta_s$ coincide [2]. We therefore carried out an investigation to determine the form of the rheological curves of enamel slips, and to determine the class of bodies to which they belong.

The true values of $\theta_s$ and $\eta'$ (structural viscosity) were determined with a coaxial cylinder viscosimeter of the Volarovich type [3].

To determine that slips have properties characterized by $\theta_s$ and $\eta'$, and to show that these values do not depend on the experimental conditions, we used the methods, the theory and application of which were developed by Volarovich and Tolstoi [3]:

1. When the slip under investigation fills the annular space between the inner (stationary) and the outer (rotating) cylinders of the apparatus, and when the outer cylinder rotates under the influence of the moment set up by the minimum load $P_0$ (which just commences rotation), the following relationship should be satisfied:

$$P_0gR = 2\pi r_0^2h\theta_s \tag{1}$$

where $g$ is the acceleration due to gravity, $R$ is the radius of the flywheel of the apparatus which imparts rotation to the outer cylinder, $r_0$ is the radius of the inner cylinder, $h$ is the height of the portion of the inner cylinder immersed in the slip; in this case $\theta_s$ is determined from the weight of the minimum load $P_0$. The condition $\theta_s$ = const may be verified by using inner cylinders of different diameters.

2. If the moment which causes the outer cylinder to rotate is set up by a given load $P$, then the following relationship holds:

$$PgR = 2\pi r^2h\theta_s , \tag{2}$$

where $r$ is the radius to which the flow of the slip in the apparatus reaches. In these conditions $\theta_s$ is determined from the value of $r$ for a given value of $P$. The conditior $\theta_s$ = const will hold if Equation (2) is found to be valid for different values of $P$.

3. When $\theta_s$ = const, the following relationship should exist:

$$\theta_s = \frac{g^R}{2\pi h} \cdot \frac{P_0}{r_0^2} = \frac{g^R}{2\pi h} \cdot \frac{P'_0}{r'^2_0} = \frac{g^R}{2\pi h} \cdot \frac{P}{r^2} = \text{const}, \qquad (3)$$

where $P_0$ and $P_0'$ are the loads which correspond to the start of rotation of the outer cylinder for different values $r_0$ and $r_0'$ of inner cylinder radii. It follows from Equation (3), that

$$\frac{P_0}{r_0^2} = \frac{P'_0}{r'^2_0} = \frac{P}{r^2} = \text{const}. \qquad (4)$$

This may be verified by determining the constancy of the ratio $P/r^2$ for different rotating loads $P$ (for a given radius $r_0$ of the inner cylinder), or of the values of $r_0$ for the same load $P$, and also by determining the constancy of the ratio $P_0/r_0^2$ for different values of $r_0$.

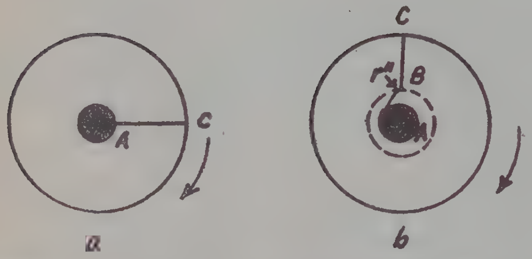

Fig. 1. Scheme of observation of the distribution of flow rates of the slip.

In addition to the above, to determine whether enamel slips obey the laws of plastic flow for Bingham-Volarovich bodies, it is necessary to determine values of $\eta'$ and to verify the condition $\eta'$ = const. For this we used the equation for plastic flow in the form deduced by Volarovich for the coaxial cylinder apparatus:

$$\eta' = \frac{\theta_s \left( \frac{P - P_0}{P_0} - \ln \frac{P}{P_0} \right)}{2\,\omega}, \qquad (5)$$

where $P$ is the load which rotates the outer cylinder with an angular velocity $\omega$. Equation (5) is valid for conditions when flow does not extend to the outer cylinder, which we observed in a study of the distribution of flow rates of slips in the annular space between the inner and the outer cylinders even for large values of $\omega$.

The values of $r$ at a given rotating load were determined by applying to the surface of the slip in the apparatus a thin strip AC (Figure 1, a) of white kaolin suspension, which showed clearly on the darker background of the slip. After rotation of the outer cylinder the strip stretched and assumed the outline shown in Figure 1, b.[1] The region between the points B and C represented the rotation of the slip as a " solid", with an angular velocity equal to that of the outer cylinder. The dotted line represents the limit of the spread of the "liquid" phase, exact determination of the radius of which was made difficult by the smooth passage of the Curve ABC along a certain radius r'' from the region of flow into the region of steady rotation of the slip. Therefore the results of experiments based on measurement of the radius r were less accurate than those obtained by other methods. All the methods enumerated above were used.

---

[1] A similar effect was observed by Volarovich and Tolstoi in their study of clay suspensions [3].

The substances studied were two acid-resisting and one ground-coat enamel on steel; the chemical composition is given in the Table.

TABLE

Chemical Composition of Enamels for Steel in %

| Enamel | $SiO_2$ | $TiO_2$ | $Al_2O_3$ | CaO | $K_2O$ | $Na_2O$ | $B_2O_3$ | $CaF_2$ | $MnO_2$ | CoO | NiO |
|---|---|---|---|---|---|---|---|---|---|---|---|
| Cover coat, acid-resisting, I . . . . | 61.3 | 5.0 | 2.0 | 5.0 | 5.1 | 18.2 | 1.0 | 2.4 | – | – | – |
| Cover coat acid-resisting, II . . | 57.3 | – | 6.6 | – | 4.3 | 14.5 | 4.5 | 5.4 | 7.4 | – | – |
| Ground Coat | 52.8 | – | 7.0 | – | 4.6 | 15.3 | 12.4 | 6.1 | – | 0.9 | 0.9 |

To obtain slips of varying consistency, different amounts of $MgSO_4$ were added. The specific gravity of the slips was kept within the range 1.73-1.74, for a fineness of grinding corresponding to approximately 18% residue on a No. 80 screen. Chasov-Yar clay (Chl) was added to the mill, to give 4% of the weight of granulate and clay.

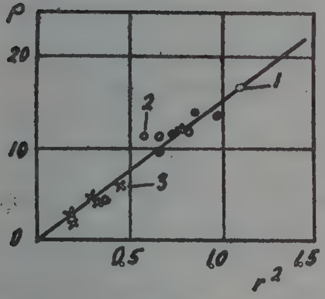

Fig. 2. Dependence of the square of the radius of spread of flow of enamel slip in the coaxial cylinder apparatus, on the loads P which rotate the outer cylinder; 1 - $r_0$ = 0.42 cm; 2 - $r_0$ = 0.55 cm; 3 - dependence of $P_0$ on $r^2_0$.

The results of the check of the validity of Equation (4) in the case of enamel slip are shown graphically in Figure 2, which shows the dependence of the square of the radius of spread of flow, r, on the loads P which rotate the outer cylinder. This dependence is shown for two values for the radius of the inner cylinder: when $r_0$ = 0.42 cm and when $r'_0$ = 0.55 cm. The dependence of $P_0$ on $r_0^2$ is shown in Figure 2. It is seen that within the limits of accuracy of the measurements, the values are in a linear relationship, which serves as a proof that such slips have a static limiting shear stress the value of which is constant.

Figure 3 shows the results of determinations of the values of $\theta_s$ and of verification of the relationship $\theta_s$ = const according to Equation (3), from measurements of $P_0$ for different dimensions of the inner cylinder, and from determinations of r for different loads P; the following notation is used in the Figure: $\theta_{P_0} = \theta_s$ determined from $P_0$; $\theta_r = \theta_s$, determined from r.

The calculations which were made when the graphs were plotted showed that the average error in the determination of the limiting shear stress from values of r (for given values of P and $P_0$) lies in the limits 1.5 - 14.2%. The greatest error, as was to be expected, was in the determination of $\theta_r$.

In these error limits, the values of $\theta_s$ for the slips remained constant independently of the experimental conditions, as we verified for the range of absolute values from 65 to 325 dynes/cm$^2$. The above inaccuracy of the determinations, apart from the reason given, is also explained by the impossibility of achieving, in practice, completely identical conditions of preparation of the slips, and their high sensitivity to these conditions.

With regard to the structural viscosity coefficient $\eta'$, it was established that the relationship $\eta' = \text{const}$, calculated from Formula (5) is valid only in the range of relatively low values for the rate of rotation of the outer cylinder. Figure 4 shows the results for acid-resistant cover coat enamel slip I. Curves 1, 2, and 3 represent $\eta' = f(\omega)$ for the slips, corresponding to values of $\theta_s$ equal to 181 (slip with normal covering properties), 232, and 320 dynes/cm$^2$, respectively.

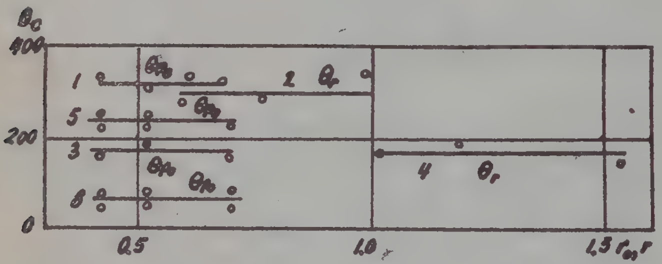

Fig. 3. Static limiting shear stress $\theta_s$ for acid-resistant enamel slips I and II, with the following $MgSO_4$ contents per 100 cm$^3$ of the slip: 1 and 2 - 0.984 g (enamel II); 3 and 4 - 0.738 g (enamel II); 5 - 1.23 g (enamel I), 6 - without electrolyte (enamel I).

For all these values of $\theta_s$ in the angular velocity range of $\omega \approx 2$-3 rev/sec, the value of $\eta'$ increases only insignificantly. The viscosity increases considerably with increasing rate of rotation of the outer cylinder. For angular velocities to the left of $\omega = 2$ (Figure 4), it may be expected that the values of $\eta'$ for these slips will remain constant down to the minimum velocities at which the effect of structure becomes apparent.

Increase of $\eta'$ with $\omega$ was observed also for slips of cover coat II and ground coat enamels. For example, an increase of $\omega$ from 6.73 to 15.8 rev/sec corresponded to an increase of $\eta'$ from 13.7 to 34.4 poises, and as $\omega$ increased from 6.73 to 23.7 rev/sec, $\eta'$ increased from 20.87 to 48.78 poises.

Increase of the values of $\eta'$ when a definite rate of rotation is reached is explained by the transition from a laminary to a turbulent flow regime, when the ratio $P/\omega$ begins to increase, and $Re > Re_{cr}$. The commencement of turbulent flow at relatively low flow rates of enamel is caused by the action of particles of the disperse phase, irregular in form, which produce eddying.

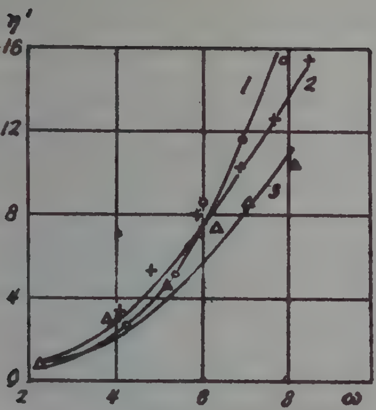

Fig. 4. Curves for the relationship $\eta' = \underline{f}(\omega)$ for enamel slips, for values of $\theta_s$ equal to: 1-181; 2-232; 3-320 dynes/cm$^2$.

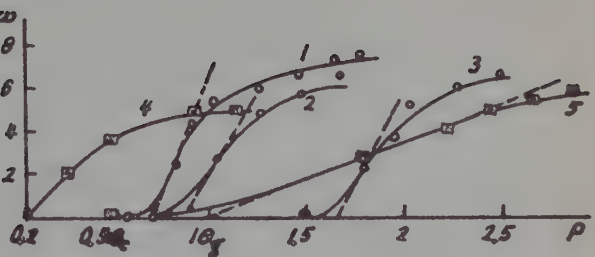

Fig. 5. The relationship $\omega = \underline{f}$ (P) for acid-resistant enamel slip I with different values of $\theta_s$ : 1-181; 2-232; 3-320 dynes/cm$^2$ ($\eta'$ from 2.47 to 8.56 poises); 4-33 dynes/cm$^2$; 5-the same, for slips with a viscosity of 21.2-27.4 poises.

These results agree with the data of Rebinder [4], according to which turbulent flow in disperse systems commences for values of $Re_{cr}$ which are smaller by a factor of 10 or more than $Re_{cr}$ for true structureless liquids. This was verified by determination of $\omega_{cr}$ (critical velocity corresponding to the commencement of turbulent flow) for varying degrees of grinding of the enamel slip. As the particle size decreases, their eddying influence should decrease, and $\omega_{cr}$ should increase; this was found to be so. For example, for a fineness corresponding to 0% residue on a No. 80 screen, $\eta'$ remained constant, within the limits of experimental error, for angular velocities of 3.5-5.5 rev/sec, which was considerably higher than in experiments with coarser slip - 18% residue on a No. 80 screen. In the latter case, as is seen from Figure 4, the viscosity remained approximately constant at velocities not in excess of 2-2.5 rev/sec.

Variation of the value of $\eta'$ in the flow of enamel slip produces yet another factor which opposes turbulence. While turbulence of flow causes $\eta'$ to rise, the second factor - the influence on $\eta'$ of the disruption of the structure of the dispersion medium - decreases the value.

The following possible cases arise from this:

1. $\theta_s$ is small. Considerable disruption of structure takes place, even at small values of the angular velocity $\omega$, with liberation of a large amount of dispersion medium. The disperse particles become capable of disorderly progressive and rotatory motion, as their concentration decreases. This leads to relatively early commencement of turbulent flow. In that case the predominant action of the tubulency of the stream affects the increase of $\eta'$, as against the opposing action of disruption of structure, even at small values of $\omega$, which results in low values of $Re_{cr}$.

2. $\theta_s$ is large. In this case the predominant influence of the eddying action of the particles on the increase of $\eta'$, as against the opposing action of the dispersion medium liberated by disruption of structure, takes effect at higher velocities than in the previous case, which leads to higher values of $\omega_{cr}$.

The above was confirmed experimentally. For example, $\omega_{cr}$ for an enamel slip with $\theta_s = 132$ dynes/cm$^2$, was approximately 3.5 rev/sec. The critical rotation of the slip, $\theta_s = 33$ dynes/cm$^2$ was not reached even at 2 rev/sec. An increase in the values of $\omega_{cr}$ was observed also with an increase of the structural viscosity of the slips.

Figure 5 shows Curves 1, 2, and 3 for the relationship $\omega = \underline{f}(\underline{P})$ and also curves for the same relationship for slips with the low value of $\theta_s = 33$ dynes/cm$^2$ (Curve 4) and with a viscosity value within fairly high limits, 21.2-27.4 poises (Curve 5).

It may be concluded from Figure 5, as from the other results given above, that enamel slips, within limits of relatively high values of their limiting shear stress (Curves 1, 2, 3, and 5), are bodies characterized by presence of $\theta_s$, $\theta_d$, and a constant value of $\eta'$ (the latter within certain limits of flow speeds, but within the limits of laminar flow). Enamel slips are also characterized by the presence of two elastic deformations: one below the static limiting shear stress, that is, before disruption of structure, and the other above $\theta_s$. It follows that enamel slips may be classed as elastic - plastic bodies (Shvedov bodies) and may be described by the following qualitative model [2], shown in Figure 6. It must be taken into account that the region $\eta' =$ const is maintained within comparatively narrow limits of velocities, because of the rapid transition of laminar flow into turbulence (the portions of the Curves 1, 2 and 3 which coincide with the dotted lines in Figure 5). However, in conditions which favor increase of $\omega_{cr}$ (increase in the values of $\eta'$, fineness of grinding of the slip, and increase of the values of $\theta_s$) the region $\eta =$ const should be widened (Curve 5, Figure 5).

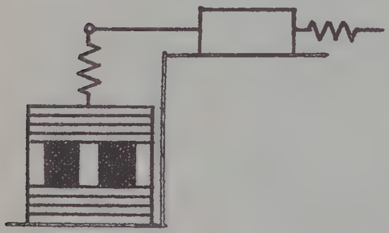
Fig. 6. Qualitative model of an elastic-plastic body.

At fairly low values of $\theta_s$ and $\eta'$ (compare Curves 4 and 5, Figure 5), because of the absence of elastic deformations above $\theta_s$ the region $\eta' =$ const, if it exists, persists only at very low values of angular velocity

When the enamel slip is applied (by immersion, pouring, or spraying) it is necessary to maintain conditions of regular spreading on the surface and of the formation of a layer of definite thickness. It is necessary to try to achieve these conditions with a minimum shaking of the enameled article when the slip is applied. This will be achieved more fully as the slip becomes less viscous, and with increasing agreement between $\theta_s$ and the necessary thickness of the layer of slip left on the article. If $\eta'$ of the slip is high, then a consequence will be that it will flow off the article slowly and irregularly in the conditions and in the time in which the process takes place. This will occur even if $\theta_s$ satisfies requirements. Slip which remains on the article in an irregular thick layer will continue to flow off after application. This effect, often observed in practice, results in reject goods ("secondary slippage"). Unfortunately, this fault is still being wrongly attributed to decreased viscosity of the slip.

If, at the minimum value of the structural viscosity of the slip, its static limiting shear stress exceeds a certain definite value, this should result in an excessively thick layer of applied enamel, which will lead to peeling off or to appearance of cracks in the coating. On the other hand, at low viscosities the thickness of the applied layer of slip will decrease with decreasing values of the static limiting shear stress. This may, in the final analysis, explain the appearance of breaks in the freshly applied layer, its slippage, especially near the edges of the article, and other faults caused by an abnormally thin coating.

According to our measurements, the values of the static limiting shear stress of slips with normal coating properties lay between the limits 110-180 dynes/cm$^2$. The viscosity at the critical velocity was of the order of 1 poise, and at $\omega$ which corresponded approximately to the spreading velocity of the slip on the article (about 30 cm/sec), it was of the order of 15 poises.

## SUMMARY

1. It is established that enamel slips are elastic-plastic bodies (Shvedov bodies).

2. It is established that the condition $\eta'=$ const for enamel slips is maintained only within narrow limits of flow velocities. The explanation, on the one hand, is the relatively early commencement of turbulent flow, when viscosity increases with velocity, and on the other hand, by the existence of a region of elastic deformations produced by forces somewhat in excess of $\theta_s$. In this region viscosity decreases with increasing velocity.

3. The covering properties of enamel slips may be characterized by the values of the static limiting shear stress and the viscosity; the latter, within the limits of flow velocities attained in practical conditions.

4. The values of the static limiting shear stress for a series of enamel slips, and the values for their viscosities at different flow velocities, have been determined. The values of static limiting shear stress of enamel slips with normal covering properties were in the limits of 110-180 dynes/cm$^2$. The viscosity of these slips varied from a value of the order of 1 poise at the critical velocity, to 15 poises at rotation velocities of the outer cylinder of the apparatus, approximately corresponding to the spreading rate of the slip on the article during application.

5. It is experimentally shown that the value of the critical flow velocity of enamel slips depends on the fineness of grinding, value of the static limiting shear stress, and the viscosity.

The V.I.Lenin Polytechnic Institute,
Kharkov

Received January 14, 1953

## LITERATURE CITED

[1] G.V.Kukolev and L.D.Svirsky, Trans. Lenin Polytech. Inst. Kharkov, 1, Chem. Tech Series, No. 1 (1952).

[2] G.I.Fuks, Viscosity and Plasticity of Petroleum Products, State Technology Press, p. 25 (1951).

[3] M.P.Volarovich and D.M.Tolstoi, J.Phys.Chem., 4, No.6, 815 (1933).

[4] Paper by P.A.Rebinder, see N.A.Tsurinov, Knowledge Concerning Clays and Clay Suspensions Used in Boring for Oil, p.103 (1940).

# STRUCTURE AND PROPERTIES OF LOADED RUBBER MIXTURES

## XII. DIELECTRIC PROPERTIES OF CARBON BLACK MIXTURES WITH NATURAL RUBBER

A.I. Lukomskaya and B.A. Dogadkin

In a study of the influence of the ability of carbon black to form structures on the dielectric properties of sodium butadiene rubber, we established [1,2] that the principal changes of properties on loading are related to the nature of the intermolecular action in the mixture, both between the rubber and the filler, and between the particles of the filler itself. The effect of intermolecular action in the rubber phase, or, in other words, the influence of the choice of rubber type, was not studied. At the same time, it is known [3] that rubbers may be divided into two classes by their behavior on filling: 1) rubbers which crystallize on stretching; and 2) rubbers which do not crystallize. The first of these classes gives vulcanizates which are sufficiently strong without filler, and which are not greatly reinforced by fillers; the second class requires reinforcement. The sodium butadiene rubber studied by us [1,2] belongs to the second group of rubbers (non-cyrstallizing), the properties of which are affected significantly by addition of filler. It appeared of interest to carry out a study of the dielectric properties of mixtures with rubbers of the crystallizing type. Natural smoked sheet rubber was chosen for the study.

The characteristics of the carbon blacks used in the investigation are given in our previous paper [1]. As previously [1,2], the non-vulcanized rubber and the two-component "rubber-carbon" mixtures were prepared in the form of films from benzene solutions, while the multicomponent rubber-carbon mixtures had the same degree of vulcanization. Changes in the physico-mechanical properties of non-vulcanized two-component "rubber-carbon" mixtures with degree of loading are shown in Table 1. The specimens were torn at two rates. In the Table the figures without brackets refer to a rate of 550 mm/min, and the figures in brackets to a rate of 94 mm/min.

The dielectric data (dielectric constant $\epsilon'$, and the tangent of the dielectric loss angle $\tan\delta$) were determined at frequencies from 50 to $25 \cdot 10^6$ cycles/sec at 20°, and at frequencies from $10^3$ to $4 \cdot 10^4$ cycles/sec in the temperature range from -75 to +152°.

The dielectric constant $\epsilon'$ and the tangent of the dielectric loss angle tan for $\delta$ natural rubber change in the same manner as $\epsilon'$ and $\tan\delta$ for sodium butadiene rubber [1], if the natural rubber specimen is tested under conditions which preclude the possibility of its crystallization. Neither the temperature nor the frequency curves for $\tan\delta$ (or the dielectric loss coefficient $\epsilon'' = \epsilon' \tan\delta$) show any maxima. For a frequency of $10^3$ cycles/sec at 20°, $\epsilon' = 2.41$, and $\tan\delta = 0.0027$. Tan $\delta$ increases slightly with increase of frequency. Examples of the experimentally found dependence of the dielectric loss coefficient $\epsilon''$ on frequency for two-component non-vulcanized "rubber-carbon" mixtures (at 20 and 100°) are shown in Figure 1.

On the basis of the frequency-temperature curves for two-component mixtures we carried out an analysis analogous to that described in the paper on non-vulcanized mixtures of sodium butadiene rubber with carbon black [1].

TABLE 1

Physico-Mechanical Properties of Two-Component Mixtures with Natural Rubber. (Determined on Smirnov's Apparatus).

| Content of carbon, in ml per 100 g rubber | Channel gas black | | | Extracted channel gas black | | | Thermal black | | |
|---|---|---|---|---|---|---|---|---|---|
| | Breaking strength kg/cm$^2$ | Relative elongation, % | Residual elongation, % | Breaking strength kg/cm$^2$ | Relative elongation, % | Residual elongation % | Breaking strength kg/cm$^2$ | Relative elongation, % | Residual elongation, % |
| 0.0 | 4.19 (1.83) | 1000 (880) | 80 (120) | — | — | — | — | — | — |
| 5.0 | 3.86 (1.66) | 900 (950) | 135 (80) | 2.6 (1.265) | 700 (930) | 85 (180) | 1.63 (0.9) | 740 (590) | 75 (100) |
| 7.5 | 5.282 (2.78) | 790 (750) | 120 (140) | 3.76 (1.58) | 800 (850) | 95 (70) | — | — | — |
| 10.0 | 6.0 (3.29) | 700 (600) | 70 (130) | 5.73(3.16) | 750 (970) | 100 (180) | 2.5 (1.242) | 780 (750) | 100 (140) |
| 15.0 | — | — | — | — | — | — | 2.8 (1.5) | 820 (1100) | 110 (250) |
| 20.0 | — | — | — | — | — | — | 3.38(1.85) | 710 (650) | 85 (110) |
| 30.0 | — | — | — | — | — | — | 5.32(3.75) | 780 (800) | 150 (160) |

TABLE 2

Data for Two-Component Mixtures of Natural Rubber with Carbon Black

| Filler | Content of carbon in ml per 100 g rubber | Parameter of distribution of relaxation times, b | k | Dielectric constant at very high frequencies, $\epsilon_\infty$ | Coefficient of structural dielectric loss, $\epsilon''_{str}$ | Shape factor, $\Phi$ |
|---|---|---|---|---|---|---|
| Channel gas black | 5 | ∞ | 0.0077 | 2.725 | 0.050 | 1.015 |
| | 10 | 1.0 | 0.071 | 4.10 | 0.105 | 2.77 |
| | 15 | 0.8 | 0.088 | 5.13 | 0.145 | 3.10 |
| Extracted channel gas black | 5 | ∞ | 0.0085 | 2.73 | 0.045 | 1.03 |
| | 10 | ∞ | 0.037 | 3.63 | 0.080 | 2.0 |
| | 15 | 1.0 | 0.069 | 4.78 | 0.121 | 2.7 |
| Thermal black | 5 | ∞ | 0.0075 | 2.72 | 0.001 | 1.00 |
| | 10 | ∞ | 0.0150 | 3.015 | 0.031 | 1.00 |
| | 15 | ∞ | 0.0216 | 3.3 | 0.068 | 1.02 |
| | 20 | ∞ | 0.0270 | 3.5 | 0.090 | 1.01 |
| | 30 | ∞ | 0.0417 | 4.0 | 0.113 | 1.02 |

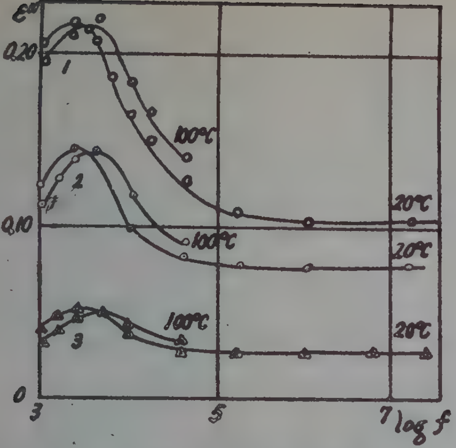

Fig. 1. Dependence of the dielectric loss coefficient on the frequency f of the alternating current, for two-component nonvulcanized mixtures of natural rubber with 10 volumes of: 1) channel; 2) extracted; 3) thermal black.

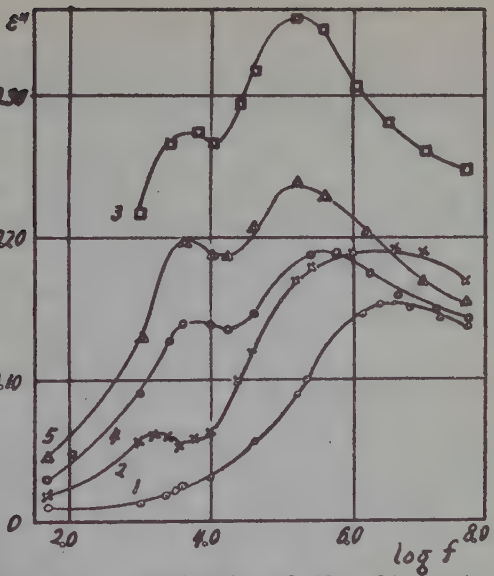

Fig. 2. Dependence of the dielectric loss coefficient $\epsilon''$ on the frequency of the alternating field f at 20°, for natural rubber vulcanizates: 1) unfilled; 2) with 5; 3) with 10 volumes of channel black; 4) with 15; and 5) with 30 volumes of thermal black.

The experimentally determined dielectric loss coefficient $\epsilon''_{exp}$ is composed of three dielectric coefficients: 1) loss coefficient due to the heterogeneity of the dielectric, $\epsilon''_{het}$, 2) loss coefficient due to direct current, $\epsilon_{cond}$; 3) the structural loss coefficient, $\epsilon''_{str}$; each of these components is due to the presence of carbon black in the mixture. As a result, as in the case of mixtures with sodium butadiene rubber, the parameters b, k, $\tau_0$, and $\epsilon_\infty$ for the equations for $\epsilon'$ and $\epsilon''$ for a heterogeneous dielectric were obtained, and the shape factor $\Phi$, which characterizes the ratio of the dimensions of the carbon formations in the mixture, was determined. The shape factor for carbon black which does not have the capacity for structure formation is equal to unity, while for structure-forming carbons it increasingly differs from unity as the tendency of the carbon to structure formation becomes greater. The results of the calculations of these values are shown in Table 2. From the data of this Table it is possible to calculate the values of $\epsilon'$ and $\epsilon''$ for any frequency and temperature.

At 20° the frequency $f_M$ which corresponds to maximum $\epsilon''$ for mixtures of rubber with channel gas black is $2.12 \cdot 10^3$, for mixtures with extracted black it is $2.5 \cdot 10^3$, and with thermal black, $2.68 \cdot 10^3$ cycles/sec.

The dielectric properties of loaded vulcanizates from natural rubber were next studied. Examples of experimental curves showing the variation of the dielectric loss coefficient $\epsilon'' = \epsilon' \cdot \tan \delta$ with frequency are shown in Figure 2. The existence of a high-frequency maximum for loaded vulcanizates, as in the case of vulcanizate without carbon (Figure 2, Curve 1) is explained by the orientation of "sulfur dipoles" in the electric field; while the low-frequency maximum, characteristic only of carbon mixtures, whether the mixture is vulcanized or not, and which is not observed either in the curves for raw rubber, or for vulcanizate without carbon (Figure 2, Curve 1), is due to the heterogeneity of the rubber-carbon mixture. By removing the dipole components ($\Delta\epsilon'_{dip}$. and $\epsilon''_{dip}$ ) from the experimental data for the dependence of $\epsilon'$ and $\epsilon''$ on temperature and frequency (by elimination of $\Delta\epsilon'_{het}, \Delta\epsilon'_{str}, \epsilon''_{het}, \epsilon'_{cond}, \epsilon''_{str}$) we obtain curves, analogous to those shown in Figures 3 and 4, which were determined experimentally by us for vulcanizates without carbon.

Table 3 shows: 1) frequencies $\underline{f}_{mdip}$, which correspond to the dipole maxima $\epsilon''_{dip}$ at 20°; 2) values of the activation energy of the dipole orientation process $\underline{U}$, calculated from the displacement of $\underline{f}_{mdip}$ with variation of temperature; 3) the parameter of the selection of dipole relaxation times, $\alpha$, at 20°; 4) the dipole moments of the vulcanizates, calculated per monomer unit of rubber; 5) the relative change in the dimensions of the dielectric segments $\underline{a}_{rel}$, determined from the Debye formula $\tau o = \frac{4\pi\eta a^3}{kT}$ for the relaxation time $\tau_0 = \frac{1}{2\pi \underline{f}_{M\,dip.}}$ and the relative viscosity $\eta_{rel}$. The latter was calculated as the ratio of the viscosity of the loaded mixture to the viscosity of the nonloaded mixture, determined under the same conditions. As in the case of sodium butadiene rubber, the nature of the dependence of the relative viscosity on the loading and temperature remains the same independently of the testing method. The viscosity $\eta$ was calculated both from data obtained with a Höppler consistometer for multicomponent nonvulcanized mixtures by Bartenev's method [4], and from the values of the mechanical loss coefficient ($\sin\varphi$) and dynamic modulus $\underline{E}$, determined for vulcanizates on the Kornfeld apparatus [2]. The variation or relative viscosity with loading, type of carbon, and type of rubber is shown in Figure 5.

TABLE 3

Frequencies, Activation Energy, Parameters of Relaxation Times, and Dipole Moments for Loaded Vulcanizates

| Filler | Content of carbon in ml per 100, g rubber | Frequency $\underline{f}_{m\,dip}$ corresponding to the dipole maximum at 20°C, $\cdot 10^5$ | Energy of activation of the dipole orientation process $\underline{U}$, kcal/mole | Parameter of selection of dipole relaxation times, $\alpha$, at 20° | Dipole moment for the monomer, $\mu\,10^{18}$ absolute electrostatic units | Relative change of dielectric segment $\underline{a}_{rel}$ |
|---|---|---|---|---|---|---|
| Channel gas black | 0.0 | 22.9 | 23.8 | 0.425 | 0.677 | $a_1$ |
| | 5.0 | 15.0 | 28.4 | 0.415 | 0.743 | $1.03a_1$ |
| | 10.0 | 2.965 | 27.5 | 0.421 | 0.722 | $1.49a_1$ |
| | 15.0 | 1.51 | 27.5 | 0.425 | 0.699 | $1.52a_1$ |
| Thermal black | 5.0 | 4.68 | 26.65 | 0.425 | 0.661 | $a_2$ |
| | 10.0 | 3.6 | 26.7 | 0.424 | 0.677 | $1.01a_2$ |
| | 15.0 | 1.7 | 26.6 | 0.425 | 0.681 | $1.15a_2$ |
| | 20.0 | 1.7 | 26.6 | 0.425 | 0.682 | $1.01a_2$ |
| | 30.0 | 1.7 | 26.7 | 0.427 | 0.677 | – |

Table 4 shows the results of analysis of the components of $\epsilon'$, and $\epsilon''$, relating to processes in a heterogeneous dielectric and to structural polarization in loaded vulcanizates. Figures 6 and 7, together with curves which show variations of the experimental values of $\epsilon''$ with changes of temperature and frequency for a natural rubber vulcanizate with 30 volumes of thermal black, also give the (calculated) changes in the component terms $\epsilon''_{dip}, \epsilon''_{het}, \epsilon''_{str}$.

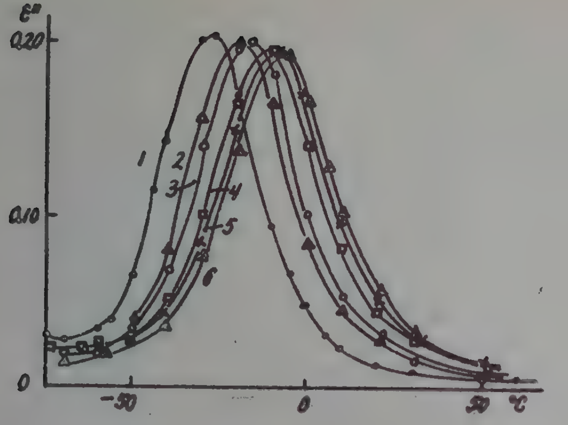

Fig. 3. Variation of the dielectric loss coefficient $\epsilon''$ with frequency and temperature for a vulcanizate of natural rubber, without carbon; frequencies in cycles per second: 1) $10^3$; 2) $4 \cdot 10^3$; 3) $6 \cdot 10^3$; 4) $27 \cdot 10^3$; 5) $34 \cdot 10^3$; 6) $40 \cdot 10^3$.

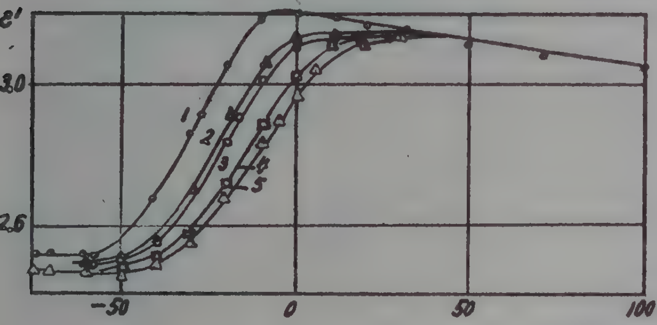

Fig. 4. Variation of the dielectric constant $\epsilon'$ with frequency and temperature for a vulcanizate of natural rubber, without carbon; frequencies in cycles per second: 1) $10^3$; 2) $4 \cdot 10^3$; 3) $6 \cdot 10^3$; 4) $27 \cdot 10^3$; 5) $40 \cdot 10^3$.

Although the results shown in Tables 3 and 4 provide evidence of the influence of the type of structure of the mixture on the dipole orientation characteristics (there is a direct relationship between changes of the shape factor $\phi$ and changes of $\underline{U}$, $\underline{a}$ and $\alpha$ in loading), they also show that this influence is far less for mixtures with natural rubber than for synthetic sodium butadiene rubber [2]. This is in agreement with the fact that the physicomechanical properties of natural rubbers vary little with loading.

It may be supposed that the effect of the type of filler and rubber on the above properties ultimately depends on the ratio of the energy of intermolecular action in the rubber phase, on the one hand, to that between the filler particles on the other. This effect is transmitted by means of "rubber-filler" bonds.

As in our previous communication, we established that the limiting value of the parameter for the distribution of dipole relaxation times $\alpha$, does not depend on the degree of loading, and is attained at 100-120° (Figure 8). It must be particularly stressed that the value of $\alpha_{max}$ differs greatly between natural and synthetic rubber. In the case of the latter, $\alpha_{max} = 0.283$, while for the former $\alpha_{max} = 0.435$. This provides further confirmation for our view that the value of $\alpha_{max}$ is mainly determined by the structure of the molecules of the polymer itself, and does not depend on intermolecular action in the mixture. Since no change of $\alpha_{max}$ with loading could be found, it may be stated that the rubber-carbon bonds formed during loading at 100-120° do not show any effect on orientation processes in the rubber phase, and so do not belong to the class of stable chemical bonds. At the same time, the dipole moment $\bar{\mu}$ also does not change with loading. Apparently the interaction of the rubber with the filler does not occur at the sites of the "sulfur dipoles".

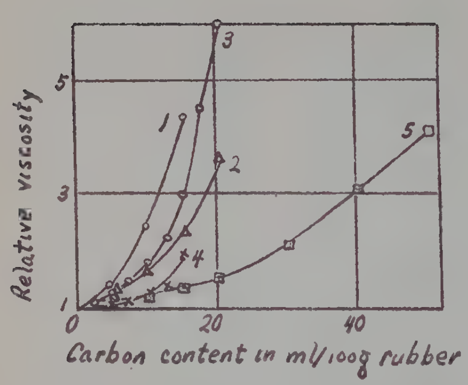

Fig. 5. Variation of relative viscosity on the carbon content in mixtures with natural rubber: 1) channel; 2) thermal black; and with sodium butadiene rubber; 3) channel; 4) extracted; and 5) thermal black.

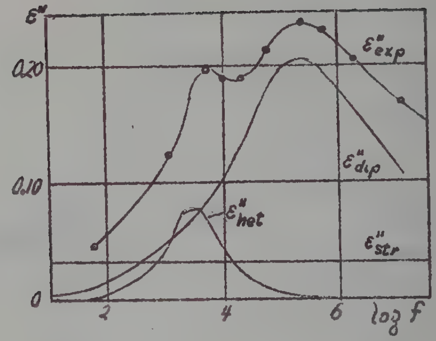

Fig. 6. Variation of the experimental coefficient of dielectric loss $\epsilon''_{exp}$ with frequency f at 20° for vulcanizates of natural rubber with 30 volumes of thermal black. $\epsilon''_{exp}$ i separated into $\epsilon''_{dip}$, $\epsilon''_{het}$, and $\epsilon''_{str}$.

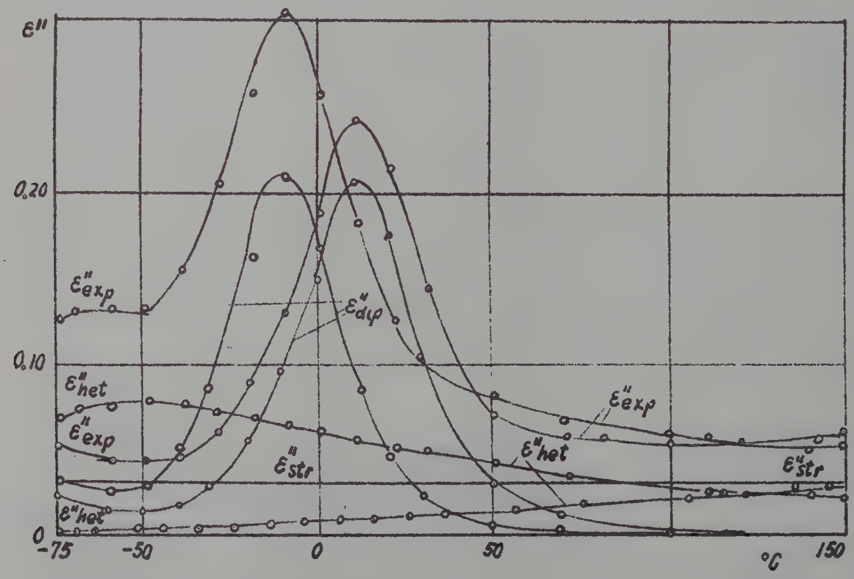

Fig. 7. Variation of the experimental dielectric loss coefficient $\epsilon''_{exp}$ with the temperature at $10^3$ cycles ( – ∘ – ) and $4\cdot10^4$ cycles ( – • – ) for a vulcanizate of natural rubber with 30 volumes of thermal black. $\epsilon''_{exp}$ is separated into $\epsilon''_{dip}$, $\epsilon''_{het}$, and $\epsilon''_{str}$.

TABLE 4

Parameters Characterizing Processes in a Heterogeneous Dielectric, and Structural Polarization in Unfilled Vulcanizates

| Filler | Content of carbon in ml per 100 g rubber | Parameter of distribution of relaxation times, b | Parameters of equations for heterogeneous dielectric | | Coefficient of structural dielectric losses, $\epsilon''_{str.}$ | Shape facto $\Phi$ |
|---|---|---|---|---|---|---|
| | | | k | $\epsilon_{\infty het}$ | | |
| Channel gas black | 5.0 | $\infty$ | 0.0103 | 4.10 | 0.0225 | 1.07 |
| | 10.0 | 1.0 | 0.0219 | 9.13 | 0.080 | 2.51 |
| | 15.0 | 0.8 | 0.04 | 13.0 | 0.140 | 3.30 |
| Thermal black | 5.0 | $\infty$ | 0.0051 | 3.670 | 0.00 | 1.2 |
| | 10.0 | $\infty$ | 0.010 | 4.243 | 0.004 | 1.0 |
| | 15.0 | $\infty$ | 0.0173 | 5.79 | 0.015 | 1.5 |
| | 20.0 | $\infty$ | 0.0175 | 5.90 | 0.020 | 1.11 |
| | 30.0 | $\infty$ | 0.018 | 8.34 | 0.030 | 1.10 |

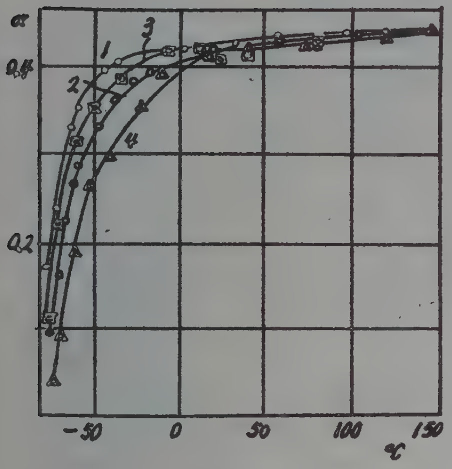

Fig. 8. Temperature dependence of the parameter for the distribution of relaxation times (α) for vulcanizates of natural rubber: 1) without filler; 2) with 5 ml, and 3) 10 ml channel black; 4) 15 ml thermal black.

## SUMMARY

1. Curves have been studied for the variation of the dielectric constant $\epsilon'$ and the dielectric loss coefficient $\epsilon''$ with temperature and frequency, for non-vulcanized natural rubber and two-component "rubber-carbon" mixtures, and also for vulcanizates of natural rubber with varying contents of thermal and channel gas black, in the frequency range of 50 to $2.5 \cdot 10^7$ cycles/sec at 20°, and temperature range from -75 to 152° at frequencies from $10^3$ to $4 \cdot 10^4$ cycles/sec.

2. As in the case of mixtures of sodium butadiene rubber[2]:

a) addition of carbon black to the mixture leads to three types of dielectric loss: due to heterogeneity of the dielectric, due to the passage of current (conductivity), and structural;

b) vulcanization of rubber leads to dipole dielectric losses, explained by orientation of "sulfur dipoles" in the electric field;

c) loading of vulcanizates produces changes in the dipole dielectric properties, which depend both on the content and type of filler, and on the type of rubber.

3. For all the types of rubber, the nature of the dependence of the dipole dielectric characteristics which determine the orientation processes in the rubber phase on the shape factor, which indicates the capacity of the carbon to form structures, corresponds to the nature of the dependence of the physicomechanical properties of the vulcanizates on the degree of loading with carbon.

We express our gratitude to Prof. G.P.Mikhailov and Candidate of Chemical Science K.A.Pechkovskaya for their assistance and advice in discussion of the paper.

Research Institute for the Tire Industry,
Moscow

Received December 16, 1952

## LITERATURE CITED

[1] B.A.Dogadkin and A.I.Lukomskaya, Colloid J., 15, 183 (1953).[1]

[2] B.A.Dogadkin and A.I.Lukomskaya, Colloid J., 15, 259 (1953).[2]

[3] A.P.Aleksandrov and Yu.S.Lazurkin, Proc. Acad. Sci. USSR, 45, No.7, 308, (1944).

[4] G.M.Bartenev, J. Phys. Chem., 24, No.10, 1210 (1950).

[5] A. Jager, Phys. 7, 434, 1936.

[6] R.M.Fuoss, J. G. Kirkwood, J. Am. Chem. Soc. 63, 385 (1941).

[7] A.P.Aleksandrov and Yu.S.Lazurkin, Caoutchouc and Rubber, No.10, 34 (1939).

---

[1] See Consultants Bureau Translation, p. 187.

[2] See Consultants Bureau Translation, p. 267.

# SULFIDES OF COPPER, LEAD, AND ZINC AS SOLID EMULSIFIERS

S.G.Mokrushin and T.P.Avilova

It is known that in the study of the stabilizing power of any emulsifier it is important to elucidate the influence of electrolytes on its protective power.

In all the experiments on the effect of electrolytes on the quality of the emulsions formed, stabilized by film sulfides of copper, lead, and zinc (certain properties of these emulsions were described in our previous papers [1]), dispersion was effected by a standard shaking method. The weight of sulfide, volumes of the dispersion medium and disperse phase, the time of preliminary shaking, and the dispersion time, were all kept constant. Water was replaced by the corresponding electrolyte solution. The degree of dispersion of the emulsion was determined microscopically. At the same time, changes in the degree of dispersion of the sulfide itself under the action of the same electrolytes were examined. The degree of dispersion of the sulfides was determined by Figurovsky's method [2],

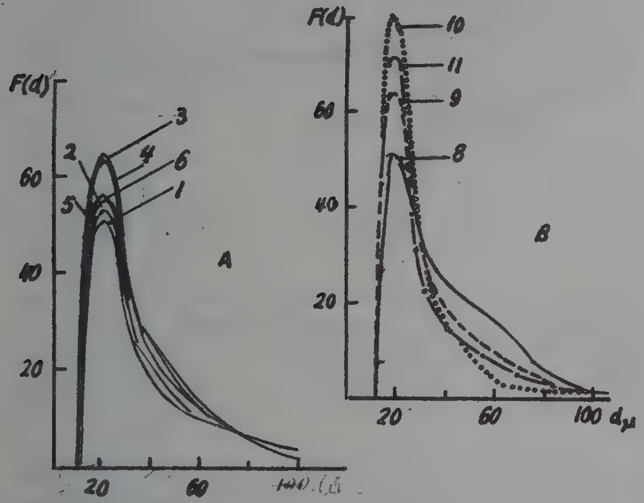

Fig. 1. Effect of electrolytes on the dispersivity of o/w emulsions: A) stabilized with CuS after 12 hours: 1) w/e (without electrolyte);2) 0.13 M; 3) 0.65 M; 4) 1.30 M $CuSO_4$; after 60 days: 5) w/e; 6) 0.13 M; 7) 1.30 M $CuSO_4$. B) stabilized with ZnS after 12 hours: 8) w/e; 9) 0.84 M; 10) 1.68 M; 11) 3.36 M $ZnSO_4$.

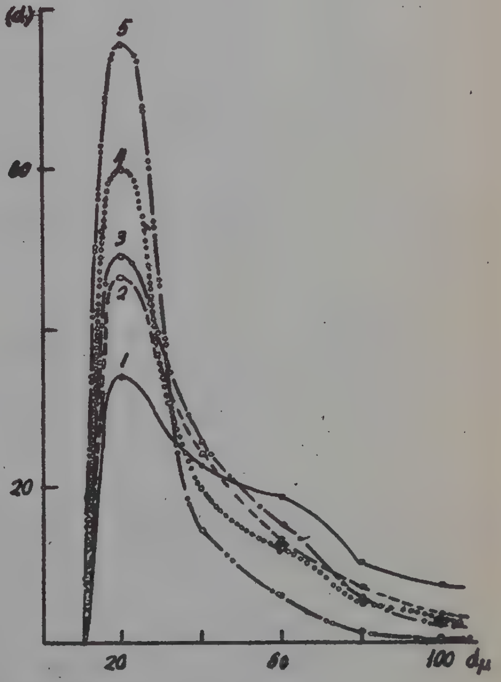

Fig. 2. Effect of electrolytes on the dispersivity of w/o emulsions, stabilized by PbS; 1) w/e; 2) 0.21 M; 3) 0.42 M; 4) 0.84 M; 5) 1.69 M $Pb(C_2H_3O)_2$.

Changes in the charge on the films in presence of electrolytes were not specially studied, the data of Mokrushin and co-workers being used [3].

The following electrolytes were used:

1. Solutions of salts, up to saturation, containing a cation common with the cation in the crystal lattice of the sulfide (solutions of sulfates of copper and zinc, and lead acetate).

2. Solutions of alkalies.

3. Solutions of salts with the univalent $Cl^-$– anion and cations of increasing valency: $K^+$, $Ba^{2+}$,, $Al^{3+}$.

4. Solutions of salts with the same univalent cation $K^+$ and anions of increasing valency: $Cl^-$, $SO_4^{2-}$, $[Fe(CN)_6]^{3-}$.

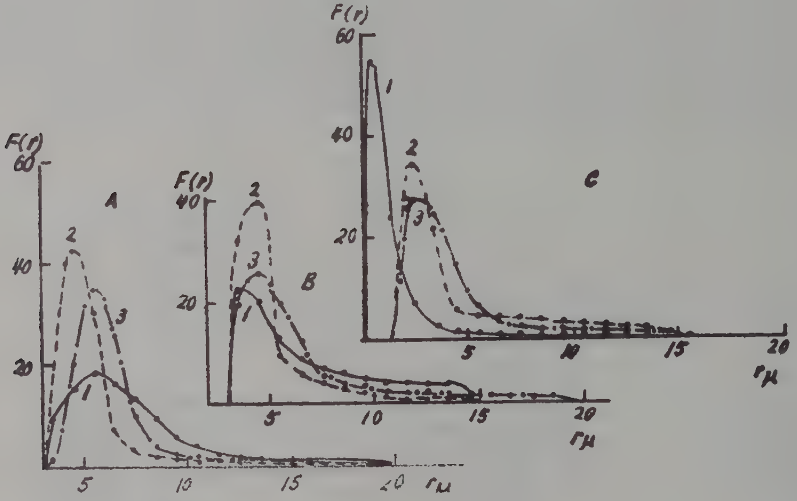

Fig. 3. Effect of electrolytes on the dispersivity of suspensions of sulfides of copper (A), lead (B), and zinc (C):
A)-1) w/e; 2) 0.005 M; 3) 0.065 M $CuSO_4$;
B)-1) w/e; 2) 0.0067 M; 3) 0.0845 M $Pb(C_2H_3O)_2$;
C)-1) w/e; 2) 0.134 M; 3) 0.0672 M $ZnSO_4$.

The investigations showed (Figures 1 and 2) that addition to the aqueous medium of salt solutions containing a cation contained in the crystal lattice of the sulfide increases the degree of dispersion of both direct and reverse emulsions, without displacing the maximum on the distribution curve. In the case of reverse emulsions this increase extends up to saturated solutions of the electrolytes, while for o/w emulsions it reaches definite concentrations, after which it either remains constant (for sulfides of copper and lead) or decreases a little, but still remains considerably above the original value (zinc sulfide).

In our view, these effects for emulsions protected by sulfides of copper and zinc can be explained only by an increase, by the action of the electrolytes, of the positive charge on the film, which opposes the coalescence of droplets, as a complete parallel was not observed between changes in the dispersivity of the emulsion and the dispersivity of the emulsifier under the action of the electrolyte (Figures 1 and 3). Changes in the wettability of the sulfides, which undoubtedly occur, cannot play a decisive role here, as otherwise additions of electrolytes would have different effects on direct and reverse emulsions.

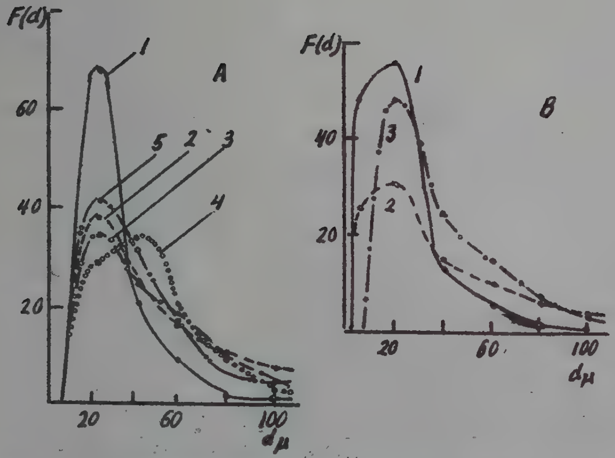

Fig. 4. Effect of alkali on the dispersivity and stability of o/w emulsions:

A) stabilized by PbS: 1) after 2.5 min. emulsification with NaOH; 2) same after 20 min; 3) after 6 days' storage with NaOH; 4) after 2.5 min. emulsification w/e; 5) same after 20 min.

B) stabilized by CuS: 1) after 20 min. emulsification with NaOH; 2) after 48 hours' storage with NaOH; 3) after 20 min. emulsification w/e.

Systems stabilized by zinc sulfide, in which increase in the dispersivity of the emulsions themselves was accompanied by a decrease in the dispersivity of the emulsifier, are in a somewhat different position. The dispersivity of the emulsifier may have a considerable effect on the increase of the dispersivity of the emulsions, as a definite degree of coagulation of the powder is needed for the formation of a stable protective layer. It should be noted that in the presence of zinc sulfate the dispersivity of zinc sulfide approaches that of the sulfides of copper and lead (see Figure 3). The stability of the emulsions decreased with increasing electrolyte concentration.

The stability of emulsions stabilized with zinc sulfide is particularly strongly affected by electrolytes. (In concentrated solutions of zinc sulfate, lower fractions of zinc sulfide are soluble). The decrease of stability is in all probability explained by an intensification of the recrystallization and aging processes in the films under the action of electrolytes.

## Effect of Solutions of Alkalies on Direct and Reverse Emulsions

The effect of alkalies was studied only with emulsions stabilized by sulfides of cooper and zinc.

The addition of caustic soda at first increases the dispersivity of o/w emulsion, but after some time (several minutes for systems stabilized by lead sulfide, and hours for those protected with copper sulfide) coalescence processes become noticeable (Figure 4).

Coalescence processes in systems stabilized by lead sulfide proceed so rapidly that the initial increase of dispersivity may be observed only by taking samples in course of emulsification (for comparison, samples were taken from emulsions with a pure aqueous phase). A similar state of affairs, but with a smaller initial increase of dispersivity, was also observed in a reverse emulsion, stabilized by lead sulfide (Figure 5).

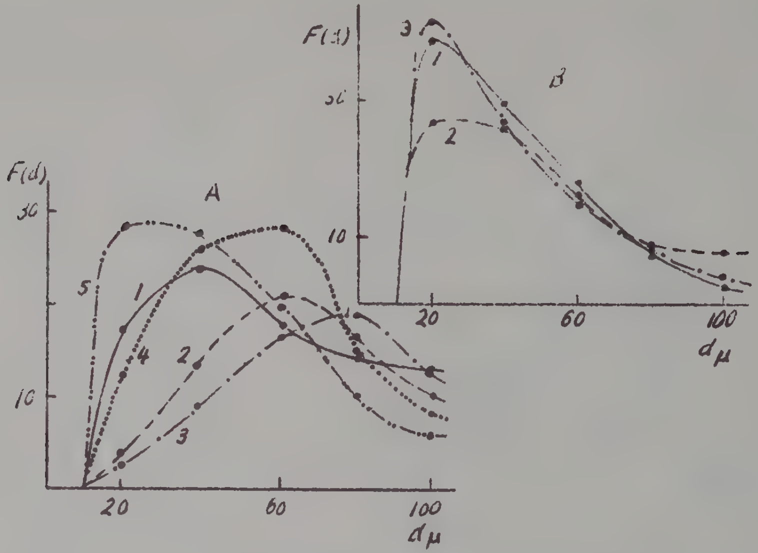

Fig. 5. Effect of NaOH on the dispersivity and stability of w/o emulsions:

A) stabilized by PbS: 1) after 2.5 min emulsification with NaOH; 2) same after 20 min; 3) after 6 days' storage with NaOH; 4) after 2.5 min emulsification w/e; 5) same after 20 min.

B) stabilized by CuS: 1) after 20 min emulsification with NaOH; 2) after 48 hours' storage with NaOH; 3) after 20 min emulsification w/e.

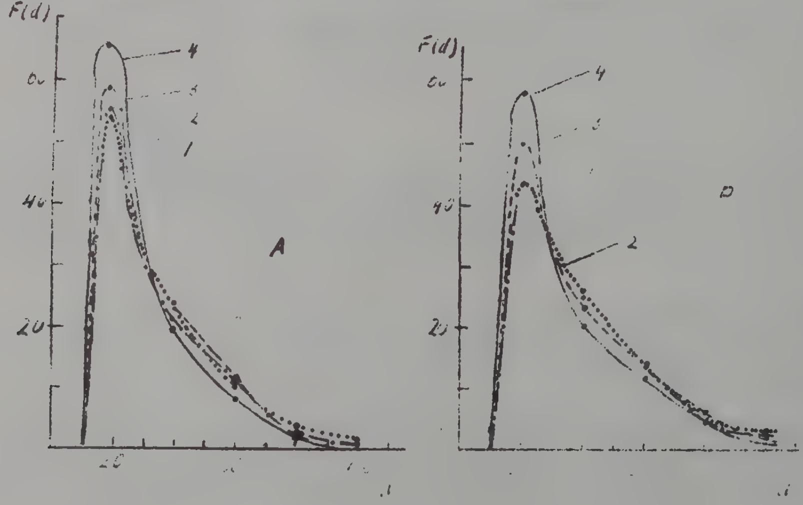

Fig. 6. Effect of electrolytes on the dispersivity of o/w and w/o emulsions stabilized by CuS:

A) o/w emulsions; 1) w/e; 2) 0.1N KCl; 3) 0.1N $BaCl_2$; 4) 0.1N $AlCl_3$;

B) w/o emulsions; 1) w/e; 2) 0.05N KCl; 3) 0.05N $BaCl_2$; 4) 0.5N $AlCl_3$.

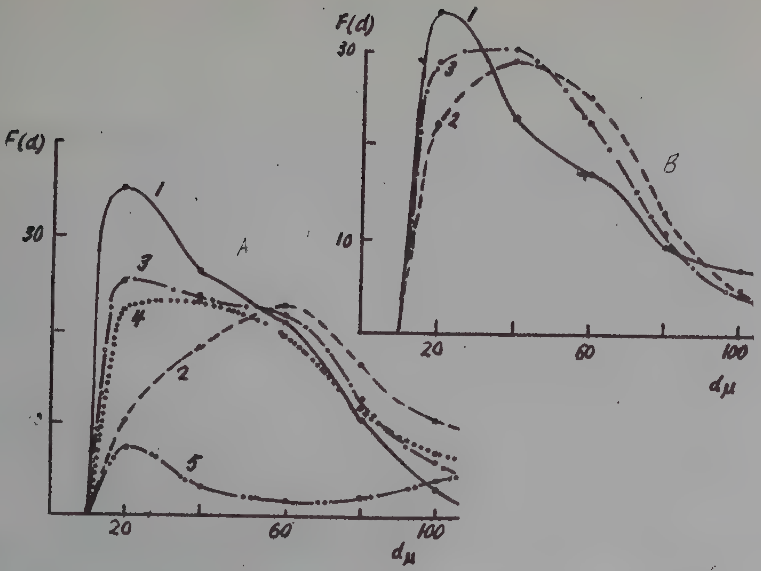

Fig. 7. Effect of electrolytes on the dispersivity of o/w and w/o emulsions stabilized by PbS:

A) o/w: 1) w/e; 2) 0.01N $K_2SO_4$; 3) 0.1N $K_2SO_4$; 4) 0.01N $K_3Fe(CN)_6$; 5) 0.1N $K_3Fe(CN)_6$.

B) w/o: 1) w/e; 2) 0.05N $K_2SO_4$; 3) 0.05N $K_3Fe(CN)_6$.

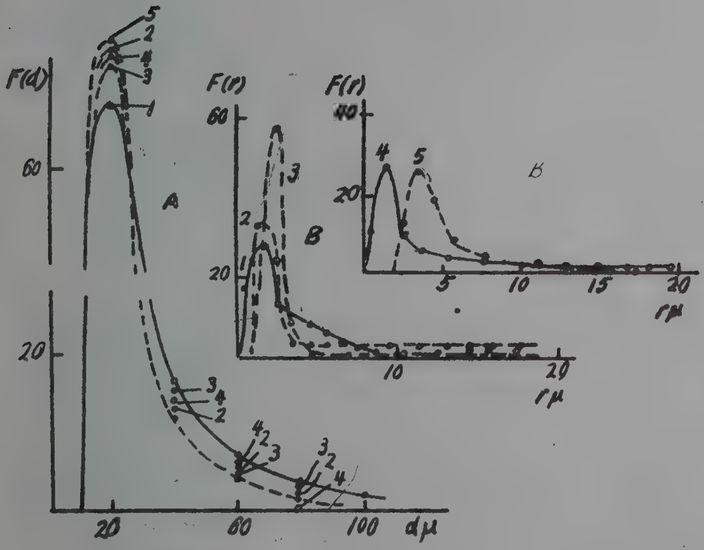

Fig. 9. Effect of electrolyte solutions:

A) on the dispersivity of emulsions stabilized by ZnS: 1) w/e; 2) 0.1 KCl; 3) 0.1N $BaCl_2$; 4) 0.1N $AlCl_3$; 5) 0.1N $K_2SO_4$. B) on the dispersivity of ZNS: 1) w/e; 2) 0.01N $AlCl_3$; 3) 0.05N $AlCl_3$; 4) w/e; 5) 0.01N $K_2SO_4$.

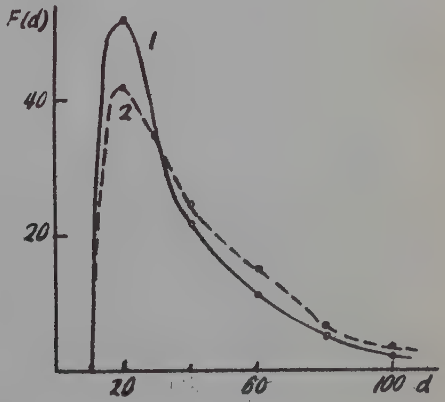

Fig. 8. Effect of $K_2SO_4$ solution on the dispersivity of o/w emulsions stabilized by CuS: 1) on the first day, 2) on the sixth day after preparation.

No increase in the dispersivity of a w/o emulsion, stabilized by copper sulfide, was observed after 20 minutes' emulsification. Dispersion analysis of such an emulsion after 48 hours' storage showed clearly defined coalescence (Figure 5).

## Effect of the Valencies of the Anion and Cation on the Emulsions Obtained

Introduction of barium chloride and aluminum chloride into the aqueous phase of direct and reverse emulsions stabilized by sulfides of copper and lead increase their dispersivity, and this increase becomes greater with increase in the valency of the ion and the concentration of the electrolyte (Figure 6). This effect may be most correctly explained by a change in the surface charge in accordance with the Schulze-Hardy rule (there is no parallel change in the dispersivity of the emulsions and emulsifier, as also in the case of solutions of potassium sulfate and ferricyanide).

Solutions of potassium chloride, because of the equal valencies of anion and cation, caused no clearly defined decrease or increase of dispersivity, which fluctuated close to mean values near to those obtained in absence of electrolytes.

The addition of salts containing di- and trivalent anions ($SO_4^{2-}$, $[Fe(CN)_6]^{3-}$) with a univalent cation, decreases the degree of dispersion of direct and reverse emulsions protected by sulfides of lead and copper (in the case of copper sulfide the effect of potassium sulfate only was studied) (Figures 7 and 8).

Emulsions stabilized by lead sulfide are strongly influenced by the $SO_4^{2-}$ ion, apparently because of its greater adsorption, due to the formation of a sparingly soluble compound, lead sulfate, with the cations of the lattice. The increase of the dispersivity may be explained be a decrease in the charge of the protective layer with preferential adsorption of negative ions.

The correctness of this view is also supported by the increase in the degree of dispersion of emulsions stabilized by lead sulfide on passing from lower (0.01N) to higher (0.1N) concentrations of potassium sulfate, overcharging of the film being possible at the latter concentration. The stability of emulsions in presence of $SO_4^{2-}$ ions decreases, and even after 6 days appreciable coalescence is observed.

The degree of dispersion of emulsions stabilized by zinc sulfide increases to an equal extent with any of the electrolytes named, with the exception of potassium ferricyanide, which sharply decreases the dispersivity and stability of the systems. This increase is always accompanied by coagulation of the powder, the significance of which was examined above (Figure 9).

In conclusion it should be noted that in many cases coalescence of the emulsions was accompanied by a displacement of the maximum on the distribution curve in the direction of the coarser fractions. In no case was a displacement of the maximum observed for an increase of the dispersivity of the emulsions (this maximum corresponded to the 10 - 30 $\mu$ fraction). This constant position of the maximum may again be explained by a similarity in the dimensions of the emulsion droplets and protective particles[1], which, of course, does not exclude the influence of other factors on the dispersivity and properties of the emulsions formed.

---

[1] The dispersivity of which also varies within relatively narrow limits.

## SUMMARY

1. The effect of electrolytes on the properties of emulsions protected by sulfides of copper, lead and zinc was studied.

2. A connection was found between the dispersivity of the emulsions and increase in the charge of the protective film.

3. The necessity for a certain degree of coagulation of the stabilizing powder was confirmed. It was found that for sulfide films the best emulsions are obtained when the effective radius of the particles is not less than 2 μ.

The A.M.Gorky Ural State University
Sverdlovsk

Received April 22, 1953

## LITERATURE CITED

[1] S.G.Mokrushin and T.P.Avilova, Colloid J., 14, 103 (1952)[1]; 15, 208 (1953).[2]

[2] N.A.Figurovsky. Modern Methods of Sedimentometric Analysis of Suspensions and Emulsions. Trans. of the Zelinsky University, Moscow (1939).

[3] S.G.Mokrushin and Z.G.Sheina, Colloid J., 5, 707 (1939).

---

[1] See Consultants Bureau Translation, p. 113.

[2] See Consultants Bureau Translation, p. 213.

# FORCES RETAINING DYESTUFF ON THE FIBER

F.I. Sadov

In recent times the special attention of investigators has been attracted to studying the nature of the bond between direct dyes and cellulose fibers. Most authors who study this problem give different explanations for the forces which retain the dye on the fiber. Views have been put forward concerning the existence of van der Waals forces between the macromolecules of the cellulose fiber and the molecules of the dye; and concerning partial valencies, that is, free partial valencies on the surface of the cellulose macromolecules, which are saturated by partial valencies of the dye. Later studies [1] particularly stress the significance of electrostatic forces of interaction, and also the formation of hydrogen bonds between the dye molecules and the macromolecules of the cellulose fiber.

Despite the large number of investigations, the question of the forces retaining direct dyes on the fiber remains unclarified and requires further study. The last decade showed considerable development in the chemistry of high polymers and dyes. Knowledge in the field of fiber structure has extended considerably, and modern physico-chemical methods of studying dyeing processes were widely applied.

It is known that the glucose residue of the cellulose molecule contains three hydroxyl groups; their effect in the dye absorption by cotton fiber was shown by the present author together with Kalinina [2].

Cellulosic fibrous material may be dyed in the form of fiber, yarn, fabric, and various finished articles. The interaction between the fiber and the dye solution may proceed in different ways: either between the dye and the external surface of the fabric, that is, between the warp and filling threads and the dye (in typical fabrics the distances between the threads are approximately 10 - 100 microns), or between the dye and the external surface of the elementary fibers in the yarn, with inter-fiber distances of approximately 1 micron; in both cases, for a stable dyeing, the dye must diffuse into the elementary fiber and react both with its external and its internal surface.

When cellulose fibers come in contact with water or aqueous solutions of dyes, a negative electrokinetic potential is set up at the fiber-water boundary, the significance of which in dyeing is vigorously debated in the current literature.

All water-soluble dyes used in the textile industry are electrolytes; they dissociate in aqueous solutions, and in the case of direct dyes the dye ion of the dyestuff has a negative charge. Observations of the behavior of aqueous solutions of direct dyes have shown the complex nature of dye solutions. However, only the ions or molecules of the dye can diffuse into the elementary fiber.

The concept of the formation of hydrogen bonds in the interaction of dye with fiber makes it easier to understand how the negatively charged dye ion is retained by the negatively charged cellulose. The formation of hydrogen bonds between fiber and dye is facilitated by the linear and plane nature of the dye molecules on the one hand, and on the other hand by the small dimensions of the submicroscopic canals in cellulose, which create favorable conditions for electrostatic interaction between the cellulose macromolecules and the dye ions. However, in these conditions the possibility is also not excluded of the formation of hydrogen bonds between the dye ions to form dye aggregates in the submicroscopic canals of the fiber [3].

Neale established, by measurement of flow potential, that bleached cotton in presence of 0.001N NaCl solution has a potential of 0.021 V, and in presence of 0.005 N solution this falls to 0.0143 V. For viscose fibers, the corresponding values of 0.0202 and 0.0130 V were obtained. Consequently, if the dye anion has valency $\underline{n}$ and carries a charge $\underline{n}\epsilon$ (where $\epsilon = 96500$ coulombs) and is adsorbed on a cellulose surface with a negative potential of $\psi$ volts with respect to the solution, then the work of approach of the dye anion to the fiber surface will be $\underline{n}\ \epsilon\psi_0$ electron-volts. According to Neale, the energy required for this work is determined by the thermal movement of the dye particles.

The interaction of the dye with the fiber commences when the forces of repulsion of ionic origin decrease as the result of shrinkage of the ionic layer, the energy barrier also decreases in consequence, and the dye becomes bound to the fiber by hydrogen bonds and van der Waals forces.

According to Neale, only a definite part of the dye ions, equal to $e^{-\frac{n\epsilon\psi_0}{300kT}}$, has sufficient energy to reach the fiber surface and is adsorbed by the latter.

The negative potential $\psi_0$ of cotton fiber may be lowered by the addition of electrolyte to the dye solution. As the electrolyte concentration increases, $\psi_0$ approaches zero, the energy barrier decreases, and the amount of adsorbed dye tends to a maximum. On the other hand, as the amount of dye adsorbed by the fiber increases, the negative charge of the fiber increases. This may explain why the amount of adsorbed dye does not increase proportionally to the dye concentration in solution, but corresponds approximately to the cube root of the dye concentration at equilibrium. Neale calculated that only 0.177 of the total dye ions in solution were adsorbed by the fiber.

According to the law of electroneutrality, dyeing will only be completed when the equivalent quantity of cations is on the dyed fiber. It follows from the work of Crank [4] that the concentration of (sodium) cations combined with dyed cellulose is 32 times as great as the concentration of dye anions. It was thus experimentally proved that sodium ions are also adsorbed by the fiber.

## EXPERIMENTAL

The influence of specific bonds between dyes and fibers can be varied only by changes in the structure of the dye molecule, while the magnitude of the electrostatic repulsion may be decreased by lowering the negative potential of the fiber or by the use of dyes with ions of lower charge (that is, with lower values of $\underline{n}$), for example, with fewer sulfo groups in the dye molecule.

On the basis of the above views concerning the forces retaining direct dyes on cellulose fibers, our aim was to study the effect of electrolyte additions, and also of the number and position of sulfo groups, on the substantivity of a number of direct dyes.

The fibers were purified from natural impurities by the standard method. The measured properties correspond to normally purified fiber. All the experiments were carried out with these fibers.

TABLE 1

Properties of Bleached Fiber

| Moisture, % | Cellulose content, % | Specific viscosity | Ash, % | Waxes, % | Nitrogen by Kjeldahl | COOH group content, % |
|---|---|---|---|---|---|---|
| 5.95 | 98.8 | 0.45 | 0.12 | 0.15 | 0.03 | 0.10 |

To determine the effect of the number of sulfo groups in direct dyes, and their position, on the dye take-up by cellulose fibers, five dyes were selected, which were prepared by coupling dianisidine with different nitrogen compounds with varying numbers and positions of sulfo groups. The following dyes were used in the study:

1) Direct Sky Blue, with the following structure:

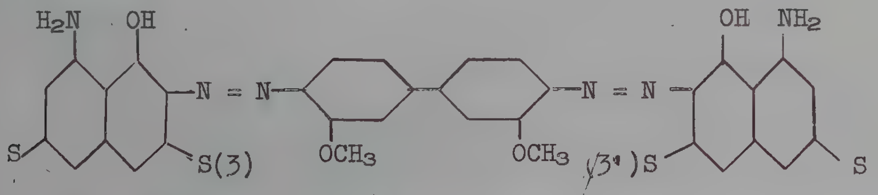

The (3) and (3') sulfogroups are in the quinoid position with respect to the ( – N = N – ) chromophores.

2) Sky Blue FF

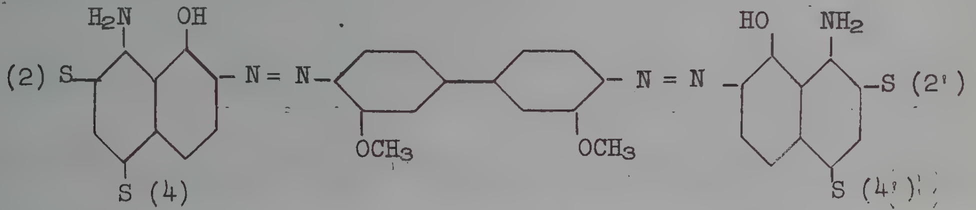

The (2) and (2') sulfo groups are bound to the auxochromes ($NH_2$ groups) by short conjugated double bonds. The (4) and (4') sulfo groups are in the quinoid position with respect to these auxochromes.

3) Direct Blue RW

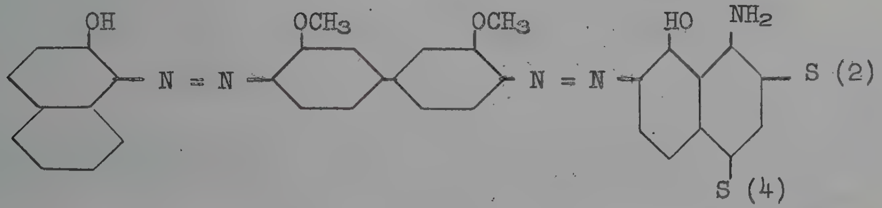

In this dye only one sulfo group (2) is linked to the auxochrome ($-NH_2$) by a short double bond, while the (4) sulfo group is in the quinoid position to the auxochrome.

4) Benzo Azurine

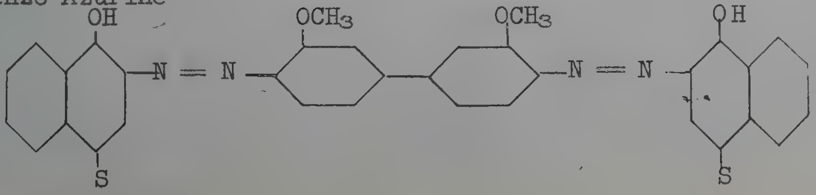

This dye has two sulfo groups, in quinoid positions to the (OH) auxochromes.

5) Direct Blue KM

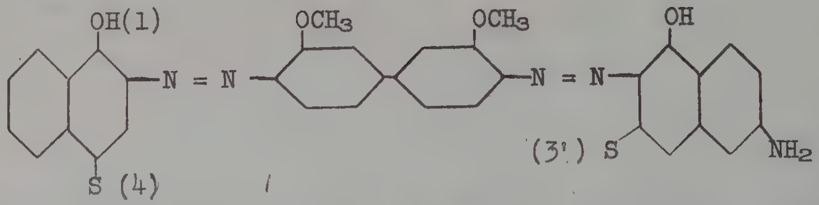

The (3') sulfo group is in the quinoid position to the chromophore ( − N = N − ).
The (4) sulfo group is in the quinoid group to the auxochrome OH (1).

All the dyes were purified by precipitation of the benzidine salt or by salting out with sodium acetate followed by separation by alkali from aqueous alcohol solution. The dye content was estimated by means of titanium chloride.

The following were used in the investigation:

Sky Blue FF with a dye content of 84%
Direct Sky Blue with a dye content of 84%
Direct Blue RW with a dye content of 82%
Direct Blue KM with a dye content of 87%
Benzo Azurine with a dye content of 91%.

On the basis of the expression $n\epsilon\psi_o$, equal to the work, in electron volts, which must be done to bring the dye particles to the fiber surface and so to increase the substantivity of the dye (that is, to increase the selectivity of the fiber for the dye), we used dyes for which n = 4 and 2. In addition, the value for the work can be decreased by varying the value of $\psi_o$, the fiber potential, by the addition of electrolyte to the dyebath.

The effect of the number of sulfo groups in direct dyes on the dye take-up of cotton fiber was studied at the following constant parameters:

| | |
|---|---|
| Concentration of dye in solution | 0.05 g/liter |
| Bath ratio | 1:200 |
| Cotton fiber | 0.5 g |
| Electrolyte | 0.1 g/liter |
| Dyeing temperature | 95° |

To study the effect of dyeing time up to equilibrium, two points were taken, 4 and 48 hours. The results are shown in Table 2.

Increase of dyeing time to 48 hours changes the adsorption of dyes insignificantly. On the basis of these results it was considered possible to continue the dyeing investigations with a dyeing time of 4 hours.

The effect of the number of sulfo groups and their position in the dye molecule, and also of the dyeing temperature, on the adsorption (in grams per 100 g fiber) are shown in Table 3.

It is seen from the results of Table 3 that dyes with two sulfo groups in the molecule are adsorbed by cellulose in greater amounts than dyes with four sulfo groups. The results are in complete agreement with the above views on the forces which retain the dye on the fiber. The position of the sulfo groups in the dye molecule also has an effect on the magnitude of the adsorption. It is seen from

TABLE 2 1)

Effect of Dyeing Time on Adsorption of Fibers

| Dye | Dyeing time | |
|---|---|---|
| | 4 hrs. | 48 hrs. |
| Direct Sky Blue | 0.098 | 0.118 |
| Sky Blue FF | 0.113 | 0.129 |
| Direct Blue RW | 0.150 | 0.155 |
| Benzo Azurine | 0.195 | 0.275 |
| Direct Blue KM | 0.407 | 0.542 |

Note. Dye take-up in grams per 100 g fiber.

TABLE 3

Effect of the Number of Sulfo Groups and Temperature on the Adsorption

| Dye | Number and position of sulfo groups in dye molecule | Dye concentration 0.05 g/liter NaCl concentration 0.05 g/liter Dyeing time 4 hours at a temperature: | | | |
|---|---|---|---|---|---|
| | | 25° | 55° | 75° | 95° |
| Direct Sky Blue | 4(3; 6-3'; 6') | 0.039 | 0.048 | 0.055 | 0.088 |
| Sky Blue FF | 4(2; 4-2'; 4') | 0.058 | 0.064 | 0.074 | 0.097 |
| Direct Blue RW | 2(2-4) | 0.048 | 0.103 | 0.134 | 0.139 |
| Benzo Azurine | 2(4-4') | 0.016 | 0.134 | 0.164 | 0.172 |
| Direct Blue KM | 2(4-3') | 0.082 | 0.154 | 0.243 | 0.283 |

the results that dyes with two sulfo groups in quinoid positions to the auxochromes have a greater effect on the selectivity of the dye than a short conjugated system between the sulfo group and the auxochrome. All the dyes show a tendency to a regular increase in the amount of dye taken up with increased temperature of dyeing.

The effect of changes in the negative potential of cellulose, $\psi_0$, with changes in the amount of electrolyte, on the dyeability of cotton fiber is shown in Table 4.

It is seen from Table 4 that the adsorption of dye by the fiber increases with increasing concentration of electrolyte in the dyebath. The effect of the number and position of the sulfo groups in the molecule of the dye follows the same laws as before.

It follows from the above that: a) Direct Sky Blue and Sky Blue FF dyes – with four sulfo groups – are adsorbed in a different way from the quantitative aspect. The hydroxyl and amino groups of these dyes have the same positions,

---

1) The experimental work was carried out by diploma student Kondratyeva.

TABLE 4

Effect of Electrolyte Concentration, NaCl, on the Adsorption of Dye (in Grams per 100 g Fiber). Dye Concentration 0.5 g/l; Temperature 95°, Dyeing Time 4 Hrs.

| Dye | Concentration of NaCl, g/liter | | | | |
|---|---|---|---|---|---|
| | 0.05 | 0.5 | 1 | 2 | 2.5 |
| Direct Sky Blue | 0.088 | 0.141 | 0.178 | 0.318 | 0.737 |
| Sky Blue FF | 0.097 | 0.177 | 0.210 | 0.351 | 0.462 |
| Direct Blue RW | 0.139 | 0.198 | 0.221 | 0.328 | 0.535 |
| Benzo Azurine | 0.172 | 0.387 | 0.422 | 0.539 | 0.619 |
| Direct Blue KM | 0.281 | 0.553 | 0.739 | - | 0.923 |

while all four of the sulfo groups of Sky Blue FF are in quinoid positions to the chromophores or auxochromes. Direct Sky Blue has only two sulfo groups in quinoid positions to the chromophore; it is adsorbed to a smaller extent by cotton fiber. Consequently it may be supposed that Direct Sky Blue has a greater negative charge than Sky Blue FF.

b) Comparison of the adsorption of the three dyes with two sulfo groups each shows that Direct Blue KM has the greatest adsorption, the value for Benzo Azurine is less, and still less for Direct Blue RW. In Direct Blue KM one sulfo group is in the quinoid position to the chromophore and the other, in the quinoid position to the auxochrome, and they are in different halves of the dye molecule. The $-NH_2$ group in the (6') position evidently tends to decrease the charge of the sulfo group in the (3') position. In Benzo Azurine the sulfo groups are in different halves of the dye molecule, in quinoid positions to the auxochromes. There are no amino groups. In Direct Blue RW both sulfo groups are in the same half of the dye molecule: one in the quinoid position to the auxochrome ($-NH_2$ group), and the other forms a conjugated double bond system with the same auxochrome.

Consequently it may be concluded that the most powerful influence on an increase of adsorption, that is, on a decrease of the negative charge of the dye ion, is exerted by a sulfo group in the quinoid position to the chromophore, and this is followed by sulfo groups in the quinoid position to the auxochrome. The influence of the sulfo group which forms a conjugated double bond system with the auxochrome of the dye molecule apparently depends on the length of this system, but the short chain 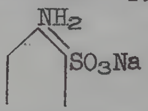 has apparently a smaller influence on the lowering of the ionic charge than have sulfo groups in the quinoid position to the auxochrome.

c) On the addition of increasing amounts of electrolyte to the dye solution, electrostatic repulsion is decreased and therefore the amount of dye adsorbed tends to a maximum (Table 4).

# SUMMARY

1. The effect of the number of sulfo groups, their position in molecules of direct dyes, and of the amount of electrolyte (NaCl) in the dyebath on the substantive properties of dyes in the dyeing of cellulose fibers has been studied.

2. It was established that electrostatic potential is one of the important factors which effect the adsorption of ions of direct dyes by cellulose fibers.

3. The view is put forward that the cellulose fiber binds direct dyes by hydrogen bonds and van der Waals forces.

Moscow Textile Institute
Chair of Chemical Technology of Fibrous Materials

Received March 5, 1953

# LITERATURE CITED

[1] S.M. Neale, J. Soc. Dyers and Colorists, 63, No. 12 (1947).

[2] F.I. Sadov and K.G. Kalinina, Colloid J., 14, No. 2, (1952).1)

[3] W. Harrison, J. Soc. Dyers and Colorists, 64, No. 7 (1948).

[4] J. Crank, J. Soc. Dyers and Colorists, 63, No. 12 (1947).

---

1) See Consultants Bureau Translation, p. 131.

# INVESTIGATION OF THE STRUCTURE OF SYNTHETIC POLYAMIDE FIBERS

## II. INTEGRAL HEATS OF WETTING OF CAPRON FIBER BY WATER

S.M.Skuratov, N.V.Mikhailov, and E.Z.Fainberg

In the previous communication, devoted to a study of the sorption of water vapor by Capron fiber, the effect of physical structure and "age" [1] of Capron fibers on their hygroscopicity was shown. Measurements of the sorption of water by Capron fiber in relation to its physical structure led to the view that differences in the sorption of water by non-oriented and oriented fibers are explained by different energies of combination between water molecules and polycaprolactam. In this connection measurements were made of the integral heats of wetting of Capron fiber by water in relation to its physical structure.

The heats of wetting of textile fibers by water were studied by numerous workers. The materials studied have been various kinds of cotton cellulose and certain artificial fibers, mainly hydrate cellulose. Only the integral heats of wetting of fibers of different moisture contents were determined experimentally; the differential heats were found from the integral values. The heats of wetting of synthetic fibers in general, and polyamide fibers in particular, have not been studied to date. The results of different authors for the integral heats of wetting of the same fibers differ considerably. The calculated values of the differential heats differ still more [2,3].

It is quite clear that the discrepancies between the data of different authors may be attributed only to a small extent to experimental errors, and they are largely a consequence of the compexity of the materials themselves, and of differences in their manufacturing technology, preliminary treatment, drying, and humidity conditioning. Therefore for the study of the heats of wetting of artificial and synthetic fibers there is no sense in laying down a very precise calorimetric technique. Principal attention should be paid to the preparation of such specimens as will ensure an adequate reproducibility of results.

### METHOD

Measurement of integral heats of wetting consists in principle of placing a sealed ampoule with the specimen into a calorimeter, the wetting liquid being used as calorimetric medium. At the appropriate instant the ampoule with the specimen is broken by some suitable means, and the thermal effect of interaction between the liquid and the wetted substance is measured. The wetting process occurs relatively rapidly and the chief factor which limits the accuracy of the measurements is only the small value of the thermal effect, especially when the wetted substance already contains a considerable amount of moisture. The small thermal effect demands a decrease in the heat capacity of the calorimeter, which is made difficult by the necessity of including in the latter a stirrer, the ampoule with the substance, and a thermometer.

Previous workers used a Dewar flask as a calorimeter for determining heats of wetting of fibers, and only a few used the complicated adiabatic calorimeter of Lipsett, Johnson, and Maass [4], with radiation thermocouples, which has not found acceptance here. We were able to use for the present investigation the calorimeter for determination of the heat capacity of liquids and solids designed by one of us [5], with some improvements in the construction, and with the calorimetric ampoule modified suitably for the purpose of the present study.

---

[1] The age of the fiber is the term given to the time which elapses from the instant of formation of the fiber to the time of investigation.

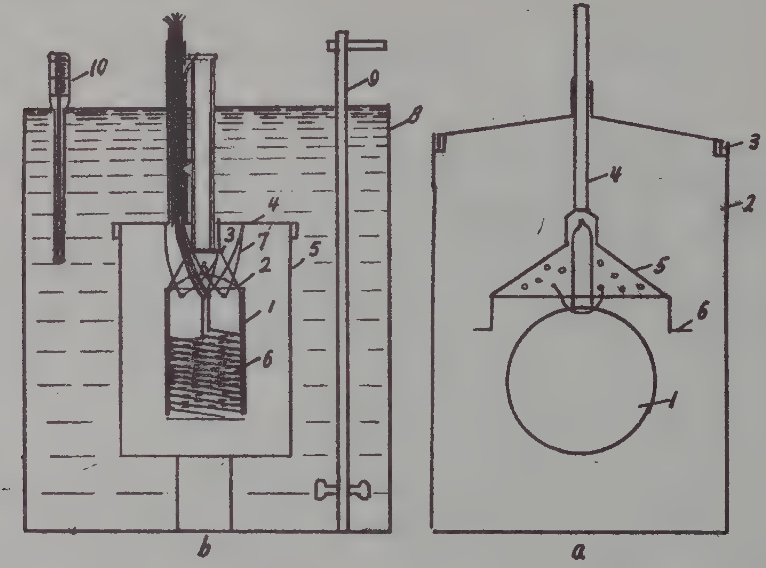

Fig. 1,a, and 1,b. Diagram of the calorimeter.

Without going into details already published [5], we will indicate only the principle of the calorimeter and note the constructional changes made for the present study. The weighed specimen of fiber, from 0.4 to 1.2 g, sealed in a spherical and thin-walled glass ampoule 1 (Figure 1,a) was placed into the calorimetric vessel 2, filled with a weighed amount of water (28-30 g), made from silvered red copper 0.3 mm thick. The calorimetric vessel was firmly closed with a lid. The gap 3 between the vessel and the lid was sealed with plastelin (0.4 - 0.5 g). The glass ampoule with the fiber was suspended from the rod 4, by a movement of which it could be broken against the bottom of the metal vessed; the hood 5 and wire 6 were to ensure some measure of mixing (by hand) of the fiber with the wetting liquid. The calorimetric vessel fitted closely into a thin-walled copper cylinder 1 (Figure 1,b) fixed by three copper plates 2 and an ebonite ring 3 to the lid 4 of the brass jacket 5. To the outer surface of the copper cylinder a heating element 6, manganin wire of 20 ohms resistance and three junctions of a copper-constantan thermocouple battery 7, were attached by means of Bakelite. The second junctions of the thermocouples were attached by Bakelite to the lid 4. The gap round the lid was also sealed by plastelin and the whole brass jacket 5 was immersed in an outer vessel 8 filled with water, and fitted with a paddle stirrer 9 rotating at a speed of 1500 revolutions per minute. The ampoule was broken by a blow from a wooden hammer on a wooden rod (not shown in the Figure) joined to the rod of the calorimetric vessel. The experiment was carried out adiabatically. Deviations from the adiabatic state were recorded from the e.m.f. of the thermocouples every 30 seconds. In all cases the correction for lack of adiabatic conditions was zero. The sensitivity of the galvanometer made it possible to record temperature differences between the calorimeter and the outer vessel to an accuracy of 0.0003°. The calorimeter temperature was not directly measured; it could be found from the temperature of the outer vessel and the temperature difference between the calorimeter and the outer vessel.

The temperature of the outer vessel was measured with a metastatic thermometer 10 with 0.005° divisions. It was thus possible to make temperature measurements with an accuracy of 0.0005°.

The heat capacity of the calorimetric system was determined by heating it by an electric current. The energy of the current was measured with an accuracy of 0.02%. As in the different experiments the heat capacity of the system varied only slightly because of small differences in the amounts of water, glass in the ampoule, fiber, and plastelin, separate determinations of the heat capacity are not necessary for each experiment; it may be determined exactly for a particular case beforehand, and used in the other cases with a small, easily calculated correction.

The experimental technique of using a calorimeter of this type was fully investigated in the paper cited above [5]. In the present study, only certain particular questions had to be elucidated: 1) would the thermal inertia of the calorimeter be significantly increased by the introduction of an evacuated glass ampoule with the fiber; 2) would the impact energy in breaking of the ampoule produce an appreciable thermal effect; 3) what is the magnitude of the thermal effect when an evacuated ampoule is broken in a calorimeter under atmospheric pressure.

TABLE 1

Integral Heat of Wetting of Hydrate Cellulose Fiber by Water [1]

| Author | Heat of wetting in cal per g dry substance |
|---|---|
| Wahba [8] | 20.3 |
| Hermans [2] | 22.4 |
| Rees [3] | 25.2 |
| Guthrie [7] | 25.2 |
| Data of the present paper | 25.86 |

The first question was solved by special experiments in which the calorimetric system was heated in presence and absence of the ampoule. Thermal equilibrium, naturally, was reached more rapidly in absence of the ampoule, but even in presence of the ampoule thermal equilibrium was established 20-25 minutes after the end of heating. This duration of the experiment did not lower the accuracy, as the experiments were carried out in adiabatic conditions.

The second question was solved by breaking unevacuated ampoules without fiber, with thicker walls than those used in the experiments, in the calorimeter. The thermal effect associated with breaking of the ampoules was found to be negligible. The third question was investigated by breaking empty evacuated ampoules of definite volume in the calorimeter. In these cases the thermal effect was appreciable, and was on the average 0.03 cal per milliliter of the ampoule volume. In the subsequent work this value was used for introducing a correction when calculating the results. The reproducibility of the results was checked by determining the heats of wetting of hydrate cellulose fibers, both bone-dry and containing definite amounts of water [2]. These fibers were chosen because their heat of wetting is considerably higher than that of polyamide fibers, and, in addition, the literature contains a number of papers [2,3,6,8] with the data of which the results obtained could be compared.

---

[1] Chilikin's data [6] are not included in Table 1, as they differ sharply from values obtained by others, apparently because of differences in the fibers studied.

[2] Graduate of Moscow State University, A.P.Anuchina, participated in this part of the work.

The results of the determinations of heats of wetting of hydrate cellulose fibers are shown in Table 1.

As is seen from Table 1, our results agree closely with the data of Rees and Guthrie. Deviations from the results of other authors are apparently to be explained by differences in the structure of the fibers studied.

Preparation of the specimens. The material studied was polyamide fiber (poly-ε-caprolactam) of the normal production type, unoriented and oriented. The preliminary preparation of the specimens was analogous to that used in our work on the study of sorption of water by Capron fiber [1]. The lubricant was removed by extracting the fiber with carbon tetrachloride in a Soxhlet apparatus. Low-molecular fractions were removed by repeated washing of the fiber with hot water.

The material was dried in a vacuum apparatus (residual pressure of $1 \cdot 10^{-6}$ mm mercury) at room temperature in ampoules joined in groups of 4 into a comb.[1] The weight of the dry fiber in the ampoules was determined as follows: the four ampoules were simultaneously filled with air-dry fiber. The amount of fiber placed in each ampoule was determined by weighing. All the four ampoules were then fused to the " comb" and connected to the vacuum installation. At the end of drying (the pumping time needed for this was established previously by special experiments) one of the four ampoules was detached from the comb and the weight of dry fiber in it was determined after opening from the difference in weight between the detached ampoule and the weight of the glass. As all four ampoules were dried in analogous conditions, it could be safely assumed that in the remaining ampoules of the given set the percentage of moisture removed during drying was the same.

## RESULTS OF DETERMINATIONS

Early in our investigations it was noticed that the heat of wetting of Capron fiber depends on its "age". This made it necessary to carry out special experiments to determine the effect of "age" of the fiber on its sorptional properties. Without elucidating this question we could not make a comparison of the results of our measurements. Table 2 shows the results of measurements of the heat of wetting of unoriented capron fiber with water as a function of its "age".

It is seen from the data shown in Table 2 that the heat of wetting of unoriented fiber decreases by almost 15% and reaches a constant value (within the limits of experimental error) only after 120 days.

In a study of the effect of "age" on the heat of wetting of oriented fiber by water (Table 3) as distinct from unoriented, it was found that the heat of wetting differs for fibers from different production batches, which is apparently due to inhomogeneity of the fibers, caused by different conditions of formation. The results of the determinations are shown in Table 3.

Table 4 shows the results of determinations of the heats of wetting by water of oriented fibers from one production batch.

---

[1] In some experiments the temperature of drying was raised to 120-135°. No differences in the heat of wetting of such fibers were found.

TABLE 2

Integral Heat of Wetting of Unoriented Fiber by Water as a Function of "Age"

| Age of fiber, days | Dry weight, g | Heat capacity of system, cal | Temperature rise, °C | Thermal effect, cal | Heat of wetting, in cal/g dry substance | Mean value, cal/g dry substance |
|---|---|---|---|---|---|---|
| 10 | 0.3968 | 35.49 | 0.080 | 2.66 | 6.70 | 6.78 ± 0.07 |
| | 0.7293 | 35.83 | 0.146 | 5.05 | 6.92 | |
| | 0.4060 | 35.73 | 0.082 | 2.75 | 6.76 | |
| | 0.6515 | 35.89 | 0.127 | 4.38 | 6.72 | |
| 45 | 0.7965 | 35.63 | 0.150 | 5.16 | 6.49 | 6.44 ± 0.06 |
| | 0.7058 | 35.67 | 0.131 | 4.49 | 6.36 | |
| | 0.7132 | 35.87 | 0.132 | 4.55 | 6.38 | |
| 60 | 1.3625 | 36.25 | 0.242 | 8.59 | 6.30 | 6.30 ± 0.04 |
| | 1.3383 | 36.02 | 0.237 | 8.36 | 6.24 | |
| | 1.1570 | 36.25 | 0.208 | 7.36 | 6.36 | |
| 75 | 0.4429 | 36.03 | 0.081 | 2.74 | 6.18 | 6.09 ± 0.06 |
| | 0.4059 | 35.64 | 0.074 | 2.46 | 6.06 | |
| | 0.5240 | 35.81 | 0.093 | 3.15 | 6.03 | |
| 75 1) | 0.4695 | 35.60 | 0.083 | 2.77 | 5.91 | 5.95 ± 0.08 |
| | 0.6160 | 35.71 | 0.110 | 3.75 | 6.08 | |
| | 0.5472 | 35.78 | 0.095 | 3.22 | 5.81 | |
| 60 2) | 0.5517 | 35.65 | 0.1005 | 3.41 | 6.16 | 6.13 ± 0.03 |
| | 0.5089 | 35.42 | 0.0935 | 3.13 | 6.15 | |
| | 0.4151 | 35.62 | 0.0895 | 3.01 | 6.08 | |
| 120 | 0.4562 | 35.76 | 0.0760 | 2.62 | 5.75 | 5.72 ± 0.05 |
| | 0.5819 | 35.64 | 0.0990 | 3.36 | 5.77 | |
| | 0.7781 | 35.94 | 0.1280 | 4.41 | 5.65 | |
| 140 | 0.7138 | 35.83 | 0.1210 | 4.15 | 5.82 | 5.84 ± 0.02 |
| | 0.6147 | 35.73 | 0.1060 | 3.60 | 5.86 | |
| 240 | 0.6216 | 35.65 | 0.1085 | 3.69 | 5.93 | 5.93 ± 0.08 |
| | 0.7801 | 35.80 | 0.1370 | 4.73 | 6.05 | |
| | 0.6513 | 35.62 | 0.1115 | 3.79 | 5.82 | |
| 330 | 0.6241 | 35.52 | 0.1080 | 3.61 | 5.80 | 5.85 ± 0.03 |
| | 0.5854 | 35.39 | 0.1025 | 3.45 | 5.89 | |
| | 0.5254 | 35.47 | 0.1035 | 3.49 | 5.86 | |

1) Dried at 120-135°

2) Fiber from another batch.

TABLE 3

Integral Heat of Wetting by Water of Oriented Fibers from Different Production Batches

| Age of fiber, days | Dry weight, g | Heat capacity of system, cal | Temperature rise, °C | Thermal effect, cal | Heat of wetting in cal/g dry substance | Mean value, cal/g dry substance |
|---|---|---|---|---|---|---|
| $22_1$ | 0.9351 | 35.86 | 0.1410 | 4.88 | 5.21 | 5.28 ± 0.05 |
| | 0.9019 | 36.03 | 0.1390 | 4.83 | 5.35 | |
| | 0.7171 | 35.72 | 0.1110 | 3.79 | 5.27 | |
| $90_3$ | 0.8674 | 35.84 | 0.1210 | 4.16 | 4.79 | 4.73 ± 0.12 |
| | 0.8351 | 35.89 | 0.1180 | 4.05 | 4.85 | |
| | 0.7670 | 35.77 | 0.1030 | 3.50 | 4.56 | |
| $150_3$ | 0.5931 | 35.58 | 0.1045 | 3.54 | 5.07 | 6.02 ± 0.05 |
| | 0.6710 | 35.67 | 0.1200 | 4.60 | 6.11 | |
| | 0.6931 | 35.63 | 0.1220 | 4.16 | 6.00 | |
| $270_2$ | 0.5487 | 35.34 | 0.0930 | 2.11 | 5.66 | 5.63 ± 0.03 |
| | 0.5258 | 35.50 | 0.0880 | 2.94 | 5.59 | |

Note. Subscript numberals 1,2,3 indicate fibers from different production batches.

TABLE 4

Integral Heat of Wetting of Oriented Fiber from a Single Production Batch

| Age of fiber, days | Dry weight, g | Heat capacity of system, cal | Temperature rise, °C | Thermal effect, cal | Heat of wetting in cal/g dry substance | Mean value, cal/g dry substance |
|---|---|---|---|---|---|---|
| 39 | 0.6176 | 35.52 | 0.1030 | 3.50 | 5.66 | 5.67 ± 0.02 |
| | 0.7542 | 35.88 | 0.1230 | 4.26 | 5.65 | |
| | 0.4360 | 35.64 | 0.0740 | 2.49 | 5.70 | |
| 90 | 0.4455 | 35.32 | 0.0750 | 2.48 | 5.56 | 5.57 ± 0.01 |
| | 0.4574 | 35.39 | 0.0770 | 2.55 | 5.58 | |
| 197 | 0.2454 | 35.35 | 0.0490 | 1.55 | 6.31 | 6.30 ± 0.005 |
| | 0.4999 | 32.99 | 0.1010 | 3.15 | 6.30 | |
| 224 | 0.5286 | 34.01 | 0.0990 | 3.25 | 6.15 | 6.22 ± 0.07 |
| | 0.4731 | 33.70 | 0.0930 | 2.98 | 6.29 | |

It is seen from the data shown in Table 4 that changes of the heat of wetting of oriented fiber differ from the corresponding changes of unoriented fiber (Table 2) both in magnitude and in sign. The thermal effect values reach a constant value after 190 days.

As no noticeable changes in chemical composition took place during storage of the fiber, changes in the heat of wetting can only be attributed to changes in the physical structure of the fibers themselves, which would be primarily reflected in the nature and magnitude of the forces of intermolecular action in the polycaprolactam.

It can be easily seen that the nature of these structural changes in polyamides must consist of an increase or decrease of crystalline order, that is, changes in the degree of defectiveness of the structural lattice of the crystalline material. It is evident that changes of heat of wetting with "age" will not occur or will be minimal if the crystal lattice has a maximum state of order and is free of defects.

The following general conclusions may be drawn from the experimental data obtained. The integral heat of wetting of Capron fiber by water depends on its physical structure, apparently manifested in differences in the energy of intermolecular bonding characteristic for different fiber structures. Variation of the heat of wetting with "age" of the fiber indicates the existence of a non-equilibrium state of the polycaprolactam structure. Decrease of the heat of wetting of unoriented fiber with "age" apparently indicates that attainment of equilibrium proceeds in the direction of a more perfect order of the structure. Increase of the heat of wetting with "age" for a single production batch of oriented fiber is apparently to be explained by relaxation processes in the oriented fiber.

## SUMMARY

1. A description is given of a calorimetric technique for the measurement of small thermal effects of wetting of polyamide fibers by water.

2. The integral heats of wetting of Capron fibers of different physical structure by water have been measured. Differences are shown in the values of the integral heats of wetting of the fibers, and in the nature of the variation of these heats with "age".

3. The view is put forward, on the basis of measurements of the integral heat of wetting of Capron fiber with water, that the nature of physical "aging" consists of changes in the character and magnitude of the forces of intermolecular action.

All-Union Research Institute for
Artificial Fibers

Received April 8, 1953

## LITERATURE CITED

[1] N.V.Mikhailov, E.Z.Fainberg, and S.M.Skuratov, Colloid J., 15, No.4, 271 (1953). 1)

[2] Hermans, Contribution to the Physics of Cellulose Fibres, pp 34-39, (1946).

[3] W.H.Rees, J. Text. Inst. 39, 351 (1948).

[4] Lipsett, Johnson and Maass, J. Am. Chem. Soc., 1927, 49, 925 (1940).

[5] S.M.Skuratov, Colloid J., 9, No. 2, 133 (1947).

[6] Chilikin, J. Applied Chem., 3, 221 (1930).

[7] J.G.Guthrie, J. Text. Inst. 40, 489 (1949).

[8] M. Wahba, J. Phys. and Coll. Chem. 52, 1197 (1948).

---

1) See Consultants Bureau English Translation, p. 279.

# FLOW OF CLAY SUSPENSIONS IN PIPES

B. S. Filatov

Problems of the calculation of flow of non-Newtonian liquids increasingly occupy the attention of investigators. This is explained by the fact that the field of application in technology of substances with anomalous viscosity is continuously widening. An important place among these substances is occupied by substances which obey the Shvedov-Bingham law [1], such as suspensions of clay and peat, drainage deposits, etc. Calculations of pressure losses in the flow of such substances in pipes were previously made with the empirical formulas of Tsarevich [2] and Shumilov [3] for drilling muds, of Petrenko [4] and the MTI1) Chair of Physics [5] for peat suspensions, and from experimental graphs [6]. Most empirical formulas do not make due allowance for the effect of the physical properties of suspensions (density, structural viscosity) on the p pressure loss in steady and turbulent flow. Therefore these methods of calculation give rise to considerable errors when the conditions of the problem differ from the conditions of the experiments on which the formulas are based.

In recent years a number of papers has been published in which the fundamentals of the theory of flow of viscoplastic bodies have been put forward [1,2,7]. However, these papers still do not fully clarify the problem. The theoretical views are not confirmed by sufficient experimental material; for example, the recommendations for calculation given in the paper by Shishchenko [2] do not have an adequate basis; his formulas for determining the coefficient of resistance in the turbulent flow of clay suspensions give values which are several times greater than the corresponding values for water. This contradicts the experimental data of Evilevich [6] and others, who found pressure losses in the flow of suspensions in pipes at high velocities to be not greater, but less than the losses for water, other conditions being equal.

The experiments described in the present paper were carried out in order to improve the calculation formulas based on the theory of motion of viscoplastic bodies, for the calculation of pressure losses in the flow of clay suspensions of low concentrations in pipes of circular section.

The experimental installation is shown in Figure 1. The liquid is fed by the centrifugal pumps 1 from a cemented pit, divided by an impervious partition into receiving 2 and measuring 3 parts, into the measuring system, consisting of standard gas pipes 4, 5, and 6, 8 m in length and with internal diameters of 6.72, 5.29, and 4.00 cm, respectively. For the measurement of pressure drop in these pipes during the passage of liquid, openings 5 mm in diameter were drilled exactly perpendicular to the axis of the pipe. Opposite these openings, the pipes were fitted with pressure gage rings 7, welded to the pipes, with internal annular grooves and with connecting branches for joining the rings to manometers. The lengths of the entry and exit equalizing regions (regions of the pipe from the ring to which the manometer was attached to the end of the pipe) and of the working region between the pressure gage rings are given in Table 1.

The pressure gage rings were attached to rubber tubes, the other ends of which led to the separating vessels 8. The separating vessels were joined by tubes to differential U-shaped glass manometers 10, 2 m in length. One mano-

---

1) MTI = Moscow Instituteof Technology.

meter was filled with carbon tetrachloride, and two with mercury. The first manometer was used for measuring pressure drops of up to 1 mm water column. Pressure drops from 1 to 50 mm water column were measured by the mercury manometers. Still greater pressure drops were measured by the dial manometers 9, also connected to the separating vessels.

TABLE 1

Basic Dimensions of the Working Pipes of the Experimental Installation

| Internal diameter D of the pipe, in cm | Entry region |  | Exit region |  | Working region in m |
|---|---|---|---|---|---|
|  | Length L in m | L/D | Length L in m | L/D |  |
| 6.72 | 4.72 | 70 | 1.28 | 19 | 2.00 |
| 5.29 | 2.20 | 42 | 0.80 | 15 | 5.00 |
| 4.00 | 2.00 | 50 | 2.00 | 50 | 4.00 |

Entry of the thixotropic clay suspension into the tubes joining the presure gage rings to the separating vessels during the determinations could cause errors in the pressure measurements. Therefore the separating vessels were joined to a pipeline from a high pressure water supply, and before each reading of pressure drop the tubes joining the pressure gage rings to the separating vessels were washed through with water. The consumption of liquid in each experiment was measured volumetrically by means of the measuring tank 3.

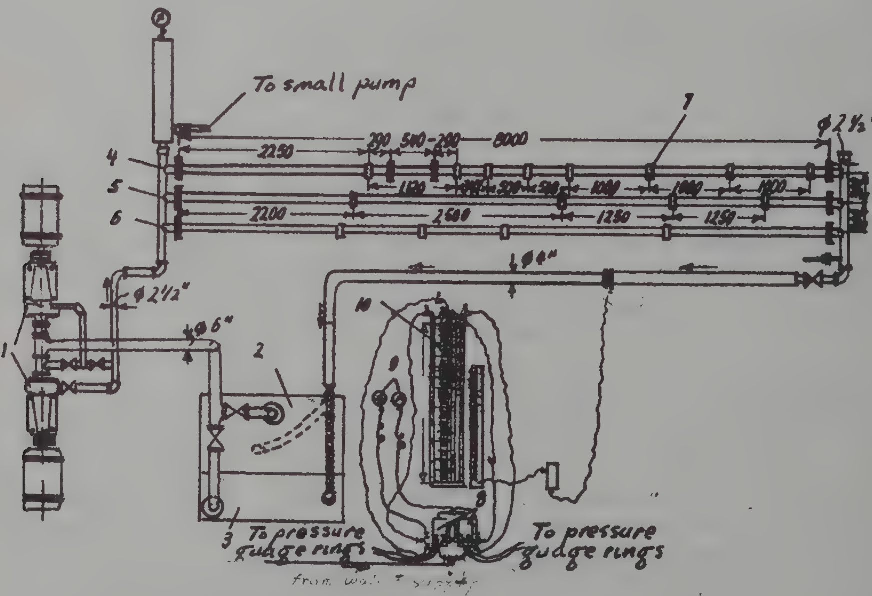

Fig. 1. Diagram of the experimental installation (explanations in text).

Description of the experiments. Four specimens of clay suspensions were studied. Suspensions 1,2, and 3 were made from powdery bentonite clay of Askan origin (Georgia), and suspension 4 from clay from Kudinovo station of the Moscow-Kursk railway. The properties of the suspensions changed during the work not only through changes of suspensions according to the designed program of experiments, but in the intervals between changes as the result of progressive dispersion of the clay particles (primary suspension 1) and of the gradual diulution of the clay suspensions by the washing of the connecting tubes, and from water in the centrifugal pump glands (suspensions 2 and 4).

The specific gravity $\gamma$, dynamic resistance to shear $\tau_0$, and structural viscosity $\eta$ of the clay suspensions are shown in Table 2.

TABLE 2

Properties of Clay Suspensions.

| Suspension | Clay type | $\gamma$ g/cm$^3$ | $\tau_0$, dynes/cm$^2$ | $\eta$, Poises |
|---|---|---|---|---|
| 1 | Askangel | 1.045 | 30-45 | 0.04 |
| 2 | Askangel | 1.047 | 108-140 | 0.10 |
| 3 | Askangel | 1.042 | 82 | 0.087 |
| 4 | Kudinovo | 1.208-1.230 | 145-180 | 0.125-0.255 |

The total number of experiments with clay suspensions was about 500. In addition, the installation was calibrated twice against water before and after the experiments with clay suspensions. The results of these experiments are shown in Figures 2 and 3. The abscissa axis gives the liquid flow in liters per second, and the ordinate axis shows the pressure drop per 1 m length of pipe, shown in Figure 2 in mm water column, and in Figure 2 in meters of the column of the piped liquid. The following conclusions may be drawn from Figures 2 and 3:

1. The positions of the points for clay suspensions clearly show the existence of two different flow regimes - a structural regime at low rates and a turbulent regime at high rates.

The structural regime has the following characteristics; a) the pressure losses greatly exceed the pressure losses for water for the same volume of liquid, and their magnitude strongly depends on the properties of the suspensions ; b) the pressure loss depends linearly on the total amount of liquid. For suspensions 1-3 with low structural viscosity the pressure losses depend little on the total volume. Increase of the total volume several-fold increases the pressure loss only by a few percent; c) when the pressure losses for clay suspensions become close in magnitude to the pressure loss for water, there is a fairly well-defined transition to turbulent flow.

The characteristics of the turbulent regime are as follows: a) the structural viscosity and dynamic resistance to shear do not affect the magnitude of the pressure losses; b) the pressure losses are directly proportional to the specific gravity of the liquid. This is clearly seen in Figure 2, where the ordinate axis gives the pressure losses in mm water column; c) the experimental points for clay suspensions on the $h = f(Q)$ graphs lie on a steeper line than the experimental points for water. This shows that the exponent in the exponential dependence of the pressure loss on the consumption of liquid is greater for clay suspensions than for water

2. The almost linear disposition of the points in the structural regime region for clay suspensions with constant structural viscosity and dynamic resistance to shear (for example, suspensions 3 and 4 in Figure 2, and all the suspensions in Figure 3) is evidence of the validity, for the clay suspensions studied, of the Shvedov-Bingham hypothesis:

$$\tau = \eta \frac{dv}{dn} + \tau_0$$

and of Buckingham's Equation:

$$Q = \frac{\pi R^3}{4\eta}\left(\frac{PR}{2L} - \frac{4}{3}\tau_0 + \frac{8}{3}\,\frac{L^3\tau_0^4}{P^3R^3}\right), \qquad (1)$$

where $\tau$ is the tangential stress in the clay suspension; $\tau_0$ is the dynamic resistance to shear; $\eta$ is the structural viscosity; $\frac{dv}{dn}$ is the gradient of the shear rate in a direction perpendicular to the direction of the velocity; $Q$ is the total volume flow of liquid in the pipe; $R$ is the radius of the pipe; $L$ is the length of the pipe; $P$ is the pressure drop in the pipe over the length $L$. The influence of the last term in the right-hand side of Equation (1), which causes deviations of the relationship $Q = f(P)$ from the linear, is noticeable only for very small total volumes.

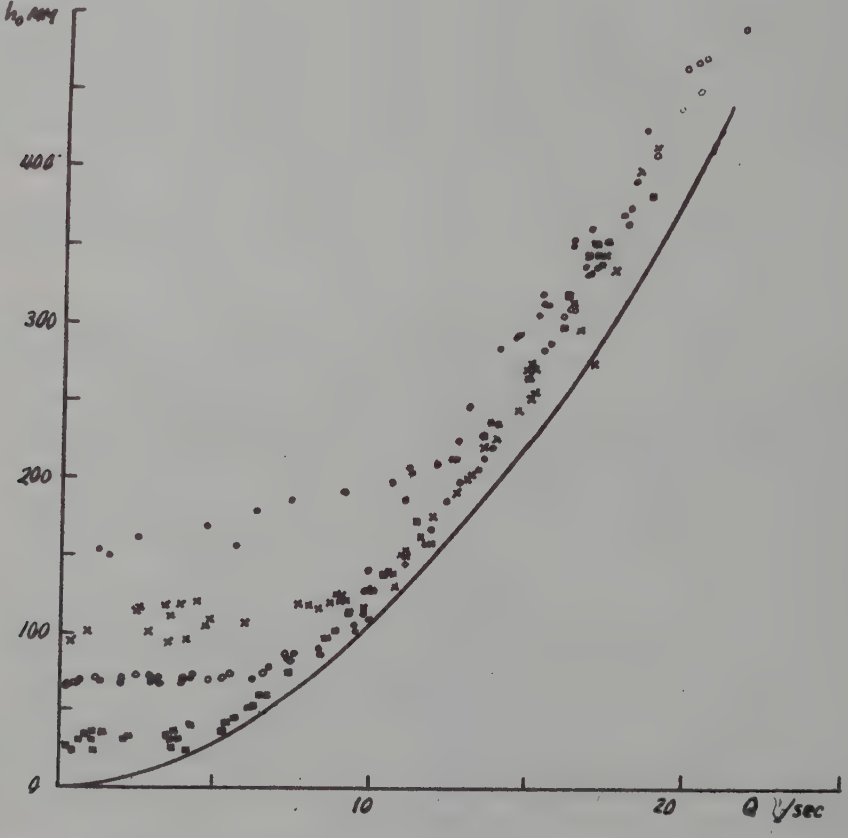

Fig. 2. Pressure loss in pipes with internal diameter 6.72 cm; □ - suspension No.1; × - No.2; ○ No.3; ● - No.4 (see Table 2).

3. In turbulent flow, pressure losses expressed in terms of meters of a column of the suspension, are greater for the less concentrated suspensions 1 and 3 than for the more concentrated suspension 2 (see Figure 3).

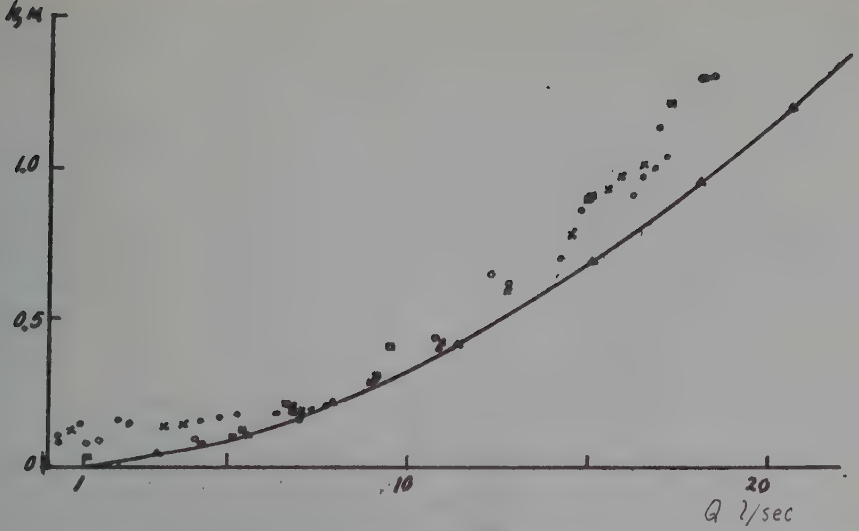

Fig. 3. Pressure loss in pipes with internal diameter 5.3 cm; △ -water; □ - suspension No.1; × - No.2; ○ - No.3; ● - No.4.

These data were also examined by another method. As was shown by Tyabin [7], Equation (1) may, by neglecting the last term of the right-hand side, be given in the criterial form as follows:

$$\frac{32L\gamma v^2}{PD} = \frac{1}{\frac{\eta}{\gamma vD} + \frac{1}{6}\frac{\tau_0}{\gamma v^2}}, \qquad (2)$$

where $v = \frac{Q}{R^2}$ is the average volume rate of flow of the liquid in the pipe, and $\gamma$ is the density of the liquid.

The expression in the left-hand side is the value $64/\lambda$, where $\lambda$ is the expression for the coefficient of resistance in the D'Arcy Formula:

$$\lambda = \frac{2PD}{L\gamma v^2}.$$

The right-hand side contains the expression for a certain criterion

$$Re^* = \frac{1}{\frac{1}{Re} + \frac{1}{6}B}, \qquad (3)$$

which Shishchenko [2] termed the " generalized Reynolds criterion".

The values of $Re^*$ and $\lambda$ were calculated for each experiment and the results plotted on a logarithmic scale. The graph is shown in Figure 4. The same graph also gives the data for water, obtained during calibration (crosses).

The points for the experimental data fall regularly on this graph, which

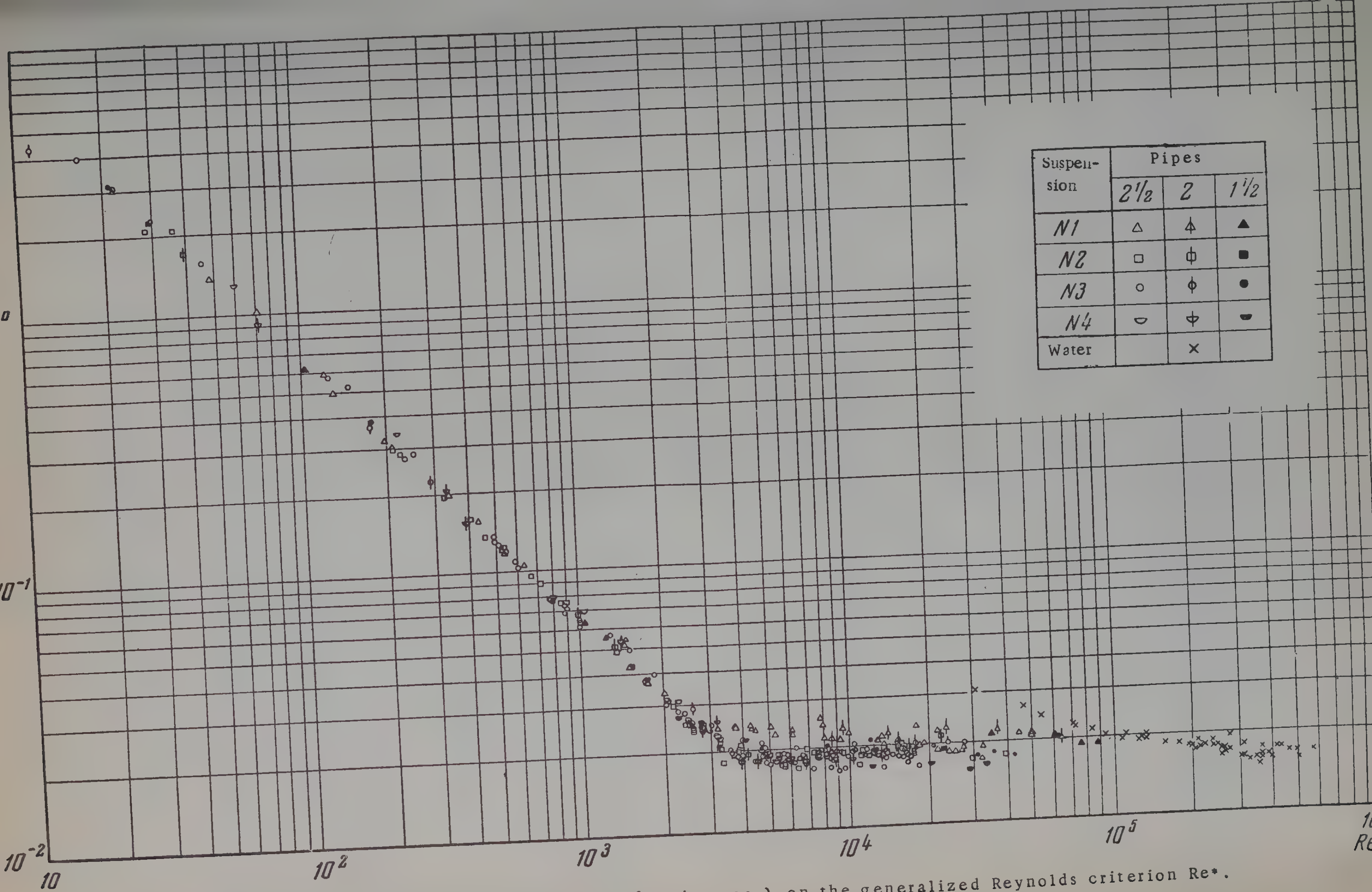

Fig. 4. Dependence of the coefficient of resistance λ on the generalized Reynolds criterion Re*.

confirms that the choice of dimensionless criteria is valid. When $Re^* < 10$, the experimental data are found to deviate from the line $\lambda = \frac{64}{Re^*}$ (not shown in Figure 2). In this region the effect of the undeformed core of the stream, which is neglected in the derivations for the expression for $Re^*$, becomes considerable, and the criterion $Re^*$ loses its meaning. It is evident that the relationship given by Equation (2) is a general one both for clay suspensions and for water, and consequently also for other non-Newtonian liquids.

For more concentrated clay suspensions the transition to turbulent flow occurs at higher values of $Re^*$ than for less concentrated suspensions. For suspension 1 the critical value $Re^*_{cr}$ is 2800, and for suspensions 2-4 $Re^*_{cr} = 3800\text{-}4000$.

It must be explained that although suspensions 2 and 3 have almost the same specific gravity as suspension 1, their consistency is much greater. The clay particles in the suspension became more and more dispersed during the experiments, and the amount of water of hydration increased correspondingly with the degree of dispersion of the clay particles. Therefore both the structural viscosity and the dynamic resistance to shear are much greater for suspensions 2 and 3 than for 1.

For turbulent flow, the value of the resistance coefficient $\lambda$ is less for more concentrated than for less concentrated suspensions.

These facts are in contradiction to the theory of "early turbulence" put forward by Wo. Ostwald [8]. According to the theory of "early turbulence", the solid phase particles in colloidal solutions are nuclei of turbulent pulsations; they cause the flow to become turbulent at lower flow rates than is the case for the pure dispersion medium in the same conditions.

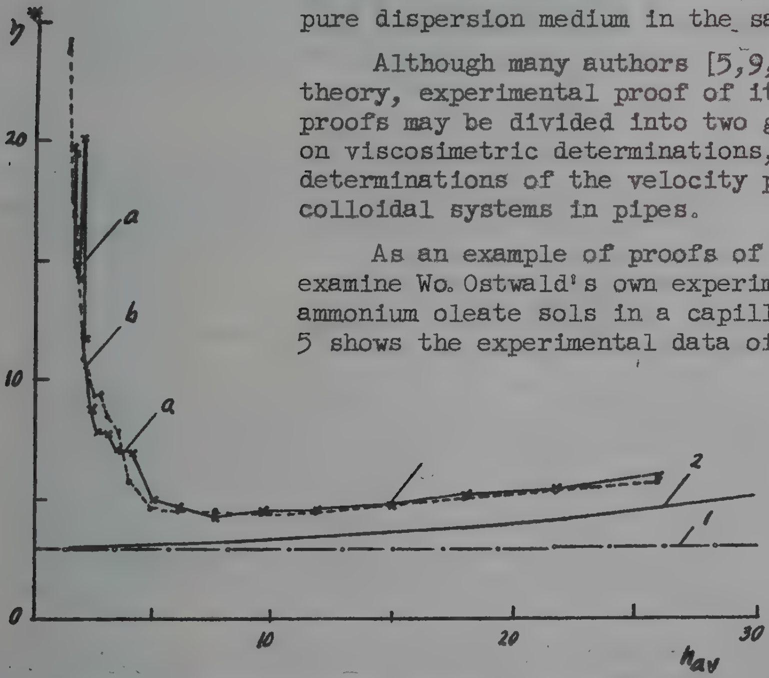

Fig. 5. Ostwald's experimental data; 1) true liquid in laminar flow; 2) water; a) "early turbulence"; b) structural branch; c) turbulence branch.

Although many authors [5,9,10,11] agree with this theory, experimental proof of it is scanty [12]. Such proofs may be divided into two groups: 1) those based on viscosimetric determinations, and 2) those based on determinations of the velocity profile in the flow of colloidal systems in pipes.

As an example of proofs of the first group, let us examine Wo. Ostwald's own experiments [8] on the flow of ammonium oleate sols in a capillary viscosimeter. Figure 5 shows the experimental data of Wo Ostwald. The abscissa axis gives the values of the pressure $h_{av}$ for which efflux of the liquid occurs, and the ordinate axis gives the values of the "apparent viscosity" $\eta^* = \frac{h_{av}}{\Delta V}$, where $V$ is the volume of liquid which flows out in a given time. For

Newtonian liquids the relationship $\eta = \underline{f}(\underline{h}_{av})$ for laminar flow is given by a straight line parallel to the abscissa axis. In presence of structural viscosity, the value of the apparent viscosity $\eta*$ decreases with increase of $\underline{h}_{av}$. In turbulent flow, on the other hand, $\eta*$ increases with increase of $\underline{h}_{av}$.

Wo. Ostwald gives the name of "structural" or "early turbulence" to small accidental rises in $\eta*$ (see Figure 5,a) which are sometimes observed on the structural branch and which are then followed by decreases of apparent viscosity until true turbulence occurs, which takes place at sufficiently high velocities and pressures. As a rule, repeat experiments with the same suspensions do not show these increases of viscosity, as can be seen from Figure 5 (dotted line). As Wo. Ostwald himself notes, he was able to observe these effects, apart from ammonium oleate, only for sols of certain organic dyes under definite conditions of measurement.

There is every reason to suppose that such accidental increases of structural viscosity at low shear rates are explained not by turbulence, but by irregular destruction of the thixotropic structure of certain colloidal systems, and therefore it is erroneous to attribute any general significance to this effect.

The proofs of the second group are based on the external resemblance between the flatter profiles of the flow rate distributions for non-Newtonian liquids with a turbulent profile of rate distributions, as compared with parabolic profile for the laminar flow of Newtonian liquids. It is, however, clear that it is impossible to prove the presence of turbulence on the basis of rate profiles only, without an examination of the nature of motion of different streams in the flow and of the dependence of pressure losses on the average rate of flow. Thus the theory of "early turbulence" as a general law for the motion of colloidal systems and suspensions, should be rejected.

## SUMMARY

1. Technical calculations for the flow of colloidal systems, which obey the Shvedov-Bingham law, in pipes of circular section may be made with the use of the usual D'Arcy formula. Here the resistance coefficient for structural flow regime should be determined from the Formula

$$\lambda = \frac{64}{Re*}.$$

For turbulent flow of clay suspensions of low concentrations and similar systems, and for pipes of diameters of the order of 5-10 cm, values of λ from 0.017 to 0.025 should be used. For more concentrated suspensions and for pipes of other diameters it is necessary to carry out further investigations.

2. In the selection of a value of λ for turbulent flow it is necessary to take into account the concentration of the solid phase in the system and also solvation of the particles, and to select lower values of λ for more concentrated systems, and vice versa.

3. To determine the flow regime it is necessary to calculate the value of the generalized Reynolds criterion Re*, which has a meaning at values > 10. The critical values of the criterion Re* at which structural flow passes into turbulent, lie in the limits of 2500 to 4000, and are determined by the content of solid phase in the system, with allowance for the hydration coatings of the particles.

The I.M. Gubkin Petroleum Institute, Moscow

Received June 22, 1953

# LITERATURE CITED

[1] M.P.Volarovich and A.M.Gutkin, Colloid J., 15, No. 2, 155 (1953).1)

[2] R.I.Shishchenko, Hydraulics of Clay Suspensions, Azerbaidzhan Petroleum Press (1951).

[3] P.P.Shumilov, Theoretical Bases of Turbine Drilling, State Fuel Technology Press (1943).

[4] F.F.Petrenko, Trans. VIMT,2) Nos. 1-4 (1938).

[5] M.P.Volarovich and co-workers, Colloid J., 8, Nos. 1-2,9 (1946).

[6] A.Z.Evilevich, Removal of Drainage Deposits by Pressure Pipes, State Construction Press (1939).

[7] N.V.Tyabin, Colloid J., 13, No. 1, 55 (1951); 14, No. 4, 270 (1952).3)

[8] Wo. Ostwald, Koll.-Z. 68, No. 2, 155, 190 (1927).

[9] N.N.Kulakov, Introduction to the Physics of Peat, GEEI (1947).

[10] P.A.Rebinder, paper in "Progress in Clays and Clay Suspensions", State Fuel Technology Press (1940).

[11] H. Umstätter, Strukturmechanik, Th. Steinkopff, (1948).

[12] W. Philippow,, Viscosität der Kolloide, Th. Steinkopff, (1944).

---

1) See Consultants Bureau Translation, p. 153.

2) VIMT = All-Union Sci. Research Inst. for Mechanization of the Peat Industry.

3) See Consultants Bureau Translation, p. 297.

# EFFECT OF ELECTROLYTES OF THE AQUEOUS PHASE OF STYRENE EMULSIONS ON THE DISPERSIVITY OF THE LATEXES FORMED

A.I.Yurzhenko and V.P.Gusyakov

In our previous communications [1,2] we presented the results of investigations of the dependence of the dispersivity of synthetic latexes formed in emulsion polymerization on the extent of polymerization, concentration, and nature of the emulsifier and monomer. It was shown that knowledge of the factors which determine the dimensions of latex particles makes it possible to draw definite conclusions concerning the topochemistry of emulsion polymerization of hydrocarbons and the kinetics of the polymerization process. In this paper we present experimental data on the effect of electrolytes (acids, bases, salts) contained in the aqueous phase of the emulsion of the polymerizing monomer, styrene, on the dimensions of the latex particles formed.

Elucidation of the effect of electrolytes contained in the aqueous phase of the emulsion of the polymerizing monomer on the dispersivity of the latexes formed is of interest for the development of a general theory of polymerization processes. Indeed, if the polymerization process takes place in the aqueous phase of the emulsion, in the emulsifier micelles, then the electrolytes in the aqueous phase should have an influence on the size of the polymer particles in the latex. This follows from the fact that additions of electrolytes to solutions of soaps and like substances may vary the size of the micelles of the latter considerably, and, consequently, also their concentration (at a constant molal concentration). This, in turn, should lead to changes in the number of polymer particles in the latex, and consequently also of their volume for a given content of polymer in the latex.

In addition to such purely colloido-chemical effects, electrolytes, particularly bases and acids, may change the rate (and the direction) of the decomposition of peroxide initiators leading to the formation of free radicals which initiate the polymerization process. This may vary the conditions of polymer accumulation in the monomer emulsion, and consequently also the dimensions of the polymer particles in the latexes formed.

The technique for the preparation of synthetic latexes in laboratory conditions was described previously [2]. The emulsifier used was Nekal (Na salt of dibutyl-α-naphthalenesulfonic acid). The pH of the aqueous phase of the monomer emulsion was varied by addition of $Na_2CO_3$, NaOH, and $H_2SO_4$ to the aqueous phase. The polymerization initiators were potassium persulfate (water-soluble), dimethylphenyl carbinol hydroperoxide, and benzoyl peroxide (oil-soluble).

The degree of dispersion of the different latexes was compared under the condition that the extent of polymerization S (percentage of monomer polymerized) in them was similar, as the extent of polymerization has a significant effect on the dimensions of latex particles [1]. The latex was diluted three times and centrifuged to remove unpolymerized monomer. Experiment showed that with such treatment of the latex nearly all the remaining monomer floated up in the form of a clearly defined oily layer; the monomer layer was then carefully separated from the remaining latex.

The polymer content of the latex was determined from the dry residue, the results obtained being compared with the extent of polymerization determined from the volume contraction (the polymerization was carried out in special dilatometers). The results obtained by these two independent methods were usually in good agreement. The degree of dispersion of the synthetic latexes was determined from the intensity of light scattering (that is, the tubidity $\tau$), the turbidity being plotted against the concentration. The dispersivity was characterized by the turbidity for equal concentrations of polymer in the latex. The radius of the polymer particle, r, in the latexes was calculated with the aid of the Rayleigh formula. The technique of turbidity measurements and determination of r was described previously [1,2].

## EXPERIMENTAL 1)

Effect of acids and bases. The concentration of $H^+$ and $OH^-$ ions in the aqueous phase of the monomer emulsion significantly affects the rate of polymerization and the molecular weight of the polymer formed. As the pH of the aqueous phase decreased, the polymerization process was retarded (Figure 1) and a product of lower molecular weight was formed (Table 1).

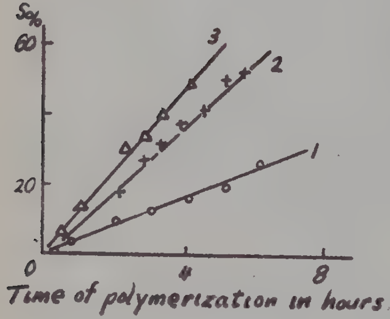

Fig. 1. Effect of pH of the aqueous phase of styrene emulsion on its polymerization rate. Emulsifier 0.5% Nekal, initiator 0.01 M $K_2S_2O_8$, at pH values of: 1) 1.8; 2) 6.8; 3) 11.8.

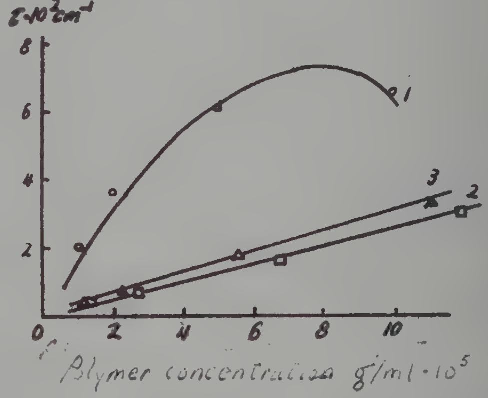

Fig 2. Effect of pH of the aqueous phase of the original styrene emulsion on the dispersivity (turbidity) of the latexes formed. Emulsifier 0.5% Nekal, initiator 0.005 M $K_2S_2O_8$ polymerization temperature 50°;
1) pH = 1.2, S = 61%, r = 60 mμ;
2) pH = 6.8, S = 68%, r = 36 mμ;
3) pH = 10.6, S = 80%, r = 39 mμ.

Our investigations showed that the degree of dispersion of latexes prepared by the polymerization of styrene in different media, differs also. The effect of pH of the aqueous phase of the emulsion on the size of the particles in the latexes, with $K_2S_2O_8$ initiator, is shown in Figure 2. Analogous results are seen if phenyl dimethyl carbinol hydroperoxide is used (Table 2).

---

1) M. S. Shteinberg participated in the experiments.

TABLE 1

Dependence of the Molecular Weight of Polystyrenes on the pH of the Aqueous Phase of the Styrene Emulsion

(Emulsifier 0.5% Nekal, polymerization temperature 55°)

| Initiator | Molecular Weight | |
|---|---|---|
| | Acid Medium (pH 1.25) | Alkaline Medium (pH 10.55 - 11.5) |
| $K_2S_2O_8$ | 52000 | 310000 |
| Phenyldimethyl carbinol hydroperoxide | 85500 | 160000 |
| Benzoyl peroxide | 41000 | 99000 |

Note. The molecular weight was determined viscosimetrically.

TABLE 2

Dependence of the Size of the Polymer Particles in Styrene Latexes on pH of the Aqueous Phase of the Original Emulsion of Styrene.

| Initiator | Polymerization temperature in °C | pH of the aqueous phase in the styrene emulsion | | | | | | | | | |
|---|---|---|---|---|---|---|---|---|---|---|---|
| | | 1.3[1] | | 3.4 | | 6.8 | | 10.6 | | 11.5 | |
| | | S% | rmμ | S% | rmμ | S% | rmμ | S% | rmμ | S% | rmμ |
| Emulsifier 0.5% Nekal | | | | | | | | | | | |
| $K_2S_2O_8$ 0.5% | 45 | 60 | 84 | - | - | - | - | 70 | 51 | - | - |
| same 1% | 45 | 65 | 77 | - | - | - | - | 70 | 34 | - | - |
| same 0.18% | 40 | 17 | 53 | 42 | 39 | - | - | 39 | 42 | - | - |
| same 0.18% | 45 | 73 | 87 | 93 | 44 | - | - | | - | - | - |
| same 0.18% | 55 | 62 | 90 | 76 | 41 | - | - | 45 | 53 | - | - |
| same 0.18% | 65 | 31 | 108 | 87 | 45 | - | - | 90 | 48 | - | - |
| Hydroperoxide 0.02M | 45 | - | - | - | - | 70 | 48 | - | - | 82 | 40 |
| same 0.02M | 50 | 60 | 53 | - | - | 73 | 43 | - | - | 64 | 37 |
| same 0.02M | 65 | - | - | - | - | 65 | 59 | - | - | 62 | 49 |
| Emulsifier 1% Nekal | | | | | | | | | | | |
| Hydroperoxide 5% | 55 | 50 | 58 | - | - | - | - | - | - | 60 | 32 |
| same 1% | 55 | 50 | 38 | - | - | - | - | - | - | 60 | 33 |

It follows from the results obtained that, for these initiators, the size of the polystyrene particles is greater in an acid than in a neutral or alkaline medium  This is found also at other concentrations of emulsifier and initiator (Table 2).

The first explanation which suggests itself for this difference in the dispersivity of latexes is the effect of the emulsifier, the properties of which vary with the nature of the medium. The studies of Yurzhenko and Kucher [3] showed that bases and acids appreciably affect micellar weight of the sulfonic

---

[1] In an acid medium, even at a lower extent of polymerization, the latexes contained the largest particles; in this case the particle radius exceeded 1/10 of the wavelength of the scattered light, and was determined approximately.

TABLE 3

Effect of Acids, Bases, and Salts on the Colloidal Properties of the Na Salt of Dibutyl-α-naphthalene Sulfonic Acid (Nekal).

| Electrolyte | pH | Micellar weight | Number of Nekal molecules in micelle | Number of micelles in 1 cm$^3$ of 0.5% Nekal, · $10^{-16}$ |
|---|---|---|---|---|
| Without added electrolytes | 6.6 | 20400 | 59 | 15 |
| Nekal + 0.1 g equiv/l $H_2SO_4$ | 1.8 | 19250 | 56 | 16 |
| Nekal + 0.1 g equiv/l NaOH | 12.0 | 32300 | 97 | 9 |
| Nekal + 0.1 g equiv/l $Na_2SO_4$ | 6.6 | 27800 | 80 | 11 |

detergent used, as well as the solubilization and other properties of the emulsifier. It was established that the largest emulsifier micelles are formed in an alkaline medium, and the solubilization of hydrocarbons in them varies correspondingly (Table 3).

If the same fraction of the emulsifier micelles (or all the micelles) participated in polymerization in an acid and an alkaline medium, then a correspondingly lower dispersivity of the synthetic latexes formed would be found in an alkali medium. This, however, does not occur in practice. Therefore, it may be supposed that in an acid medium the fraction of the emulsifier micelles which take part in the polymerization process (that is, which form the initial centers of polymerization) is less than in an alkaline or neutral medium. This must be due to the conditions of the initiated polymerization process in the micelles.

It is known that the decomposition of water-soluble initiators (inorganic and organic) to form free radicals which initiate polymerization takes place more intensively in presence of bases [4]1). Thus, in an alkaline medium we have an increased concentration of free radicals. These radicals, being formed in true aqueous solution, enter the emulsifier micelles which are saturated with the monomer, and initiate the polymerization process within them.

The rate of the initiation reaction will, evidently, be

$$V_{in} = K_{in}\,[R_w]\,[m],$$

where [Rw] and [m] are the concentrations of the free radicals and the emulsifier micelles in the aqueous phase of the emulsion. It is seen from the above equation that the concentration of emulsifier should affect the rate of initiation (and of the whole process), as was shown previously [5].

The increase of the rate of initiation of the polymerization process in micelles in an alkaline medium is associated with an increase in the fraction of the emulsifier micelles which participate in the polymerization process, which

---

1) N.M.Likholet and O.P Brazhnikova showed that potassium persulfate decomposes more rapidly in an acid than in an alkaline or neutral medium. However, the mechanism of decomposition in an acid medium is different from that in an alkaline or neutral medium, the formation of active free radicals being suppressed in an acid medium.

determines the number of polymer particles in the synthetic latex formed. As the monomer content of the original emulsion was the same in all cases, this should result in a smaller average radius of the latex particles.

TABLE 4

Effect of pH of the Aqueous Phase of the Emulsion on Particle Size in Latexes Obtained with an Oleophilic Initiator

(0.02 M benzoyl peroxide)

| Polymerization temperature, °C | pH of the aqueous phase of the original emulsion of styrene | | | | | |
|---|---|---|---|---|---|---|
| | 1.3 | | 6.8 | | 11.5 | |
| | S% | r, mμ | S% | r, mμ | S% | r, mμ |
| 45 | 91 | 39 | 40 | 41 | 58 | 46 |
| 55 | 55 | 50 | 35 | 52 | – | – |

It is an interesting fact that, in the polymerization of styrene in presence of an initiator of a different type – oil-soluble (benzoyl peroxide) – different behavior is observed. Studies of the turbidity of latexes obtained with this initiator showed (Figure 3, Table 4) that the most highly disperse latex is obtained in an acid medium, and not in an alkaline one, as was the case for the first two initiators.

This indicates that the influence of the electrolytes used on the dispersivity of the latexes formed depends on the nature of the initiator.

When an oil-soluble initiator is used, the influence of the medium on the size of the polystyrene particles may be satisfactorily explained on the basis of changes in the colloidal properties of the sulfonic detergent which occur when an acid or base is added to the aqueous phase of the emulsion, and if the use of water-insoluble initiator is taken into account. In this case the formation of free radicals from the peroxide evidently takes place not in a true aqueous solution, as in the case of water-soluble initiators, but within the emulsifier micelles by the decomposition of the solubilized initiator.

The fact that a basic latex contains the largest polymer particles is in good agreement with data which show that in an alkaline solution the micelle size is greatest [3], and the micelle concentration decreases accordingly, leading to the formation of coarsely disperse latexes. Conversely, in an acid medium the number of micelles is greater, and in consequence (other conditions being equal) the amount of monomer for each site of polymerization decreases and a more highly disperse latex is formed.

Effect of salts. The addition of neutral salts to the aqueous phase of an emulsion of polymerizing hydrocarbon also has a considerable effect on the dispersivity of the latexes formed. To study the effect of neutral salt content on the size of polymer particles, synthetic latexes were prepared in presence of KCl and $Na_2SO_4$ of different concentrations, added to the aqueous phase of the styrene emulsion (to the emulsifier solution). The results for the dispersivity (turbidity) of such latexes are shown in Figure 4.

It follows from these results that the presence of small amounts (up to 0.05 g equiv/l) of salts in the reaction system slightly increases the dispersivity of the latexes, and with further increase of salt concentration the size of the polymer particles in the latex increases sharply. The increase in the dispersivity of latexes on the addition of small amounts of salts to the emulsifier solution must be explained by the formation of a further quantity of micelles (as the result of a decrease in the critical concentration of micelle formation) due to a decrease in the concentration of molecularly dissolved sulfonic detergent. This increases the number of polymerization sites, and thus leads to a decrease in the diameter of the latex particles.

The increase in the size of polymer particles in the latex, which takes place on further addition of salts, may be explained on the basis of two suppositions: first, that the presence of salts sharply increases the size of the emulsifier micelles, and accordingly decreases their number per unit volume. Yuržhenko and Kucher [3] showed that the micellar weight of

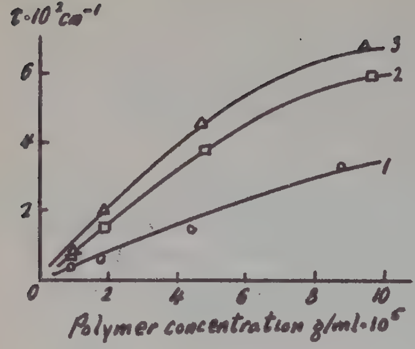

Fig. 3. Effect of pH of the aqueous phase of styrene emulsion on the dispersivity of latexes obtained with benzoyl peroxide (0.02 M). Emulsifier 0.5% Nekal, polymerization temperature 65°. 1) pH = 1.3, S = 53%, r = 39 mμ; 2) pH = 6.8, S = 58%, r = 52 mμ; 3) pH = 11.5, S = 57%, r = 56 mμ.

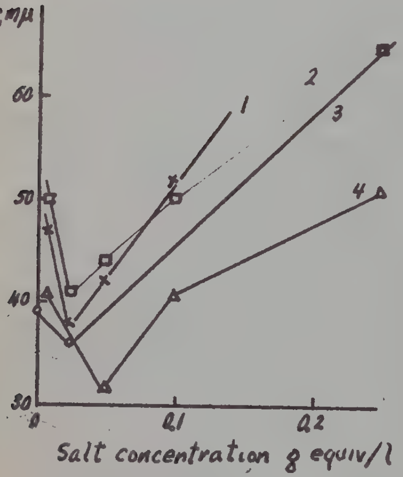

Fig. 4. Effect of salt concentration in the original monomer emulsion on the radius of polystyrene particles in the latex; emulsifier, 0.5% Nekal; 1) KCl, extent of polymerization S = 37-40%, initiator, benzoyl peroxide 0.02 M; 2) $Na_2SO_4$, S = 38-40%, benzoyl peroxide 0.02 M; 3) $Na_2SO_4$, S = 50-67%, hydroperoxide 0.02 M: 4) KCl, S = 60-73%, $K_2S_2O_8$, 0.005 .

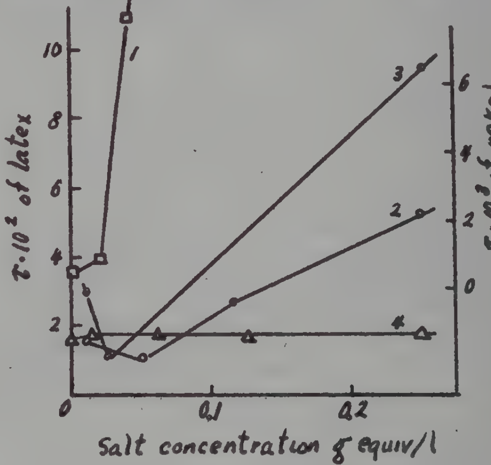

Fig. 5. Effect of salt concentration on the turbidity τ of 0.5% Nekal solution, 1, and of styrene latexes containing 0.005% (after dilution): 2) after addition of KCl to the aqueous phase of the original styrene emulsion; 3) $Na_2SO_4$; 4) KCl added to the latex formed.

sulfonic detergents increases under action of $Na_2SO_4$. We also observed an increase in the turbidity of Nekal on the addition of KCl (Figure 5, Curve 1). Decrease of the dispersivity of the emulsifier should lead to an increase in the particle size of synthetic latexes, as was found in the present investigation. Second, this effect may be attributed to the coagulation, caused by the addition of salts, of the latex formed.

To extablish which of these is the basic cause, the effect of salts on the dispersivity of the latex formed was studied. For this, different amounts of 0.5 M KCl solution were added to weighed amounts of the latex. These samples were allowed to stand for two days, diluted 500, 1000, and 2500 times, and their turbidity was investigated. The results of turbidity measurements on the addition of salts to the aqueous phase of the original emulsion of styrene (before polymerization – Curves 2 and 3) and to the prepared latex (Curve 4) are shown in Figure 5. It follows from these results that addition of up to 0.25 g-equiv/l KCl produces only an insignificant increase of turbidity, while the addition of similar amounts of salt to the emulsifier solution or to the reaction system before polymerization considerably alters the intensity of light scattering. This shows that changes in the size of polymer particles in synthetic latexes on the addition of salts to the solution of the emulsifier used in polymerization, occur chiefly as the result of a change in the colloidal state of the sulfonic detergent (size and number of micelles) by the action of the electrolytes added, which determines the number of sites of polymerization and consequently the size of the polymer particles in the latex.

## SUMMARY

1. The dispersivity of styrene latexes in relation to the content of electrolytes in the initial polymerization system has been studied. It is shown that the dispersivity of latexes obtained in an acid medium with a water-soluble initiator (potassium persulfate) is considerably lower than the dispersivity of latexes obtained in an alkaline or neutral medium. The reverse is found if the initiator is oil-soluble (benzoyl peroxide).

2. The dispersivity of latexes is considerably influenced by neutral salts contained in the aqueous phase of the polymerizing monomer (styrene); in the region of low salt concentrations the dispersivity of the latexes increases due to the formation of new micelles (decrease of the critical concentration of micelle formation); on further increase of the salt concentration the dispersivity of the emulsifier, and also of the latex, decreases.

Lvov Medical Institute

Laboratory of Physical and Colloid Chemistry

Received January 16, 1953

## LITERATURE CITED

[1] A.I.Yurzhenko and V.P Gusyakov, Colloid J., 14, No. 2, 140 (1952).1)

[2] A.I.Yurzhenko and V.P.Gusyakov, Proc. Acad. Sci., USSR, 86, No. 1, 129 (1952); Colloid J., 14, No. 6, 414 (1952).2)

[3] A.I.Yurzhenko and R.V.Kucher, Colloid J., 13, No. 3, 228 (1951).

[4] A I.Yurzhenko, Trans. 3rd Conf. on High Mol. Compds., Acad. Sci. USSR Press, 119 (1948).

[5] A.I.Yurzhenko and N.S.Tsvetkov, Proc.Acad.Sci.USSR, 85,No. 5, 1099 (1952).

---

1) See Consultants Bureau Translation, p. 153; 2) ibid, page 449.

# VLADIMIR ALDOFOVICH NAUMOV

(Obituary)

The death took place on October 9, 1953, of Doctor of Chemical Sciences Professor Vladimir Adolfovich Naumov, who played a prominent part in the development of our national colloid chemistry.

Vladimir Adolfovich Naumov was born in 1879 in Moscow, in a family of government employees. In 1904 he graduated at the Moscow higher technical school and received the title of engineer-technologist. After graduating at the technical school, V.A.Naumov specialized in organic chemistry under the guidance of Prof V.V.Sharvin; at the same time his first paper was published, on the subject of condensation of anthroquinone with phenol (1904). After graduating, V.A. taught chemistry, physics, and mathematics at a high school for several years. On the invitation of Prof V.V.Sharvin, from the fall of 1907 V.A.Naumov held the post of assistant in chemistry at the Moscow Commercial Institute (now the Plekhanov Institute of National Economy) where he worked until his death, for 47 years. In the Institute he organized the laboratory of general chemistry, and later the laboratory of qualitative analysis, which he conducted up to 1920.

In the summer semesters of 1908 and 1909 V A.Naumov worked at the University of Heidelberg, mainly in organic chemistry; the result of these studies was a paper "on the reaction between organomagnesium compounds and dibromoanthracene tetrabromide" (1910). At this time he bagan to be interested in physical chemistry.

In the summer semesters of 1913 and 1914 V.A.Naumov worked in the Göttingen laboratory of the well-known colloid scientist Zsigmondy, on colloid chemistry. From that time all his activity was devoted to research work in the field of colloid chemistry, and organization of the teaching and publicizing of this, at that time quite new, branch of science.

In 1914 V.A.Naumov published his paper " on the reaction of formation of colloidal gold solution by the formaldehyde method and the effect of carbon dioxide on its formation" . He also returned later to the study of colloidal gold solutions, and in 1921 - 1922 published two interesting papers on " the formation of colloidal gold solutions by the action of electrical spark charges" (1923).

V.A.Naumov published a number of review articles on colloid chemistry and presented addresses both to the Institute of National Economy and to other scientific and academic institutions, and in 1914 he organized, at the Moscow Institute of National Economy, the first laboratory of colloid chemistry in Moscow and one of the first in Russia, and was the first to give a systematic course in colloid chemistry in Russia.

In 1917 he published a handbook with the title " Practical Introduction to the Chemistry of Inorganic Colloids", while 1926 saw the publication of his excellent textbook " Chemistry of Colloids" which ran to three editions and which was used by many thousands of students during two decades.

At the Institute of National Economy, V.A.Naumov was first, in 1923, appointed Professor of Colloid Chemistry, and then in 1931, Head of the Department of Physical and Colloid Chemistry : this position he held to the day of his death. From 1918 to 1927 he was Lecturer in Colloid Chemistry at the Moscow Higher Technical School. From 1923 to 1938 he was Professor of Colloid Chemistry in the Moscow State University.

In addition to his vigorous teaching activities, V.A. was associated with a number of Research Institutes (VISM, Institute of Mineral Raw Materials, VIOK, etc.) where numerous investigations were carried out under his guidance on the applications of colloid chemistry to various practical problems.

V.A.Naumov was a brilliant lecturer and instructor. His lectures in colloid chemistry were accompanied by experiments which were exceptionally convincing and outstanding in design. In addition to their depth of content and clarity, these lectures were elegant and fascinating in form. His high experimental skill was displayed no less clearly in his experimental studies. V.A. displayed great enthusiasm in his experimental and teaching work. From early morning to late at night it was always possible to see him either working in his study or with his students. His attitude to his pupils was always simple and correct, while demanding a high standard. V.A.Naumov demanded high standards from himself, and a sense of duty and responsibility for all his work was very highly developed in him. In 1947 he completely lost his sight as the result of a severe disease of the eyes, but he continued his work and his lectures, the last of which he read on the eve of his death.

The role of V.A.Naumov in the history of the development of colloid chemistry in the Soviet Union is very important, and his name will be written among the pioneers of our National colloid chemistry.

V. Nazarov

TRANSLATION TO AND FROM ALL LANGUAGES

by bilingual chemists and engineers:

Rates for translation into English:

| Language | Price per 1000 words |
|---|---|
| French | $ 10.00 |
| German | 10.00 |
| Italian | 10.00 |
| Russian | 10.00 |
| Spanish | 10.00 |
| Dutch | 12.00 |
| Other languages | Rates upon request |

CONSULTANTS BUREAU
152 West 42nd Street
New York 18, N. Y.